Aus der <u>Klinik für Allgemeine, Unfall- und Wiederherstellungschirurgie</u>

Klinik der Universität München

Vorstand/Direktor: Wolfgang Böcker

The Roles of Extracellular Matrix Molecules Matrilins and Aggrecan in Bone Development and Articular Cartilage Functions

Dissertation

zum Erwerb des Doktorgrades der Humanbiologie

an der Medizinischen Fakultät der

Ludwig-Maximilians-Universität zu München

vorgelegt von

Ping Li

aus (Geburtsort)

Hebei, China

Jahr

2020

Mit Genehmigung der Medizinischen Fakultät der Universität München

Berichterstatter: PD Dr. Attila Aszodi

Mitberichterstatter: PD Dr. Jesus Buija

Prof Dr. Susanne Mayer

Prof Dr. Mohammad-Mehdi Shakibaei

Mitbetreuung durch den
Promovierten Mitarbeiter: Dr. hum,biol. Paolo Alberton

Dekan: Prof. Dr. med. dent. Reinhard Hickel

Tag der mündlichen Prüfung: 14.09.2020

Affidavit

Li, Ping

Surname, first name

I hereby declare, that the submitted thesis entitled

The Roles of Extracellular Matrix Molecules Matrilins and Aggrecan in Bone Development and Articular Cartilage Functions

is my own work. I have only used the sources indicated and have not made unauthorised use of services of a third party. Where the work of others has been quoted or reproduced, the source is always given.

I further declare that the submitted thesis or parts thereof have not been presented as part of an examination degree to any other university.

München, 16.03.2020

Place, Date

Ping Li

Signature doctoral candidate

TABLE OF CONTENTS

ABBREVATIONS

AC	Articular cartilage
ADAMTS	A disintegrin and metalloproteinase with thrombospondin motifs
AFM	Atomic force microscopy
BHMED	Bilateral hereditary micro-epiphyseal dysplasia
CS	Chondroitin sulphate
EO	Endochondral ossification
COMP	Cartilage oligomeric matrix protein
ECM	Extracellular matrix
ER	Endoplasmic reticulum
FACIT	Fibril-associated collagens with interrupted triple helix
GAGs	Glycosaminoglycans
GP	Growth plate
HA	Hyaluronan
H&E	Haematoxylin and Eosin
HSCs	Hematopoietic stem cells
HZ	Hypertrophic zone
IGD	Interglobular domains
IGF-1	Insulin-like growth factor 1
ITM	Interterritorial matrix
IO	Intramembranous ossification
kDa	Kilodalton
KS	Keratan sulphate
Leucine-rich repeat	LRR
LP	Link protein

MED	Multiple epiphyseal dysplasia
MMPs	Matrix metalloproteinases
OA	Osteoarthritis
Osteochondritis dissecans	OCD
PCM	Pericellular matrix
PG	Proteoglycan
POC	Primary ossification center
Ptc-1	Patched-1
PTHrP	Parathyroid hormone related peptide
PRG4	Proteoglycan 4
PSACH	Pseudoachondroplasia
PZ	Proliferative zone
rER	Rough endoplasmic reticulum
RZ	Resting zone
SEMD	Spondyloepimetaphyseal dysplasia
Small leucine-rich repeat proteoglycans	SLRPs
Smoothened	Smo
SOC	Secondary ossification center
TM	Territorial matrix
TSP	Thrombospondin
UPR	Unfolded protein response
VEGF	Vascular endothelial growth factors
vWFA	von Willebrand factor A

LIST OF PUBLICATIONS

This thesis is based on the following publications

I.   **Mice lacking the Matrilin Family of Extracellular Matrix Proteins Develop Normal Skeleton but are More Susceptible for Age-associated Osteoarthritis**

Ping Li, Lutz Fleischhauer, Claudia Nicolae, Carina Prein, Zsuzsanna Farkas，Maximilian Michael Saller, Wolf Christian Prall, Raimund Wagener, Juliane Heilig, Anja Niehoff, Hauke Clausen-Schaumann, Paolo Alberton, Attila Aszodi*

International Journal of Molecular Sciences. 2020 Jan 19; 21(2). pii: E666.

II.   **Aggrecan Hypomorphism Compromises Articular Cartilage Biomechanical Properties and Is Associated with Increased Incidence of Spontaneous Osteoarthritis.**

Alberton Paolo, Dugonitsch HC, Hartmann B, Li Ping, Farkas Z, Saller MM, Clausen-Schaumann H, Aszodi Attila.

International Journal of Molecular Sciences. 2019 Feb 26; 20(5). pii: E1008.

1. Introduction

Bones are important constituents of the organ systems of the vertebrates providing body support, physical protection for inner organs, movement facilitation, mineral storage and a niche for hematopoiesis [1, 2]. In human, there are more than 200 bones, which derive through two developmental pathways: 1) flat bones of the skull form directly from the condensation of the skeletogenic mesenchymal cells in the process of intramembranous ossification (IO); 2) while long bones of the appendicular and axial skeleton arise from intermediates of cartilaginous templates in the process of endochondral ossification (EO) [3]. EO starts with the condensation of the skeletogenic mesenchymal cells at the sites of the future bones, and the progenitor cells in these aggregates, under the guidance of various factors, differentiate into chondrocytes forming the cartilage template. Chondrocytes within the cartilage anlage begin to proliferate and synthesize cartilage-specific extracellular matrix, which is rich in collagen II and aggrecan [3]. The cartilage templates subsequently undergo maturation, hypertrophy, vascular invasion and mineralization, and the bones grow both laterally and longitudinally [4, 5]. As a result of the morphogenetic processes, embryonic cartilage is largely replaced by bone (transient cartilage), except the ends of long bones where it remains intact and forms the permanent articular cartilage [6, 7].

Articular cartilage (AC) is a highly hydrated, strong, resilient, avascular, alymphatic and aneural tissue. Covering the ends of long bones, AC is not only providing a lubricating, frictionless surface for the synovial, diarthrodial joints, but is also essential to distribute the mechanical loading generated during movement [8]. AC is composed of a relatively small number of chondrocytes, which lay down a specialized extracellular matrix (ECM). The major constituents of the ECM are the organic components (about 40%) and water (about 60%) [9, 10]. AC is characterized by a unique zonal structure with varying structural and biochemical properties. Generally, the AC is divided into four vertical layers: the superficial zone, the middle zone, the deep zone and the calcified cartilage zones[11]. All these zones have characteristic mechanical behavior for loading stimuli [12].

The ECM of both the transient and permanent cartilage provides physical support for chondrocytes, and acts as a sponge reserving growth factors and other cytokines, which in turn could modulate cell proliferation and differentiation. The ECM is predominantly composed of fibrillary

collagens, proteoglycans, and non-collagenous molecules [6, 13, 14]. These constituents interact with each other forming a unique protein network, which maintain the biochemical and biomechanical characters of the cartilage. The collagen fibrils provide tensile strength, whereas proteoglycans account for the elasticity of the tissue [13, 15]. The cartilage ECM is a dynamic network, which undergoes modeling and remodeling along the whole life. Homeostasis of cartilage is maintained by complex mechanisms controlling the turnover of the ECM by regulating the balance between anabolic and catabolic processes [16]. Mutations in matrix proteins resulting in abnormal organization of the ECM could eventually affect the development of

1.1. Bone and cartilage

Bone is a dynamic organ, which form either endochondral ossification or intramembranous ossification [3, 20].viscero-cranium, and a part of the clavicle develop by IO, while most bones in the body including long bones of the vertebral bodies and the ribs follow EO [7, 21]. In general, three types of cartilage can be defined in vertebrates: hyaline cartilage, elastic cartilage and fibrocartilage. Elastic cartilage, composed of collagen type II fibrils and elastic fibers, is found in the epiglottis, in the external ear, and in smaller laryngeal cartilages. Fibrous cartilage is rich in collagen type I, in addition to collagen II, and is mostly distributed in tissues with high shear stress such as the meniscus, the intervertebral discs and in pubic symphysis [7, 22]. Hyaline cartilage is the most widely distributed cartilage, typical for endochondral bone formation. The developing hyaline cartilage is surrounded by a perichondrium, and its ECM can be divided into three compartments relative to the chondrocytes: pericellular matrix, territorial matrix and interterritorial matrix. Hyaline cartilage stays permanent in the joints forming the articular cartilage, which characterized by a lubricated surface reducing the friction between the opposing bones making the movement more flexible [23].

1.1.1. Endochondral ossification

Endochondral bone formation (Figure 1) is initiated by the condensation of committed mesenchymal cells at the places where the future bony elements form [24, 25]. Under the guidance of specific molecules including

transcription factors, morphogens, cell-cell and cell-matrix adhesion molecules, the condensing progenitors form aggregates and most of them differentiate into chondrocytes, which synthetize cartilage-specific ECM and form aggregates and most of them differentiate into chondrocytes, which synthetize cartilage-specific ECM and form the initial cartilage template. Meanwhile, peripheral cells at the anlage elongate and make the perichondrium surrounding the cartilaginous core [15, 24, 26]. The early cartilage molds of long bones grow via the combination of chondrocyte proliferation and cartilage-specific ECM production, which is rich in collagen II and the proteoglycan aggrecan. Then, the proliferative chondrocytes in the central part of the anlage (diaphysis withdrawn from the cell-cycle, undergoing maturation and eventually transform into large, hypertrophic chondrocytes [27]. The hypertrophic cells produce specific ECM components like collagen X [28], express mineralization-inducing factors (e.g. alkaline phosphatase and matrix degrading enzymes (e.g. matrix metalloproteinase-13, MMP-13, and secrete vascular endothelial growth factor (VEGF, which attracts blood vessels invading the hypertrophic cartilage. The blood vessels recruit osteoclast/chondroclasts into the cartilage, which partially digest the ECM of the hypertrophic core; and osteoblasts which lay dawn trabecular bone on the remnants of the hypertrophic cartilage, thus forming the primary ossification center (POC at the diaphysis of the long bones. Simultaneously, perichondrial cells surrounding the hypertrophic core differentiate into osteoblasts, which secrete bone matrix and gradually form the bone collar. As the long bones grow, the POC is continuously expanding towards the two epiphyseal ends. The steps of endochondral ossification also occur later at the epiphyses establishing the secondary ossification centers (SOC) [29-31]. The narrow cartilaginous structure between the POC and SOC is the growth plate (GP), which is essentially responsible for spatially and timely coordinated maturation of the chondrocytes and for the longitudinal elongation of the endochondral bones. According to the metabolic status of the chondrocytes, the GP is organized into different horizontal zones: resting zone (RZ), proliferative zone (PZ) and hypertrophic zone (HZ) (Figure 2). In the RZ, the chondrocytes are rounded and they constitute a "germ-pool" of the cartilage. These progenitor cells after entering into the cell cycle generate the proliferative zone with chondrocytes characterized by columnar organization and high mitotic activity. At the lower part of the PZ, the cells stop to proliferate, mature and become hypertrophic. In the HZ, the chondrocytes enlarge, largely contributing for longitudinal elongation of long bones in mammalians,and secrete factors, which prepare the ECM for mineralization, vascular invasion, and for replacement of cartilage by bone. The last terminal layer of hypertrophic chondrocytes either die by apoptosis or transdifferentiate into osteoblasts.
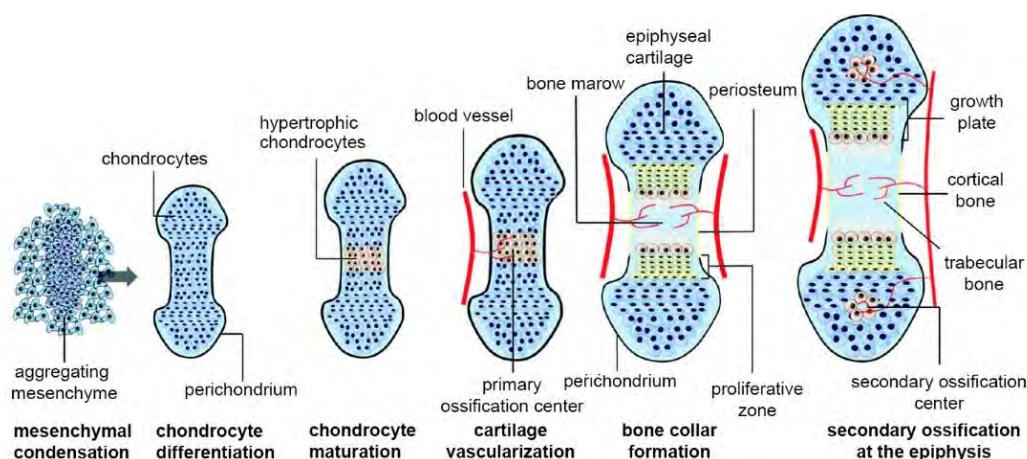
Figure 1: Endochondral bone formation. The figure is adapted and modified from Xie et.al, 2014 [32].

Plethora of molecules participate in the control of EO regulating mesenchymal condensation and aggregation, chondrocyte differentiation, proliferation, maturation and death. Fibroblast growth factors (FGFs), Sry-related high mobility group box (Sox) transcription factor 9 (Sox9) and Wnt signaling among the most important ones which direct the condensation process and the differentiation of precursors towards chondrogenic lineage. Sox9 acts uninterruptedly during endochondral bone formation by regulating mesenchymal-chondrocyte transition, chondrocyte proliferation and maturation [33, 34]. Sox5 and Sox6 are also expressed during the early chondrocyte differentiation, but unlike Sox9, are not required for mesenchymal condensation [35, 36]. The Indian hedgehog-Parathroid hormone-related protein (Ihh-PTHrP) signaling pathway plays the most critical role during chondrocytes proliferation, chondrocyte and perichondreal osteoblast differentiation. Ihh is produced by pre-hypertrophic chondrocytes, it binds to its receptor Patched-1 (Ptc-1) thus activating Smoothened (Smo) and transcription factors of the Gli family, which then triggers transcription gene activation. The expression of Ihh promotes synthesis of PTHrP in periarticular chondrocytes at the end of the epiphysis, which diffuse back to the GP and prevent proliferative chondrocytes become hypertrophic. Hence, Ihh-PTHrP signaling forms a negative feedback loop that regulates chondrocyte maturation [36-38]. Bone morphogenetic protein (BMP) signaling another mechanism which is important during EO. BMPs could promote cell proliferation and inhibit the terminal hypertrophic; meanwhile, BMPs could increase the expression of Ihh, which is opposite to that of FGFs [26, 39]. Runx2 is well recognized for its functions in endochondral ossification through modulating the proliferation and hypertrophic of chondrocytes and osteoblast, but different from sox9, which initiates chondrogenesis, Runx2 is vital mainly for the late stages [33, 40-42].
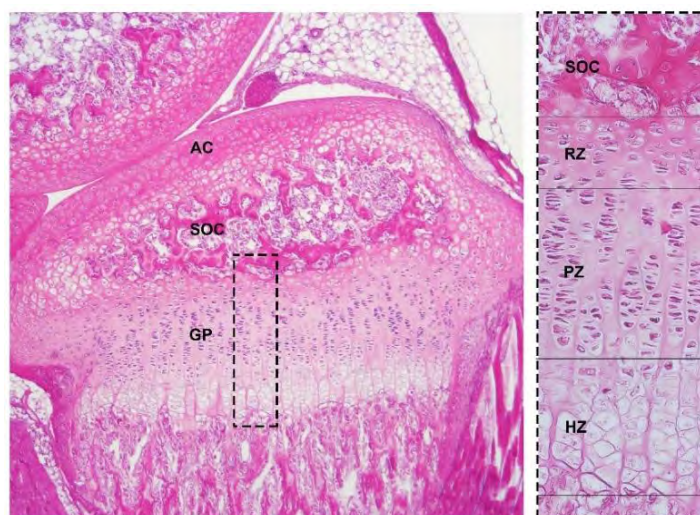
Figure 2: Structure of the mouse epiphysis and the growth plate. AC, articular cartilage; GP, growth plate; HZ, hypertrophic zone; PZ, proliferative zone; RZ, resting zone; SOC, secondary ossification center.

1.1.2. Articular cartilage.

Articular cartilage is hydrated, strong and resilient avascular hyaline cartilage. It covers the ends of long bones providing a lubricating, frictionless surface for the synovial joints and helps to distribute the loading generated during moving [8]. AC is characterized by a specialized ECM, which is produced by a relatively small number of chondrocytes. The ECM of the AC composed of the macromolecular assemblies of type II collagen fibrils and the proteoglycan aggregates aggrecan, which networks are interconnected via multiple adaptor glycoproteins [9]. The collagen network responsible for the tensile strength of the cartilage, while the aggrecan aggregates retain a huge amount of water and provide resistance against compressive forces. The chondrocytes are scattered throughout the ECM and, in contrast to cells in many other tissues, there is no direct chondrocyte-chondrocyte interactions, thus the cellular communication relies solely on the extracellular matrix [9, 10]. Throughout the AC, the orientation of the collagen fibrils, chondrocyte morphology and arrangement as well as the proteoglycan composition of the ECM greatly vary, allowing the separation of four distinct AC zones. In the uppermost superficial (or tangentional) zone (SZ), the chondrocytes are flattened and together with the tightly packed collagen fibrils align parallel to the joint surface. Compared to the other zones, the narrow SZ is further characterized by low proteoglycan content and by the expression of lubricating protein lubricin. The middle (or transitional) zone (MZ), is populated by roundish chondrocytes and contains highly intercrossed, obliquely oriented collagen fibrils. In the deep (or radial) zone (DZ), the chondrocytes form column-like structures and the thick collagen fibers align perpendicular to the surface. The DZ has the highest

proteoglycan deposition and the lowest water content in the AC. The calcified zone (CZ) connects the non-mineralized AC to the subchondral bone, and contains hypertrophic-like chondrocytes. Notably, the interface between the DZ and the CZ, which is called the tidemark, has a peculiar high deposition of proteoglycans and glycoproteins [43, 44] **(Figure 3**. The unique structure and composition of different zones allow the AC to respond differently for loading stimuli. The SZ exhibits the lowest level of hydrostatic pressure and the highest resistance to shear stress. In contrast, the DZ bears the highest hydrostatic pressure and the greatest resistance to compression. The mechanical properties of the MZ range between the two flanking zones [45].
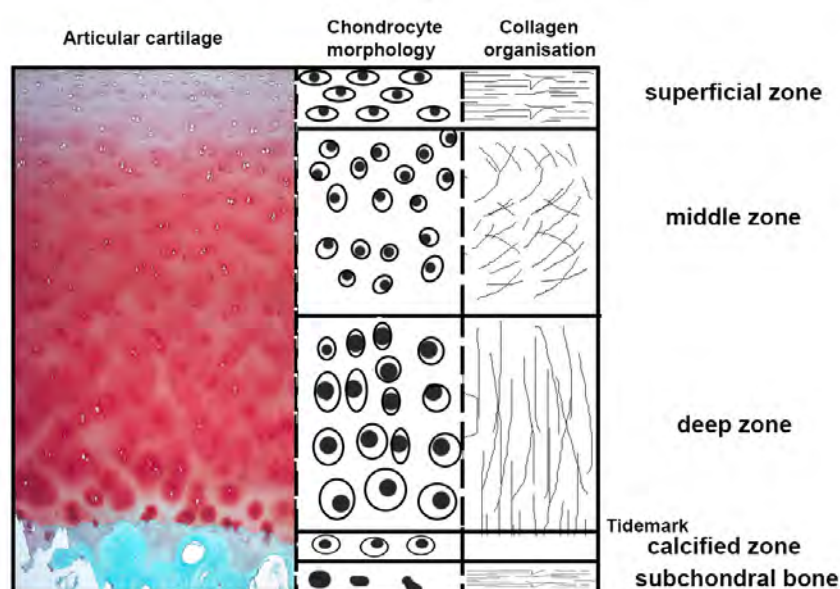

Figure 3: Structure of the articular cartilage. SZ- Superficial zone, MZ- Middle zone, DZ- Deep zone, CZ- Calcified zone SB- Subchondral bone. The figure is adapted from (Sam L. Francis, 2018)[46]

Damaged articular cartilage is generally inefficient to recover after injury or chronic diseases like osteoarthritis (OA), primarily due to the lack of efficient regenerative capacity of the tissue [47, 48]. Owing to the lack of vessels and lymphatics, nutrients and waste exchange could only occur via diffusion of ECM. Absence of nerve fibers makes it difficult to transmit the damage signals to chondrocytes triggering adaptive changes. Furthermore, even though AC chondrocytes are metabolically active, they have a very restricted proliferative capacity [9, 10]. Although previous studies have identified a considerable number of progenitors at the SZ of articular cartilage, they are apparently unable to

rescue the tissue degradation [49]. Over the past decades, many efforts have been made in searching for cartilage regenerative therapies, some are even applied in the clinic, but none of them was found to be effective in the long term. Such a lack of success can be ascribed to the fact that current methods fail in eliciting repair with an outcome which would properly mimic the architecture and function of the native AC.

1.2. Extracellular matrix of the hyaline cartilage

The ECM determines the structural, mechanical and physico-chemical properties of the hyaline articular cartilage. The major components of the cartilage ECM are the collagen fibrils and the proteoglycans (PGs) **(Figure 4**, which form a specialized macromolecular network providing tensile strength and resilience for the tissue, respectively [13, 50]. Numerous non-collagenous proteins are also present in cartilage, which regulate matrix assembly and involved in chondrocyte adhesion. Cartilage collagens may include fibrillar collagens (collagen I, II, III, V, and XI), fibril-associated collagens with interrupted triple helix (FACITs) (collagens IX, XII, XIV, XVI, and XXII), short chain collagens (collagen X), network-forming collagens (collagen IV), and others (collagen VI, VII and XIII) [51]. Classical collagens build up the heterotypic collagen fibrils of the cartilage composed of type II, IX and XI collagens. The collagen meshwork entraps the proteoglycan aggregates composed of aggrecan molecules bound to a hyaluronan backbone via link protein. The two supramolecular components of the ECM, the collagen fibrils and the aggrecan gel, are mainly responsible for cartilage physical properties providing tensile strength and resistance against compressive forces. The non-collagenous glycoproteins, e.g. matrilins and cartilage oligomeric matrix protein (COMP), could bridge the collagen network and the hyaluronan-aggrecan gel together together contributing to the stability and integrity of cartilage. The cartilage ECM not only provides physical support for the chondrocytes but also functions as sponge reserving different kinds of growth factors and cytokines which modulate chondrocyte activities [9, 52-54]. Cartilaginous ECM undergoes continuous remodeling by the combination of synthesis and degradation, which in turn regulate cell behavior by modulating proliferation, survival and differentiation [55]. The ECM molecules in the cartilage are organized into different compartments according to the relative distance from the cell membrane and to the structural organization and abundance of the individual ECM components (Figure 4). The pericellular matrix (PM) is the nearest and narrowest ECM compartment, which surrounds each chondrocyte. PM contains mainly proteoglycans, adhesive glycoproteins and a very fine collagen fibrillary

network and is primarily mediates cell-matrix interactions [56]. The territorial matrix (TM) is situated around the PM of individual our grouped chondrocytes. This compartment is thicker than the PM, and it characterized by a relatively fine collagen fiber network which protects the cells from mechanical overload. The interterritorial matrix (ITM) makes the largest part of the ECM with collagen bundles and proteoglycans, hence, predominantly responsible for the mechanical properties of the cartilage [57, 58].

1.2.1. Collagens

Collagen II is the major component of the collagen fibrils and is ubiquitously present throughout of the cartilage ECM zones and compartments [59, 60]. Collagen II is a homotrimer of three identical α chains encoded by a single gene (COL2A1). The quantitatively minor collagen types IX and XI are also important constituents of the heterotypic collagen II/IX/XI fibrils controlling fibrillogenesis and lateral growth. The collagen fibers in developing cartilage are slightly different from that in permanent articular cartilage, characterized by changes from thin collagen fibers, consisting of 10% collagen IX, 10% collagen XI and 80% collagen II, to much thicker collagen fibrils, containing approximately 1% collagen IX, 3% collagen XI, and 90% collagen II [61, 62].

Mutations in collagen types II, IX and XI result in various chondrodysplasias ranging from lethal to mild phenotype. The other collagen types, including collagens III, VI, X, XII and XIV, may exist in minor amount and are considered as factors modulating matrix maturation [61, 63]. Specifically, collagen VI is enriched in PM surrounding the chondrocytes. It is involved in cell-matrix communication and mechano-transduction, allowing the chondrocytes to perceive its microenvironment changes and make adaptive reactions maintaining the tissue homeostasis. [59, 64]. Collagen X is mainly synthesized by hypertrophic chondrocytes, and it is an important differentiation marker for the hypertrophic zone and the calcified cartilage of the GP and the articular cartilage, respectively [65, 66]. FACIT collagens could only bind to the surface of the fibrils, where they participates in the stabilization and network organization of the fibrils [62, 63, 67-69].
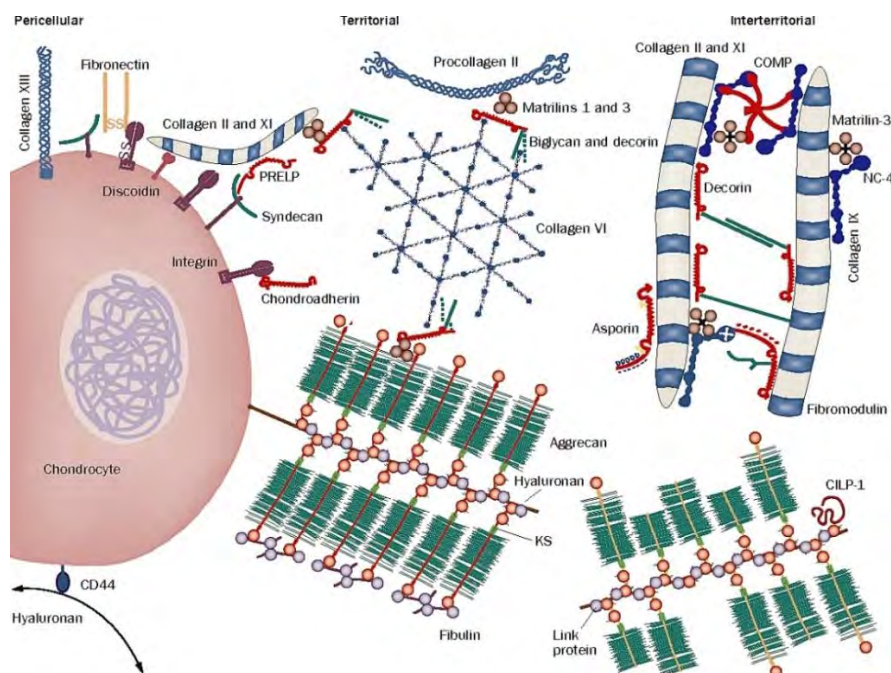
Figure 4: Extracellular matrix of hyaline cartilage. The figure is adapted and modified from Heinegård, 2009 [70].

1.2.2. Proteoglycans

Proteoglycans (PGs) are complex molecules, which composed of a core protein and one or more covalently attached glycosaminoglycan (GAG) chains. The GAG chains build up from various repeating disaccharide units defining distinct GAGs: hyaluronan (HA), chondroitine sulphate (CS), keratine sulphate (KS), dermatan sulphate and heparin sulphate. Expect HA, all other GAGs are directly attached to a core protein and establishing the diverse superfamily of cartilage proteoglycans. The most abundant cartilage PG is the aggrecan, which form macromolecular aggregates binding to the elongated, linear HA via cartilage link protein **(Figure 5**. These PG aggregates occupy the space in between the collagen fibrils, due to their high water binding capacity, and are regarded as a main structural constituent of the cartilage ECM [71-73]. The aggrecan core protein carries two N-terminal globular domains, G1 and G2, an interglobular domain between G1 and G2, an extended domain for KS and CS chains, and one C-terminal globular domain (G3). Among all the composing unites, only G1 is involved in the aggregation processes with LP and HA [72, 74]. The function of the G2 domain is largely unknown, while the G3 region containing several disulfide-bonded domains with homology to epidermal growth factor (EGF), C-lectin and complements regulatory protein motifs is involved in interaction of other cartilage ECM proteins [50, 75-77]. The extended domain between the G2 and G3 bears more than hundred CS and about 30 KS chains. 100 CS and 30 KS chains. The high negative charge density of the CS chains attracts counter ions and draw H_2O into the tissue creating a positive osmotic pressure, which

endows articular cartilage to resist compressive forces. The KS chains mainly interact with the fibrillar collagens [78]. Besides the structural role, the aggrecan–hyaluronan aggregates also play important roles in cell-ECM crosstalk through their numerous CS chains. When the sulphation of aggrecan CS chains is impaired, Ihh signaling is reduced, thereby affecting the normal morphogenesis of the cartilage [79]. Small leucine-rich repeat proteoglycans (SLRPs) are another PGs present in the cartilage ECM. SLRPs belong to the leucine-rich repeat (LRR) protein superfamily and characterized by a central LRR region stabilized by N- and C-terminal cysteine bridges [80]. Decorin and biglycan are prominent members of the cartilage SLRPs, which able to bind to collagen fibrils and carry only one or two CS chains at the N-terminal extension [81, 82].

1.2.3. Perifibrillar adapter proteins

Perifibrillar adapter proteins in the cartilage convey interactions between the collagen fibrils and the aggrecan aggregates, thereby stabilize those two supramolecular networks **(Figure 4)**. This diverse group of ECM proteins includes collagens like the FACIT collagen type IX, SLRPs like decorin and biglycan, and other non-collagenous matrix glycoproteins such as matrilins and cartilage oligomeric matrix protein (COMP). The collagen IX molecule composed of three distinct polypeptide chains ($\alpha1/\alpha2/\alpha3$) and it associates with the surface of collagen II/XI fibrils in an anti-parallel orientation. Its short arm at the N terminus sticks out of the fibril and provides binding sites for other perifibrillar adaptor proteins, whereas the long arm mediates covalent interactions with type II collagen and other collagen IX molecules [83-85]. The pentameric glycoprotein COMP belongs to the thrombospondin family and in the developing cartilage catalyzes collagen fibril formation. In more maturated cartilage in which fibrillogenesis is limited, however, it is functioning as cross-linker, thereby stabilizing the collagen network through binding to ECM proteins like collagen IX and matrilins. Furthermore, COMP connects the collagen network to the PG gel by binding to aggrecan [86-88]. Members of the matrilin family, such as matrilin-3, interact with collagen II/IX, COMP, biglycan, decorin and aggrecan forming a multimolecular complex, which interconnect collagen fibrils and aggrecan/HA aggregates via collagen VI microfibrils [89, 90]. In summary, perifibrillar adapter proteins are important for stabilization of the ECM by connecting of its constituents and for fibrillogenesis by controlling fibril diameter [91, 92]. Mutations or absences of perifibrillar adapter proteins results in a range of skeletal diseases including chondrodysplasias and premature osteoarthritis [93] .

1.2.4. Matrilins

Matrilins are non-collagenous, oligomeric extracellular matrix proteins which form a family with four

members: matrilin-1, matrilin-2, matrilin-3 and matrilin-4. All the four members share a similar modular protein structure containing one or two von Willebrand factor A-like (vWFA) domains, several epidermal growth factor-like domains and a C- terminal coiled-coil domain [94, 95] **(Figure 6)**. In addition, matrilin-2 and matrilin-3 carry positively charged amino acids at the N termini, just before the vWFA domain, and matrilin-2 has a unique domain preceding the coiled-coil domain. This modular structure enables matrilins with multiple molecular interactions [96, 97]. Through the C-terminal coiled-coil domain, matrilins form homo- or heterooligomers: matrilin-1 and matrilin-4 can form homotrimers, matrilin-2 and matrilin-3 form homotetramers, while only matrilin-1 and matrilin-3 able to form heterooligomers in cartilage with different stoichiometry [96]. No direct interactions exist between matrilin-2 and matrilin-3 or matrilin-3 and matrilin-4 [98]. Through their vWFA domain(s), matrilins bind to a diverse set of cartilage ECM constituents including COMP, decorin and biglycan, collagens II, IX and XI, and aggrecan, and contribute to matrix integrity and assembly [99-104]. Matrilin-3 consists of only one vWFA domain, while the other matrilins composed of two vWFA domains interconnected by the EGF-like motifs. Through the EGF- like domains, matrilins may interact with different growth factors such as bone morphogenetic protein-2 (BMP-2) and TGF-beta [96, 97]. Matrilins can form both collagen-dependent and independent networks in the cartilage. The collagen-independent network is typically found in the pericellular matrix and it may have a role in mechanotransduction of chondrocytes.
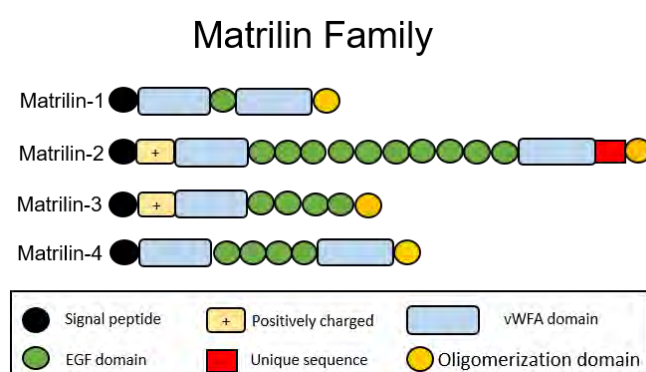
Figure 5: The domain structure of matrilins. The figure is adapted and modified from Wagener et al, 1998 [105].

1.2.4.1. Expression pattern and predicted functions of matrilins

According to tissue distributions in mice, matrilins can be sorted into two groups: matrilin-1 and matrilin-3 are almost exclusively cartilage-specific proteins, while matrilin-2 and matrilin-4 are present not only in cartilage but also in numerous extra-cartilaginous tissues.

Matrilin-1 (previously named cartilage matrix protein, CMP) first appearing around embryonic days 12.5 (E12.5) in the differentiated cartilage templates of long bones, and is enriched in the epiphyseal and growth plate cartilages during limb development. At the layers of the forming articular cartilage matrilin-1 is absent. In the adult joint, however, matrilin-1 is weakly expressed at the peripheral areas of the articular cartilage [106]. Matrilin-1 may take part in collagen fibril assembly and interact with the aggrecan core protein bridging the two main ECM components together in cartilage [94, 97]. Matrilin-1 (*Matn1*^{-/-}) knockout mice have no obvious skeletal phenotype, although ultrastructural irregularities of the collagen fibrils, and increased stiffness of the cartilage have been reported [98, 107]. Except for cartilaginous tissues, matrilin-1 exhibits minor expression in the heart and the eye[108].

Matrilin-2 is the biggest member of matrilin family and in the skeletal system it is first detectable in the developing limb cartilage at E13. Matrilin-2 is expressed in the proliferative and upper hypertrophic zones of the growth plate, in the superficial layer of the forming articular cartilage and in the perichondrium. Matrilin-2 is present in a broad range of extra-skeletal tissues including tendons, dermis, heart, smooth muscles, alimentary canal and peripheral nerves [98, 106, 109]. The function of matrilin-2 in cartilaginous tissues largely remains unknown, hence *Matn2*^{-/-} knockout mice have no reported skeletal abnormalities. Outside of the skeleton, matrilin-2 has been suggested to participate in peripheral nerve regeneration [110], muscle regeneration [111] and in the control hepatocarciogenesis [112] and autoimmune neuroinflammation[113].

Matrilin-3 also starts appearing in cartilage at E12.5 and displays largely an overlapping expression pattern with matrilin-1 [106, 109]. Matrilin-3 is expressed in the deep region of the developing articular cartilage, but it is present only in minor amount of the peripheral areas of the permanent articular cartilage. Similar to that of matrilin-1, matrilin-3 is primarily involved in connecting of the cartilage ECM networks and could modulate of the collagen diameter during fibrogenesis [64, 114]. Matrilin-3 deficient mice (*Matn3*^{-/-}) generated in the Aszodi lab show onl ay slight ultrastructural abnormality of the collagen fibrils, while mice generated in the Chen lab display transiently accelerated hypertrophic chondrocyte differentiation and knee osteoarthritis in animals older than one year [115, 116]. Recently, a beneficial role of matrilin-3 for repair of osteoarthritic lesions has been suggested [117].

Matrilin-4, the last member of the family being discovered, exhibits the most ubiquitous expression pattern. Matrilin-4 is abundantly expressed in the growth plate and epiphyseal cartilage, and in the whole surface of the forming articular cartilage. In the growth plate, the deposition of matrilin-4 in the hypertrophic

zone is weaker compared with that in the proliferative zone. In the adult articular cartilage, matrilin-4, just like the other matrilins, is weakly expressed in the peripheral joint areas. Beyond the skeletal system, matrilin-4 can be found in the heart, lung, kidney, central and peripheral nervous system [109]. Matrilin-4 knockout mice (*Matn4*$^{-/-}$) do not display obvious skeletal abnormalities by visual inspection but show abnormal proliferation of hematopoietic stem cells upon stress conditions [118].

1.3. Skeletal diseases associated with matrilins and aggrecan

The chemical composition and the architecture of the ECM are pivotal the normal physical properties of the cartilage, for skeletal morphogenesis and for the normal functions of the AC. Defects in ECM assembly or abnormal ECM composition may results in pathological conditions including chondrodyslasias and degenerative joint diseases such as osteoarthritis.

1.3.1. Chondrodysplasia

Osteo-chondrodysplasias are heterogeneous genetic disorders with over 400 conditions affecting bone and cartilage development. Chondrodysplasias often result in disproportionate dwarfism due to defects in genes affecting growth plate structure and function. Mutations can alter the integrity of the cartilage matrix or disturb cell-matrix interactions leading to misguidance of proliferating cells into columns, which are essential for the elongation of long bones [119, 120]. Mutations in genes encoding various cartilage ECM proteins could induce chondrodysplasia, including mutations in matrilin-3 and aggrecan [121].

Although all the four matrilins are present in the cartilage throughout endochondral bone formation, only mutations in the human gene coding for matrilin-3 (*MATN3*) have been clearly assigned to any form of chondrodysplasias. Mutations in *MATN3* are linked to the autosomal dominant form of multiple epiphyseal dysplasia (MED), a genetically heterogeneous, mild form of chondrodysplasia characterized by abnormal ossification of the epiphysis, joint stiffness and early onset of osteoarthritis. MED-causing *MATN3* mutations are missense and are mainly located in β strands of the von Willebrand domain [122-125]. Mutations close to the β-sheet regions lead to bilateral hereditary micro-epiphyseal dysplasia (BHMED), a skeletal condition similar but still distinct to MED. Additional MED-like disorder is the spondylo-epi-metaphyseal dysplasia (SEMD), which can be caused by mutations in the EGF domain of matrilin-3 [123, 126]. Mechanistically, most MED and SEMD *MATN3* mutations result in defective protein secretion and accumulation in the endoplasmatic reticulum. Furthermore, a linkage of *MATN3* to spinal disc degeneration has been reported [127]. Mutations in the gene coding for matrilin-1 (*MATN1*) have been excluded from several types of

osteochondrodysplasias (including MED), while the association of *MATN1* with idiopathic scoliosis, mandibular prognathism and SEMD with joint laxity have been found [128]. To date, no genetic linkage between *MATN2* and *MATN4* to any heritable skeletal disorder has been identified.

Mutations in the aggrecan gene (*ACAN*) cause various forms of skeletal dysplasias defining a still growing group of genetic disorders collectivelly called as aggrecanopathies [71, 129, 130]. The essential importance of aggrecan in cartilage development has been illustrated by the naturally occouring mutations in various species including the embryonic lethal cartilage matrix deficiency (*cmd*) in mouse and *nanomelia* in chicken, and the the recessive Dexter bulldog dwarfism. The *cmd* -/- mice, which carry a functional null mutation of *Acan*, die shortly after birth, while the heterozygotes mice are born normal but suffer from late-onset of spinal disorder [130, 131]. Further *ACAN* mutations distributed all over the molecule cause SEMD, spondyloepiphyseal dysplasia Kimberley type, osteochondritis dissecans and various idiopathic short stature syndromes. [132]. Recent genetic studies on the variation of human height have suggested *ACAN* as a potential modulator of height [126]. Mechanistically, aggrecanopathies can be caused by mutations either leading to haploinsuffiency or inducing a dominant-negative pathomechanism disrupting the normal cartilage function[133].

1.3.2. Osteoarthritis

Osteoarthritis (OA) is a multifactor-induced disease characterized by progressive loss of the AC associated with limited joint flexibility, swelling, severe pain and stiff joints. OA is the major cause of disability in adults which seriously affects the life quality of middle-aged and elderly patients [134-136]. Besides AC destruction, OA impacts multiple joint tissues including the synovial membrane, subchondral bone, menisci, ligaments and tendons. Owing to the lack of effective therapies for rescuing the degraded cartilage, the long disease duration and high cost for joint replacement make OA one of the most concerned musculoskeletal disease worldwide [137-139]. Decades' studies about the pathophysiology of OA have clarified that the OA is raised from an imbalance of cartilage homeostasis shifting from anabolism to catabolism [140-142], which is caused by multiple factors including genetic susceptibility, weight, inflammation and abnormal biomechanical stimuli [143-145]. As a net effect, degradation of aggrecan complexes and disruption of the collagen fibrillary network result in a structurally and biomechanically compromised tissue which eventually leads to cell death and progressive erosion of the AC [146, 147].

Matrilins, as integrative players of the cartilage ECM, can be indirectly or directly associated with osteoarthritis. MATN3 MED patients may have early onset osteoarthritis due to abnormal development and shaping of the epiphysis. In addition, a mutation in the first EGF domain of MATN3 has been associated with hand osteoarthritis but not with knee OA [148-150]. MATN3 expression is upregulated in the joint of OA patients [151-154] and in vitro studies revealed that it may play a complex role in the control of anabolism-catabolism in the cartilage [155-157]. The weak association of *MATN1* with OA has been reported [158] and the ectopic deposition of the matrilin-1 protein was demonstrated in the AC of human knee OA cartilage [159]. Dysregulation of MATN2 and MATN4 expression has been linked to the onset and progression of OA, respectively [160, 161].

Aggrecan endows the cartilage with load-bearing properties and plays essential roles in mediating acell-matrix interactions. Degradation of aggrecan is considered as a hallmark of early osteoarthritis which mainly attributed to the proteolytic activities of MMPs and aggrecanases (ADAMTS-4 and -5) [162, 163]. Decreased level of aggrecan molecules reduces the negative charge density of the sGAG chains leading to decreased osmotic swelling pressure accompanied by increased constraining matrix stress, and finally elevates the cartilage stiffness [164, 165]. Subsequently, collagenases (MMP-1 and -13) degrade the collagen fibrils initiating tissue erosion [162, 166]. Missense mutations in the G3 domain of ACAN result in skeletal dysplasias such us idiopathic short stature, SEMD or familial osteochondritis dissecans (OCD) [133, 167-170]. OCD is characterized by the separation of the subchondral bone and the AC and early onset osteoarthritis. A missense V2303M mutation in the G3 domain of ACAN has been described which impairs protein interactions of aggrecan with other ECM molecules [170].

1.4.　Aim of the thesis

The extracellular matrix is vital for the development of endochondral bones and for maintaining the homeostasis of the articular cartilage. Disturbances in the secretion, matrix assembly or molecular interactions of the composing macromolecules could induce a series of structural and metabolic abnormalities in the cartilage, which may accelerate pathological processes in the skeletal system. Despite the increasing information on the structural and functional importance of ECM constituents in cartilage physiology and pathophysiology, still a significant gap exists between the molecular structure of a matrix protein and its biochemical and biomechanical properties.

In this thesis, therefore, our ultimate goal was to further understand the biological roles of cartilage ECM in the sequence of endochondral bone formation and articular cartilage physiology; and to elucidate its contribution for pathological conditions of the skeleton such as osteochondrodysplasias and osteoarthritis using genetically modified mice as model organism. Specifically, we aimed to investigate:

1. the role of matrilin family of cartilage adaptor proteins in morphogenesis and function of the skeleton utilizing a set of single or multiple matrilin knockout mice;

2. the consequence of reduced aggecan expression on cartilage properties by analysing the hypomorphic $Agc1^{CreERT2/CreERT2}$ mouse line.

Particularly, the following milestones were defined:

1. clarifying possible functional compensation among matrilins in cartilage;

2. dissecting the role of matrilins in morphogenesis of the appendicular and axial skeleton;

3. understanding the role of matrilins for the structural biomechanical properties of the cartilage;

4. establishing the link between matrilin-deficiency and osteoarthritis;

5. assessing the contribution of aggrecan protein level to spontaneous, age-associated osteoarthritis.

1.5. Own contribution

Paper I: I prepared all mouse tissue tissue samples and performed the whole-mount skeletal, histological, histochemical, in situ hybridization and immunohistochemical analyses. I isolated proteins from cartilage and performed the biochemical assays. I prepared all the samples for AFM measurement. I performed the morphometric measurements and the statistical analyses. I assessed articular cartilage degradation of the knee joint together with Paolo Alberton and Attila Aszodi. I wrote the manuscript together with Attila Aszodi and Paolo Alberton.

Paper II: I performed the immunohistochemical analysis on articular cartilage samples. I did the OA scoring together with Paolo Alberton and Attila Aszodi.

2. SUMMARY

Cartilage is composed of chondrocytes and an abundant extracellular matrix (ECM), which consists of macromolecular assemblies of collagen fibrils and aggrecan-hyaluronan aggregates interconnected with adaptor proteins. The cartilage ECM provides the proper microenvironment for chondrocytes and primarily determines the architecture, biomechanical and functional properties of the tissue. Spatially- and temporally-controlled ECM homeostasis through a sophisticated balance of protein synthesis and degradation is essential for both endochondral bone formation and the normal function of the permanent articular cartilage. Disturbance of cartilage ECM composition, assembly or turnover can lead to pathophysiological conditions such as chondrodysplasias or osteoarthritis. For a better understanding of the role of ECM macromolecules in cartilage physiology and pathology, we have focused our research on the characterization of the in vivo functions of the 1) matrilin family of adaptor proteins, and the 2) major cartilage proteoglycan aggrecan.

Matrilins are structurally related, non-collagenous proteins belonging to the vWFA domain-containing superfamily of macromolecules. Four matrilins are known, matrilin-1, -2, -3 and 4, and each are expressed in the transient growth plate cartilage and, at low levels, in the permanent articular cartilage. Mutations in the human gene encoding matrilin-3 (MATN3) are associated with autosomal dominant skeletal disorders, and all matrilins (MATN1, MATN2, MATN3 and MATN4) have been implicated in human osteoarthritis. However, mouse models carrying single null allele for matrilins display no or relatively mild skeletal abnormalities suggesting functional compensation among the family members. In the first study (Paper I) we have challenged the compensation theory of matrilins by generating and analyzing multiple matrilin knockout mice. First, we demonstrated by protein analyses of knee cartilage of various compound knockout mice that MATN4 and MATN2 are indeed upregulated in the absence of MATN1 and MATN4, respectively, evidencing the existence of biochemical compensation mechanisms among matrilins. Second, we showed that quadruple knockout mice ($Matn1-4^{-/-}$) have normal size, exhibit no obvious abnormalities in the overall structural and biomechanical properties of the growth plate, however, display a modestly increased mean diameter of the collagen fibrils. Third, we provided biochemical evidences that the lack of all matrilins in cartilage only mildly affect the extractability of their binding partners. Fourth, we showed that only $Matn1-4^{-/-}$ and $Matn4^{-/-}$ mice develop age-associated spontaneous osteoarthritis suggesting an important role of MATN4 for maintaining the normal physiological properties of the articular cartilage. Fifth, and most unexpectedly, we demonstrated that matrilin-deficiency in the axial skeleton lead to sacralization of the last lumbar vertebra in $Matn4^{-/-}$ mice. Taken

together, our data indicate that matrilins are largely dispensable for the growth of the appendicular skeleton, but are pivotal for correct patterning of the vertebral column and for preventing articular cartilage degradation.

Aggrecan is the essential proteoglycan of the cartilage ECM which, due to the high negative charge density of its GAG chains, attracts water into the tissue allowing to resist compressive forces. The absence of aggrecan in cartilage results in lethal chondrodysplasia, while mutations in the human aggrecan gene (*ACAN* or *AGC1*) cause a broad range of skeletal disorders through dominant negative mechanisms disrupting cartilage structure or by inducing reduced ECM deposition of the protein (haploinsufficiency). The number of such aggrecanopathies still increasing, however, the relationship between the disease-causing mutation and the cartilage phenotype is remains to be elucidated. We have, therefore, investigated the impact of the reduced deposition of aggrecan on skeletal development and articular cartilage function using the *Agc1*$^{CreERT2/+}$ and *Agc1*$^{CreERT2/CreERT2}$ mouse models (Paper II). We demonstrated that both heterozygous and homozygous mutant mice are hypomorphic expressing aggrecan mRNAs below the normal levels. We showed that diminished deposition of aggrecan protein into the cartilage ECM leads to a dwarf phenotype in *Agc1*$^{CreERT2/CreERT2}$ mice, which is persisted throughout the life. Most importantly, we found that *Agc1*$^{CreERT2/CreERT2}$ mice develop severe, age-associated degeneration of the knee articular cartilage. The osteoarthritis-like phenotype was not due to upregulation of ECM degrading enzymes but was accompanied by increased stiffening of the articular cartilage. Thus, our findings suggest that a reduction in the normal collagen/aggrecan ratio in the articular cartilage makes harder the joint surface, which eventually predisposes for degradation.

3. ZUSAMMENFASSUNG

Knorpel setzt sich zusammen aus Chondrozyten und einer stark ausgeprägten extrazellulären Matrix (EZM), welche aus makromolekularen Verflechtungen von Kollagenfibrillen und Aggrecan-Hyaluronan Molekülen besteht. Die Aggrecan-Hyaluronan Moleküle sind untereinander über Adapter-Proteine verbunden. Die EZM des Knorpels stellt nicht nur das angemessene mikrobiologische Milieu für die Chondrozyten breit, sondern ist zudem maßgeblich für die biomechanischen, architektonischen und funktionellen Eigenschaften des Gewebes verantwortlich. Die Homöostase der extrazellulären Matrix wird gewährleistet durch ein räumlich und zeitlich aufeinander abgestimmtes Gleichgewicht von Proteinsynthese und -degradierung, welches darüber hinaus für eine regelrecht ablaufende enchondrale Ossifikation und Funktionsfähigkeit des artikulären Knorpels essentiell ist. Kommt es zu einem Ungleichgewicht in der Zusammensetzung der EZM oder einer Störung im Aufbau und Umsatz des Knorpels, kann dies zu schwerwiegenden Krankheitsbildern wie Chondrodysplasien oder Osteoarthirtis führen. Um ein tieferes Verständnis für die Bedeutung der extrazellulären Makromoleküle an der Physiologie und Pathophysiologie des Knorpels zu erlangen, haben wir unsere Forschungsschwerpunkte auf die Charakterisierung der 1) Matrilin-Familie, einer Gruppe von Adapter-Proteinen, und 2) Aggrecan, einem Hauptproteoglycan im Knorpel, gelegt.

Matriline bilden eine Familie von extrazellulären und strukturell verwandten Proteinen mit modulärem Aufbau. Alle Matriline gehören zu einer Überfamilie der vWFA (von Willebrandfaktor A)-Domänen beinhaltenden Gruppe von Makromolekülen. Bisher sind vier Matriline, Matrilin-1, -2, -3, und -4, bekannt und alle werden im hohen Maße in der vorübergehenden Wachstumsplatte im Knorpel exprimiert. Geringe Expressionsraten der Matriline konnten im ortsständigen artikulären Knorpel nachgewiesen werden. Einige autosomal-dominant vererbte skelettale Erkrankungen sind assoziiert mit Mutationen im humanen Gen MATN3, welches für das Protein Matrilin-3 codiert. Jedoch zeigten Mausmodelle mit einem einzelnen Nullallel für Matriline keine, beziehungsweise, nur geringe Veränderungen des Skeletts. Diese Erkenntnisse lassen die Hypothese zu, dass es durch andere Mitglieder der Familie zu einer funktionellen Kompensation kommt. In einer vorherigen Studie (wissenschaftlicher Artikel I) haben wir diese Hypothese durch das Erstellen mehrerer Matrilin-Knockout Mäuse genauer untersucht. Dazu haben wir zuerst mittels Proteinanalysemethoden von murinem Knorpel nachgewiesen, dass MATN4 und MATN2, bei gleichzeitig vorliegendem Knockout des jeweils anderen Gens, hochreguliert waren und somit einen funktionellen Kompensationsmechanismus unter den Familienmitgliedern bewiesen. Weiterhin konnten wir mittels eines vierfachen Knockouts (Matn-1-4 $^{-/-}$) zeigen,

dass betroffene Mäuse eine normale Größe aufwiesen und zudem keine offensichtlichen Veränderungen bezüglich der strukturellen und biochemischen Eigenschaften der Wachstumsplatte zeigten. Ein Merkmal, welches allerdings auffiel, war ein moderat erhöhter Durchmesser der Kollagenfibrillen. Darüber hinaus haben wir aufgezeigt, dass ein Mangel an Matrilinen zu einer gering eingeschränkten Extrahierbarkeit der Bindungspartner führt. Der Befund, dass nur Matn-1-4 $^{-/-}$ Knockout Mäuse eine altersabhängige und spontane einsetzende Osteoarthritis aufwiesen, lässt auf eine wichtige Funktion von MATN4 für die Aufrechterhaltung normaler physiologischer Eigenschaften des artikulären Knorpels schließen. Zu Letzt, jedoch sehr unerwartet wiesen Matn4 $^{-/-}$ Mäuse eine Fusion des letzten lumbalen Wirbelkörpers und des ersten sakralen Wirbelkörpers auf. Zusammenfassend weisen unsere Ergebnisse darauf hin, dass die Matriline bei der Entwicklung und Ausbildung des Extremitätenskeletts eine untergeordnete Rolle, jedoch bei der Untergliederung und Formierung der Wirbelsäule eine Schlüsselrolle einzunehmen scheinen.

Aggrekan ist ein Proteoglykan und ein integraler Bestandteil der EZM des Knorpels, welches aufgrund der hohen negativen Ladung der Glykosaminoglykane-Ketten, Wasser anzieht, im Gewebe bindet und diesem so eine gewisse Elastizität verleiht. Fehlt Aggrekan gänzlich im Knorpel endet dies in letal verlaufenden Chondrodysplasien. Wohingegen Mutationen im humanen Agrrekan-Gen (ACAN oder AGC1) durch einen dominanten negativen Mechanismus zu einer Veränderung der Knorpelstruktur oder einer reduzierten EZM Ablagerung führen und somit ein breites Spektrum an skelettalen Erkrankungsbildern hervorrufen (Haploinsuffizienz). Obwohl die Anzahl an den neu endeckten Aggrekanopathien stetig zunimmt, bleibt die Beziehung zwischen krankheitsauslösenden Mutationen und dem Knorpelphenotypen weiterhin ungeklärt. Um diese Beziehung besser zu verstehen, haben wir den Einfluss einer verminderten Aggrekan Ablagerung auf die skelettale Entwicklung und die funktionellen Eigenschaften des Gelenkknorpels mittels dafür entwickelten Agc1$^{CreERT2/+}$ und Agc1$^{CreERT2/CreERT2}$ Mausmodellen untersucht (wissenschaftlicher Artikel II). Anhand dieser Modelle konnten wir aufzeigen, dass die Aggrekan mRNA Spiegel bei heterozygoten und homozygoten Mausmutanten unterexprimiert waren. Wir konnten zudem zeigen, dass eine verminderte Ablagerung von Aggrekanmolekülen in die EZM des Knorpels zu einem Zwergphenotypen in Agc1$^{CreERT2/CreERT2}$ Mäusen führt. Dieser Phenotyp persistierte über die gesamte Lebensspanne der Mäuse. Besonders hervorzuheben ist, dass Agc1$^{CreERT2/CreERT2}$ Mäuse eine schwere und altersabhängige Degeneration des artikulären Knorpels der Kniegelenke aufwiesen und, dass dieser Osteoarthiris ähnliche Phänotyp nicht einer Hochregulation von EZM zersetzenden Enzymen zuzuschreiben war, sondern dass er mit einer erhöhten Steifheit des Knorpels resultierte. Daraus lässt sich ableiten, dass eine Verringerung des normalen Kollagen/Aggrekan-Verhältnisses im artikulären

Knorpel zu einer erhöhten Härte in der Gelenkoberfläche führt und diese damit anfällig für degenerative Veränderungen macht.

Paper I

![International Journal of Molecular Sciences logo]

![MDPI logo]

Article

Mice Lacking the Matrilin Family of Extracellular Matrix Proteins Develop Mild Skeletal Abnormalities and Are Susceptible to Age-Associated Osteoarthritis

Ping Li [1], Lutz Fleischhauer [1,2,3], Claudia Nicolae [4,†], Carina Prein [1,2,‡], Zsuzsanna Farkas [1], Maximilian Michael Saller [1], Wolf Christian Prall [1], Raimund Wagener [5], Juliane Heilig [6,7], Anja Niehoff [6,8], Hauke Clausen-Schaumann [2,3], Paolo Alberton [1] and Attila Aszodi [1,2,*]

[1] Experimental Surgery and Regenerative Medicine (ExperiMed), Department of General, Trauma and Reconstructive Surgery, Munich University Hospital, Ludwig-Maximilians-University, 80336 Munich, Germany; Ping.Li@med.uni-muenchen.de (P.L.); lutz.fleischhauer@hm.edu (L.F.); carina.prein@uwo.ca (C.P.); Zsuzsanna.Farkas@med.uni-muenchen.de (Z.F.); Maximilian.Saller@med.uni-muenchen.de (M.M.S.); Christian.Prall@med.uni-muenchen.de (W.C.P.); Paolo.Alberton@med.uni-muenchen.de (P.A.)

[2] Center for Applied Tissue Engineering and Regenerative Medicine, Munich University of Applied Sciences, 80533 Munich, Germany; hauke.clausen-schaumann@hm.edu

[3] Center for NanoScience, Ludwig-Maximilians University Munich, 80799 Munich, Germany

[4] Department of Molecular Medicine, Max Planck Institute for Biochemistry, 82152 Martinsried, Germany; cnicolae@pennstatehealth.psu.edu

[5] Center for Biochemistry, Medical Faculty, and Center for Molecular Medicine, University of Cologne, 50923 Cologne, Germany; raimund.wagener@uni-koeln.de

[6] Cologne Center for Musculoskeletal Biomechanics, Faculty of Medicine and University Hospital of Cologne, 50931 Cologne, Germany; juliane.heilig@uni-koeln.de (J.H.); niehoff@dshs-koeln.de (A.N.)

[7] Center for Biochemistry, Faculty of Medicine, University of Cologne, 50931 Cologne, Germany

[8] Institute of Biomechanics and Orthopaedics, German Sport University Cologne, 50933 Cologne, Germany

[*] Correspondence: attila.Aszodi@med.uni-muenchen.de; Tel.: +49-89-4400-55481

[†] Current address: Department of Biochemistry and Molecular Biology, The Pennsylvania State University College of Medicine, Hershey, PA 17033, USA.

[‡] Current address: Department of Physiology and Pharmacology, Schulich School of Medicine and Dentistry, The University of Western Ontario, London, ON N6A 3K7, Canada.

Abstract: Matrilins (MATN1, MATN2, MATN3 and MATN4) are adaptor proteins of the cartilage extracellular matrix (ECM), which bridge the collagen II and proteoglycan networks. In humans, dominant-negative mutations in MATN3 lead to various forms of mild chondrodysplasias. However, single or double matrilin knockout mice generated previously in our laboratory do not show an overt skeletal phenotype, suggesting compensation among the matrilin family members. The aim of our study was to establish a mouse line, which lacks all four matrilins and analyze the consequence of matrilin deficiency on endochondral bone formation and cartilage function. *Matn1-4⁻/⁻* mice were viable and fertile, and showed a lumbosacral transition phenotype characterized by the sacralization of the sixth lumbar vertebra. The development of the appendicular skeleton, the structure of the growth plate, chondrocyte differentiation, proliferation, and survival were normal in mutant mice. Biochemical analysis of knee cartilage demonstrated moderate alterations in the extractability of the binding partners of matrilins in *Matn1-4⁻/⁻* mice. Atomic force microscopy (AFM) revealed comparable compressive stiffness but higher collagen fiber diameters in the growth plate cartilage of quadruple mutant compared to wild-type mice. Importantly, *Matn1-4⁻/⁻* mice developed more severe spontaneous osteoarthritis at the age of 18 months, which was accompanied by changes in the biomechanical properties of the articular cartilage. Interestingly, *Matn4⁻/⁻* mice also developed age-associated osteoarthritis suggesting a crucial role of MATN4 in maintaining the stability of the articular cartilage. Collectively, our data provide evidence that matrilins are

important to protect articular cartilage from deterioration and are involved in the specification of the vertebral column.

Keywords: matrilin; cartilage; bone development; articular cartilage; osteoarthritis

1. Introduction

Endochondral bone development is a complex process which requires the differentiation of chondrocytes and the production of a tissue-specific extracellular matrix (ECM) by forming cartilaginous templates of the future bones. Cartilage ECM provides physical support for chondrocytes maintaining the integrity and biomechanical properties of the cartilage, such as resistance against tensile strength and compressive forces. The typical transient hyaline cartilage of the developing bones and the permanent articular cartilage are composed of the heterotypic type II/IX/XI collagen fibrils and proteoglycans, mainly aggrecan, and numerous multi-domain adaptor proteins, which interconnect the two macromolecular networks. Among the perifibrillar adaptor proteins, matrilins (MATN) form a subfamily of modular, non-collagenous ECM proteins consisting of four members, namely matrilin-1, -2, -3, and -4 [1]. All matrilin members share similar structures containing one (matrilin-3) or two (matrilin-1, -3 and -4) von Willebrand factor A (VWA) domains, various numbers of epidermal growth factor (EGF) like domains and a coiled-coil (CC) α-helical oligomerization module. In mice, matrilin-1 (MATN1) and matrilin-3 (MATN3) are predominantly expressed in the developing epiphyseal and growth plate cartilages [2,3], while matrilin-2 (MATN2) and matrilin-4 (MATN4), besides cartilage, are also present in various extra-skeletal tissues [4,5]. Matrilins interacts with numerous cartilage ECM components including aggrecan (ACAN) [6], collagen II [7], collagen IX [8], cartilage oligomeric matrix protein (COMP) [9] and decorin [10], thereby may interconnect and stabilize the macromolecular networks of collagen fibrils and the aggregating proteoglycan aggrecan [1,10,11].

During skeletal development, MATN1, MATN3, and MATN4 display a largely overlapping expression pattern. These matrilins are abundant in epiphyseal and growth plate cartilage, whereas MATN2 is strongly expressed in the perichondrium/periosteum and moderately in the proliferative zone of the growth plate [12,13]. At the forming articular surface, the outermost superficial cell layers express MATN2 and MATN4, whereas the deeper cell layers of the articular surface express MATN3 and MATN4 but not MATN1 [13]. In more mature articular cartilage, all matrilins are expressed at very low levels [13].

To date, the association of a human connective tissue disorder has been only identified in the genes coding for matrilin-3 and matrilin-1. Multiple epiphyseal dysplasia (MED) is a clinically and genetically heterogeneous skeletal dysplasia characterized by joint pain and stiffness, and early onset of osteoarthritis (OA). Autosomal dominant forms of MED are caused by mutations in the genes encoding matrilin-3 (MATN3), collagen IX chains (COL9A1, COL9A2 and COL9A3) and cartilage oligomeric matrix protein (COMP) [14]. The MED mutations identified in MATN3 are missense and predominantly confined to the β-sheet regions of the VWA domain [15–17]. In vitro experiments suggest that these mutations lead to the retention of the mutant MATN3 in the rough endoplasmic reticulum, where it accumulates as an unfolded intermediate and activates unfolded protein response [18–20]. In addition to MED, mutations in MATN3 have been described in bilateral hereditary micro-epiphyseal dysplasia (BHMED) [21] and spondylo-epi-metaphyseal dysplasia (SEMD) [22] patients. Furthermore, a low occurrence of linkage of *MATN3* to hand OA and spinal disc degeneration has been reported [23–25]. The association of MATN1 with osteoarthritis was described in the Dutch but not in the British population [26,27]. More recently, *MATN1* was suggested as a candidate gene for idiopathic scoliosis [28] and mandibular prognathism [29], and as a genetic modifier of SEMD with joint laxity [30].

Despite the suggested integrative functions of matrilins in the cartilage ECM, ablation of matrilin genes in mice does not lead to an overt phenotype. Single knockout mice lacking matrilin-1 (*Matn1−/−*)

or matrilin-3 (*Matn3⁻/⁻*) [31,32] were generated in our laboratory and these null mice showed no signs of chondrodysplasia or any other obvious skeletal phenotype. In contrast, subtle defects were identified in other matrilin mutant strains generated by independent laboratories. Abnormal collagen II fibrils and stiffness of the cartilage ECM were reported in the matrilin-1 deficient mice [33,34], while accelerated differentiation of embryonic hypertrophic chondrocytes in the growth plate, increased bone mineral density and higher incidence of knee osteoarthritis were found in matrilin-3 knockout mice [35]. Although, we were unable to detect these skeletal phenotypes in our single knockout lines, we have reported a mild increase of collagen fibrillar thickness in *Matn1⁻/⁻*, *Matn3⁻/⁻* and matrilin-1/matrilin-3 double deficient mice (*Matn1⁻/⁻/Matn3⁻/⁻*) by electron microscopy [36]. This finding implies that matrilin-1 and matrilin-3 may have only a minor role in the proper ultrastructural organization of collagen network in cartilage. Interestingly, matrilin-2 and matrilin-4 deficient mice, which also develop without obvious skeletal abnormalities [12,37], instead present extra-skeletal phenotypes. *Matn2⁻/⁻* mice display impaired functional recovery after femoral nerve lesion, indicating an essential role of matrilin-2 for peripheral nerve regeneration [38], while *Matn4⁻/⁻* mice show increased proliferation of hematopoietic stem cells upon myelosuppressive chemotherapy, inflammatory stress and transplantation [37].

The similar structure, function, and expression pattern of matrilins suggest compensation among the family members. Indeed, we previously demonstrated that matrilin-4 is up-regulated in the cartilage of *Matn1⁻/⁻* and *Matn1⁻/⁻/Matn3⁻/⁻* mice, providing the first experimental evidence that biochemical compensation could exist between matrilins in vivo [36]. In order to further extend our knowledge about the skeletal function of matrilins, herein we report the analysis of mice lacking all matrilins. Quadruple mutant mice (*Matn1-4⁻/⁻*) have a reduced number of lumbar vertebrae due to lumbosacral homeotic transition and osteoarthritic-like degeneration develops in mice older than 18 months. Interestingly, similar articular cartilage degeneration was observed in aged matrilin-4 deficient mice, indicating an unexpected role of matrilin-4 in protecting articular cartilage from age-associated, spontaneous osteoarthritis.

2. Results

2.1. Biochemical Compensation in Cartilage of Mice Lacking Matrilins

Previously we have demonstrated that knockout mice lacking matrilin-1 (*Matn1⁻/⁻*), matrilin-3 (*Matn3⁻/⁻*) or both matrilin-1 and matrilin-3 (*Matn1⁻/⁻/Matn3⁻/⁻*) exhibit only mild ultrastructural abnormalities of the collagenous fibrillar network of the cartilage without manifestation of any obvious skeletal defects [31,32,36]. We have also found, however, that matrilin-4 (MATN4) is upregulated in *Matn1⁻/⁻* and *Matn1⁻/⁻/Matn3⁻/⁻* mice but not in *Matn3⁻/⁻* mice in knee cartilage tissues sequentially extracted with high salt containing 10 mM ethylenediaminetetraacetic acid (EDTA) (fraction II) and 4 M guanidine hydrochloride (GuHCl) (fraction III), while matrilin-2 (MATN2) was deposited normally in those mutants compared with controls [36]. In the present study, we have analyzed further compound knockout mice lacking MATN1, MATN2 and MATN3 in various combinations (*Matn2⁻/⁻/Matn3⁻/⁻*; *Matn1-3⁻/⁻*), and we could confirm that the homotrimeric form of MATN4 was consistently upregulated in fractions II and III, but not in neutral salt extracts (fraction I) of animals lacking MATN1 and/or MATN2 (Figure 1C). MATN4 compensatory upregulation was especially prominent in mice, which lacked MATN2 in addition to MATN1 and/or MATN3, such as *Matn2⁻/⁻/Matn3⁻/⁻* and *Matn1-3⁻/⁻* mice. Importantly, these multiple knockouts including the triple mutant *Matn1-3⁻/⁻* mice had normal gross skeleton and displayed normal growth plate and articular cartilage histoarchitectures at birth and at various postnatal stages (Figure 1A,B and not shown). Similarly, mice lacking MATN4 developed a normal skeleton without apparent abnormalities of the zonal and columnar structure of the cartilaginous growth plate of the long bones (Figure 1D). Interestingly, immunohistochemical staining revealed an upregulation of MATN2 deposition in the proliferative and hypertrophic zones of the newborn growth plate cartilage in *Matn4⁻/⁻* mice (Figure 1E). Using Western blots, we could confirm stronger signals for MATN2 in fractions II/III of matrilin-4 mutant cartilage extracts compared with wild type, while the levels of MATN1 and MATN3 did

not change significantly (Figure 1F). The expression of *Matn2* at mRNA levels was comparable between control and *Matn4⁻/⁻* mice in newborn limb cartilage (data not shown). Collectively, our data demonstrate that MATN2 and MATN4 biochemically compensate for the lack of MATN4 and MATN1, respectively, in the newborn mouse knee cartilage.
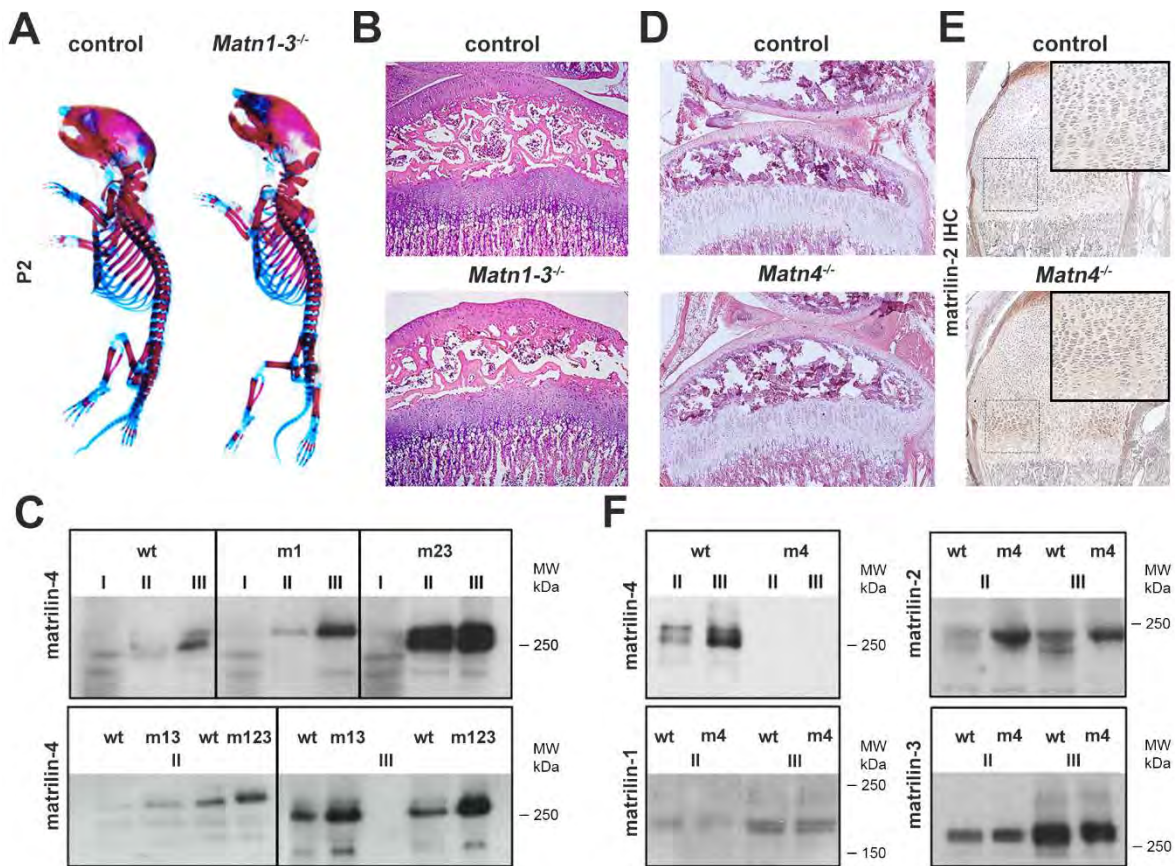

Figure 1. Biochemical compensation among matrilins. (**A**) Whole-mount skeletal staining at postnatal day 2 (P2) shows no obvious skeletal defects in mice lacking matrilin-1, -2 and -3 (*Matn1-3⁻/⁻*) compared to wild type. (**B**) HE staining of the proximal tibia (original magnification × 10) of the knee joint indicates normal growth plate and articular cartilage structures in *Matn1-3⁻/⁻* mice at 4 weeks of age. (**C**) Western blot analyses of sequential cartilage extracts (I-neutral salt; II-high salt/EDTA; III-GuHCl) from newborn mice indicates upregulation of matrilin-4 in mice lacking matrilin-1 (m1), matrilin-2 and -3 (m23), matrilin-1 and -3 (m13), and matrilin-1, -2, and -3 (m123). (**D**) HE staining of the proximal tibia (original magnification × 10) of the knee joint at 4 weeks of age demonstrates that mice lacking matrilin-4 (*Matn4⁻/⁻*) have a normal structure of long bones. (**E**) Immunohistochemistry (IHC, original magnification × 10) indicates the increased deposition of matrilin-2 in the growth plate of the humerus (rectangle, original magnification × 20) of *Matn4⁻/⁻* mice. (**F**) Western blot analyses show increased amounts of matrilin-2 in cartilage extracts of *Matn4⁻/⁻* mice (m4), while the levels of matrilin-1 and matrilin-3 are unchanged. Abbreviation: MW-molecular weight marker.

2.2. Loss of Matrilins Results in Modulation of Lumbosacral Identity of the Vertebrae

In order to assess the role of matrilins in skeletal development, we have generated quadruple knockout mice lacking all members of the protein family (*Matn1-4⁻/⁻*). Homozygous mutant breeding revealed normal litter size with offspring, which had normal life span and developed no apparent gross abnormalities. However, we have noticed by regular inspection of the cages, that *Matn1-4⁻/⁻* mice showed reduced fear and anxiety when they were picked up by the tail and, in general, were physically less active and motile in the cage compared with control mice. In this study, we have focused on the skeletal analysis of the mice, therefore, the behavioural abnormalities were not investigated further. Alcian blue and alizarin red double whole-mount skeletal staining of mutant

and wild-type (control) mice at postnatal day 2 (P2) showed normal formation of the elements of the appendicular skeleton (Figure 2A). Closer inspection of the long bones on skeletal preparations or X-ray micrographs demonstrated very moderate but significantly increased lengths of the tibia, femur, and the humerus at P2 in the *Matn1-4⁻/⁻* mice compared with control mice ($p < 0.05$). However, the lengths of these skeletal elements were comparable at the ages of four weeks and four months (Figure 2A,C,E). Similarly, the whole body length (the distance between the nose and the tip of the tail) was comparable between wild-type and *Matn1-4⁻/⁻* animals at four weeks and four months of age (Figure 2F).
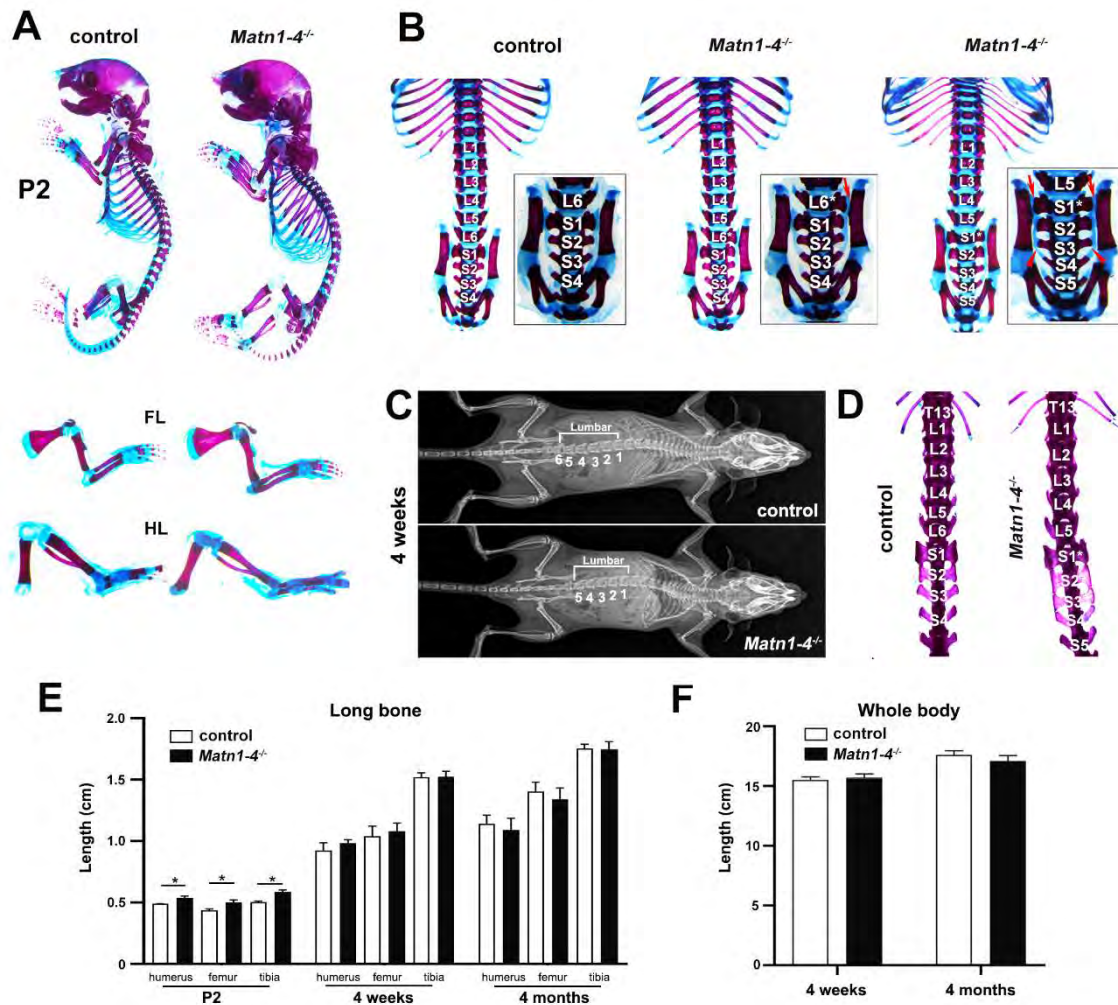

Figure 2. Skeletal phenotype in mice lacking all matrilins. (**A**) Skeletal staining at P2 showed normal formation of the elements of the appendicular skeleton. (**B–D**) Skeletal staining and X-ray analyses at P2 and 4 weeks of age revealed a highly penetrant homeotic transformation at the lumbar-sacral border of the axial skeleton. (**B**) Wild-type (control) mice have 6 lumbar (L1 to L6) and 4 sacral (S1 to S4) vertebrae, S1 articulates to the ilium and S1-S2-S3 are fused. In *Matn1-4⁻/⁻* mice, L6 is sacralized (S1*) resulting in 5 lumbar (L1 to L5) and 5 sacral vertebrae (S1 to S5). In the mutants, the sacralized L6 vertebra (S1*) gained the typical S1 wing shape (red arrows on B), S1* and S2 are articulate to the ilium and S1*/S2/S3/S4 are fused. The arrowheads depict the fusion between S3 and S4. The heterozygous offspring exhibit an intermediate pattern with only one side of L6 is sacralized (L6*) by gaining a wing-shaped transverse process and articulating to the ileum (L6*, red arrow), while the other side retained the lumbar identity. (**C**) Representative X-ray images of wild-type and *Matn1-4⁻/⁻* mice at 4 weeks. (**D**) Skeletal preparations at 4 weeks demonstrate the sacralization of L6 in the quadruple KO mice. (**E**) Measurements of the lengths of the appendicular skeletal elements indicate a moderate but significantly increased size of mutant long bones at P2. At 4 weeks and 4 months, there is no significant difference between the genotypes. Statistical significance calculated by Mann-

Whitney *U* test where * *p* < 0.05. (**F**) Comparable body length of wild-type and *Matn1-4⁻/⁻* animals at 4 weeks and 4 months of age. Abbreviations: FL-forelimb; HL-hindlimb.

In contrast to the appendicular skeleton, skeletal staining and X-ray analyses revealed a highly penetrant homeotic transformation at the lumbar-sacral border of the axial skeleton (Figure 2B–D). The mouse axial skeleton typically consists of 30 pre-caudal vertebrae including 7 cervical (C), 13 thoracic (T), 6 lumbar (L) and 4 sacral (S) ones giving the formulation of C7/T13/L6/S4 [39,40]. We found that 87.5% of *Matn1-4⁻/⁻* mice have five lumbar and five sacral vertebrae (C7/T13/L5/S5), while only 6.7% of wild-type animals presented this vertebral pattern (Figure 2B,C and Table 1). Apparently, the missing L6 vertebrae in the *Matn1-4⁻/⁻* mice gained a sacral identity (S1* in Figure 2B,D) resulting a sacral pattern of S1*/S2/S3/S4/S5. In control, S1 articulates to the ilium, S1/S2 acquire wing-shaped transverse processes and S1/S2/S3 are fused. In the mutants, the sacralized L6 vertebra (S1*) and the true S1 (now S2) articulate to the ileum (red arrows on Figure 2B), S1*/S2/S3 have wing-shaped transverse processes and S1*/S2/S3/S4 are fused. Interestingly, when a *Matn1-4⁻/⁻* male was crossed with a C57/BL6 female, the heterozygous offspring exhibited either the normal L6/S4 pattern (three out of seven mice), the homeotic transformed L5/S5 pattern (two out of seven) or an intermediate, asymmetric L6*/S4 pattern (two out of seven mice). In the latter case, only one side of L6 is sacralized (L6*) by gaining a wing-shaped transverse process and articulating to the ileum (Figure 2B, *Matn1-4⁺/⁻*, L6*, arrows), while the other side retained the lumbar identity.

Table 1. Axial skeletal phenotypes in the respective genotypes.

Lumbosacral Pattern	Control (*n* = 45)	*Matn1-4⁺/⁻* (*n* = 7)	*Matn1-4⁻/⁻* (*n* = 40)
L6/S4	42 (93.3%)	3 (42.8%)	6 (12.5%)
L6*/S4	0	2 (28.6%)	0
L5/S5	3 (6.7%)	2 (28.6%)	34 (87.5%)

2.3. Lack of Matrilins Has No Adverse Effect on Structural and Functional Properties of the Cartilaginous Growth Plate in Long Bones

Next, we examined long bone development by histological tools at various developmental stages. Hematoxylin and eosin (HE) staining of the hindlimb at embryonic day 15 (E15) demonstrated that the length of the whole tibia and percentage of the hypertrophic zone relative to the entire cartilaginous mass were similar in *Matn1-4⁻/⁻* and control animals (Figure 3A,B). At E18, the proximal tibia exhibited comparable columnar organization of the growth plate (Figure 3C) and similar length of the proliferative and hypertrophic zones in control and *Matn1-4⁻/⁻* mice (Figure 3D). Similarly, the mineralization of the primary ossification center, judged by Safranin orange-von Kossa staining (Figure 3E), and the resorption at the chondro-osseous junction, visualized by tartrate resistant acid phosphatase (TRAP) activity staining (Figure 3F), were indistinguishable between control and quadruple mutant animals. At postnatal stage two weeks, the columnar organization of the growth plate was normal, and morphometric measurements of the lengths of the resting, proliferative and hypertrophic zones and the total growth plate showed no statistically significant difference between control and *Matn1-4⁻/⁻* mice (Figure 3G,H).

Chondrocyte differentiation was investigated in the growth plate of newborn tibia by in situ hybridization. We found no difference in the expression domains of the typical differentiation markers between control and *Matn1-4⁻/⁻* mice (Figure 4A). It has been previously suggested that matrilin-3 inhibits chondrocyte hypertrophy by suppressing BMP-2/SMAD-1 signaling [41]. Therefore, we have investigated the activation of SMADs in protein extracts of primary mouse chondrocytes isolated from newborn rib cages using a phospho-specific antibody. Western blotting displayed similar phospho-SMAD-1/5/8 levels between the genotypes (Figure 4B,C), arguing against significantly altered BMP-2 signaling in cartilage lacking matrilins.
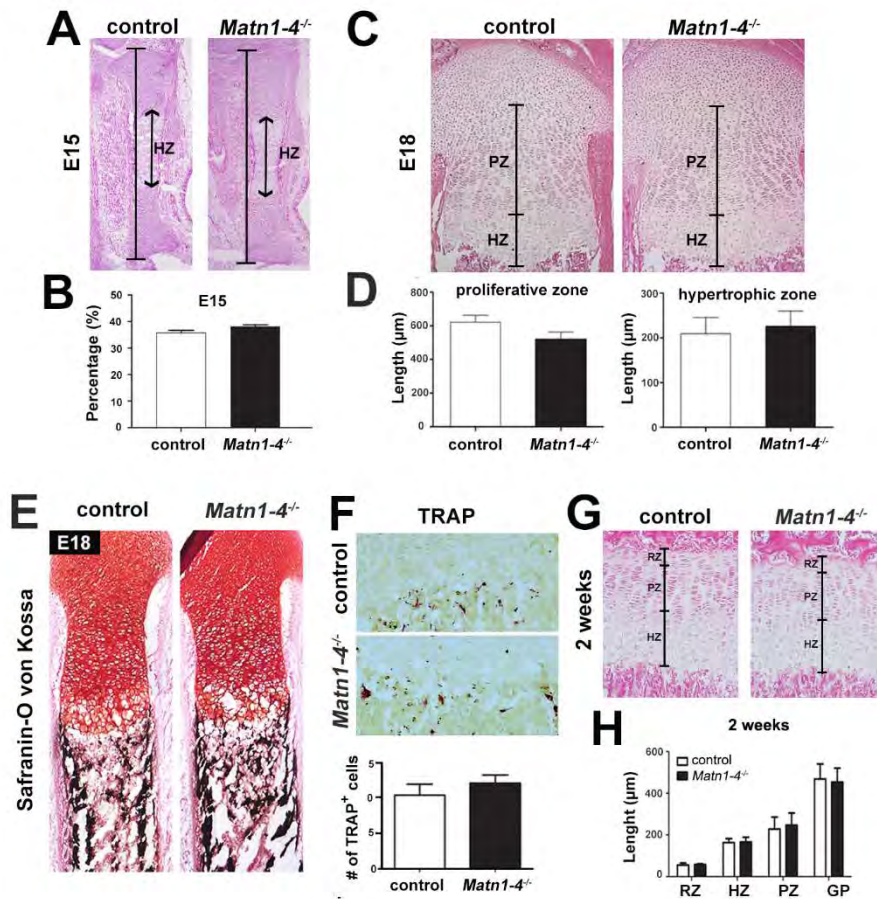
Figure 3. Normal cartilage development and growth plate structure in long bones of *Matn1-4⁻/⁻* mice. (**A**) HE-stained proximal tibiae at E15.5 show normal length, structure and hypertrophic zone (HZ) in *Matn1-4⁻/⁻* mice. (**B**) Percentage of the hypertrophic zone relative to the entire cartilaginous mass of the tibia was similar in *Matn1-4⁻/⁻* and in the control animals. (**C**) HE-stained proximal tibiae at E18 and morphometric measurements of the proliferative (PZ) and hypertrophic (HZ) zones (**D**) demonstrate normal structure of the growth plate in the *Matn1-4⁻/⁻* mice. Safranin O-von Kossa (**E**) and TRAP staining (**F**) show comparable mineralization and chondroclast/osteoclast activity at the chondro-osseous junction in control and *Matn1-4⁻/⁻* mice. Quantification of the TRAP positive cells in the tibial growth plate of control and *Matn1-4⁻/⁻* mice shows no difference at the chondro-osseous junction. (**G**) HE-staining of the tibial growth plate at 2 weeks and morphometric analysis (**H**) of the length of the entire growth plate (GP) and the separated growth plate zones (RZ-resting; PL-proliferative; HZ-hypertrophic) indicate normal columnar organization of the chondrocytes and normal GP zonality in *Matn1-4⁻/⁻* mice. Original magnifications: × 10 for (**A**), (**C**) and (**E**); x 20 for (**F**) and (**G**).

Next, we analyzed the proliferation and survival of the chondrocytes in the tibial growth plate. Proliferation was assessed by bromodeoxyuridine (BrdU) incorporation assays, which revealed a similar proliferation rate in control and *Matn1-4⁻/⁻* mice at the newborn stage (Figure 4D,E) or at four and eight weeks of age (data not shown). We further investigated cell death by terminal deoxynucleotidyl transferase dUTP nick end labeling (TUNEL) assay in newborn samples and found comparable numbers of apoptotic chondrocytes at the chondro-osseous junctions in both control and quadruple mutant mice (Figure 4F,G).

Collectively, the data above demonstrate that chondrocyte differentiation, proliferation, and survival occur normally in the growth plate of long bones in mice lacking all matrilins.
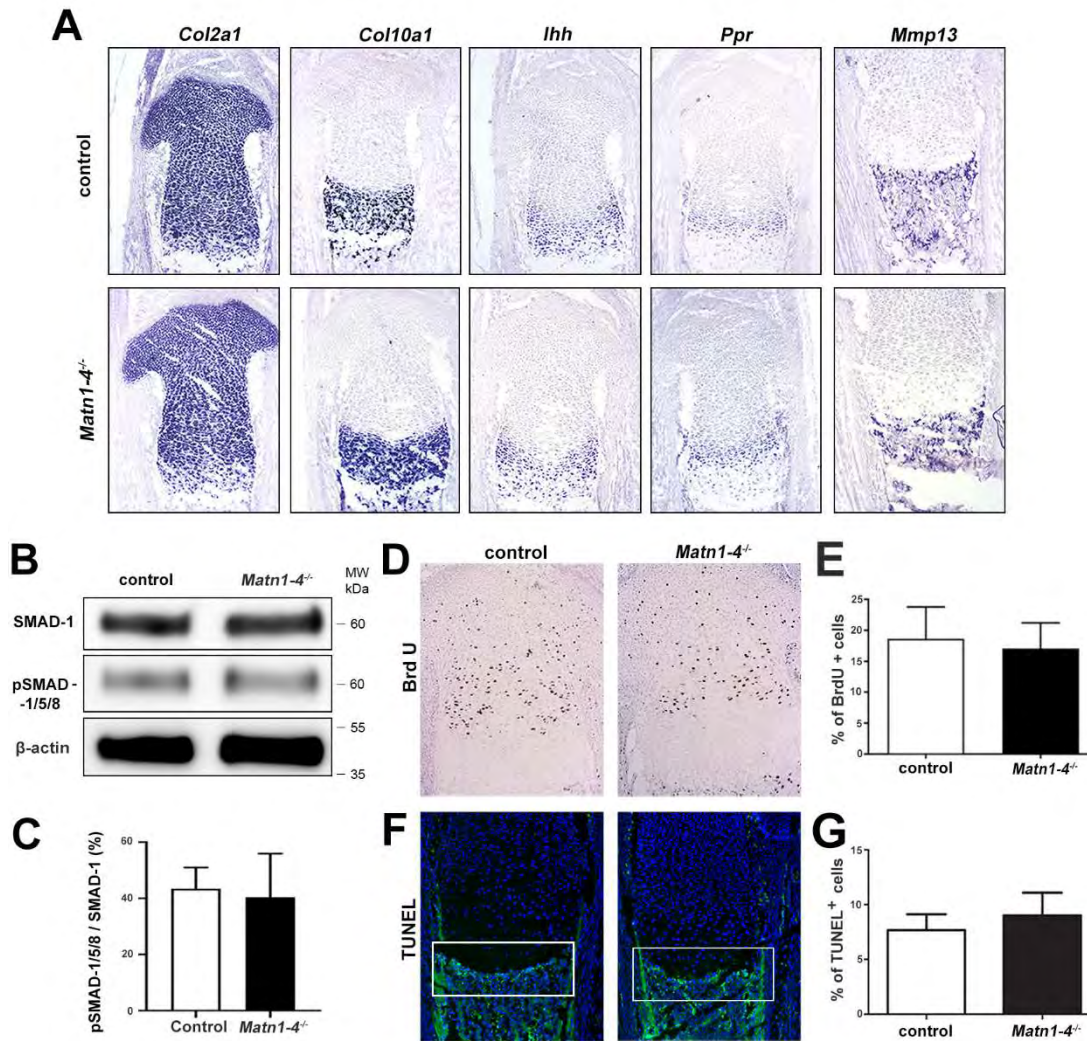
Figure 4. Chondrocyte differentiation, proliferation and apoptosis are not altered in *Matn1-4⁻/⁻* mice. (**A**) Non-radioactive in situ hybridization for collagen II (*Col2a1*), collagen X (*Col10a1*), indian hedgehog (*Ihh*), PTH/PTHrP receptor (*Ppr*) and matrix metalloproteinase-13 (*Mmp13*) show similar expression pattern in newborn control and mutant mice. Western blotting (**B**) and densitometric quantification (**C**) indicate normal activation of SMAD-1/5/8 in mutant primary chondrocytes. (**D**) BrdU incorporation assay and quantification (**E**) at the newborn stage indicate normal chondrocyte proliferation in the *Matn1-4⁻/⁻* growth plate. TUNEL staining (**F**) and quantification (**G**) do not reveal any difference in cell death at the chondro-osseous junctions (white boxes) in newborn control and *Matn1-4⁻/⁻* mice. Abbreviation: MW-molecular weight marker. Original magnifications: × 10 for (**A**), (**D**) and (**F**).

2.4. Normal Deposition but Altered Extractability of Binding Partners in the Cartilage ECM of Quadruple Knockout Mice

As matrilins are adaptor proteins of the cartilage ECM interacting with aggrecan, COMP, collagen fibrils, and small leucine-rich proteoglycans (e.g., biglycan and decorin) [1], we have investigated the expression and anchorage of some of these binding partners by immunohistochemistry and biochemical analysis. Immunostaining of the proximal tibia in newborn or four-week old limbs indicated no apparent differences in the deposition of collagen II, collagen VI, collagen IX, aggrecan and COMP between control and *Matn1-4⁻/⁻* mice (Figure 5A,B). Western blot analysis of sequential extracts of knee cartilage isolated from newborn animals showed slightly increased extractability of collagen II, collagen IX, aggrecan, collagen VI and COMP in fraction I (neutral salt) of *Matn1-4⁻/⁻* mice, when compared to wild-type controls. While the amount of matrilin

interacting proteins did not change in fraction II (high salt with 10 mM EDTA), weaker signals for collagen II, collagen IX, and COMP were detected in fraction III (4 M GuHCl) isolated from the cartilage of quadruple knockout mice compared with controls (Figure 5C). At four weeks, the amount of aggrecan increased in all fractions, the amount of collagen IX slightly increased in fraction II, and the amount of COMP moderately decreased in fraction III in *Matn1-4*^{–/–} mice compared to control (Figure 5D).
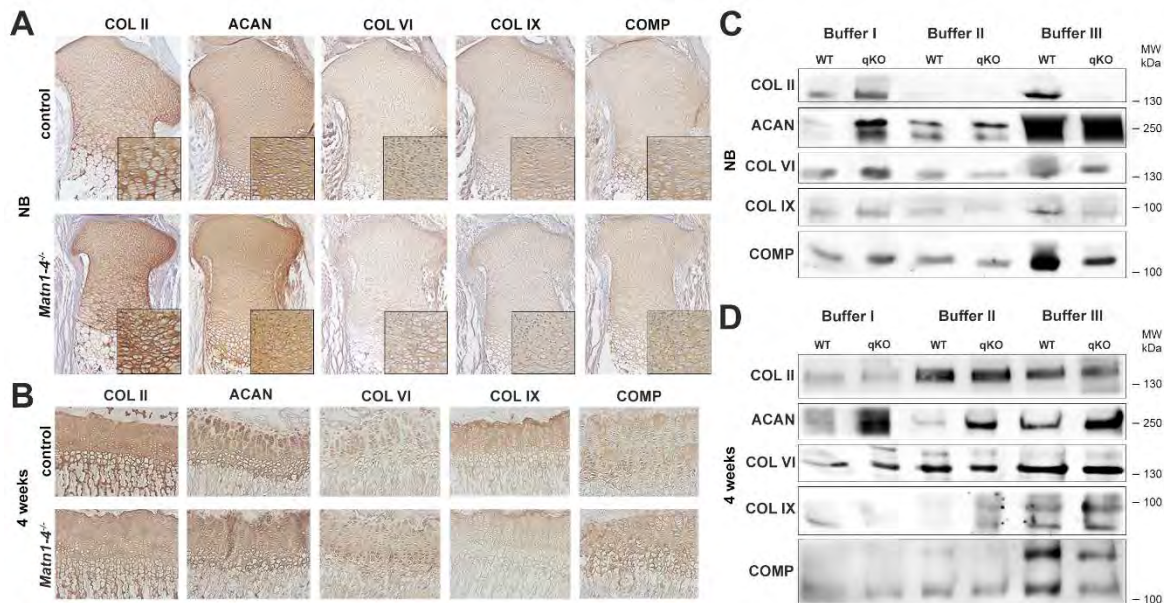

Figure 5. Immunohistochemical and biochemical analysis of the deposition and solubility of the binding partners of matrilins. Immunohistochemistry at newborn (**A**) and 4 weeks (**B**) stages indicates no apparent differences in the deposition of collagen II (COL II), collagen VI (COL VI), collagen IX (COL IX), aggrecan (ACAN) and cartilage oligomeric matrix protein (COMP) between control and *Matn1-4*^{–/–} mice. Original magnifications: × 10 for (**A**) and (**B**); x 20 for inserts in (**A**). Western blot analysis of cartilage extracts in newborn (**C**) and 4 weeks old (**D**) animals. In newborn, slightly increased extractability of collagen II, collagen IX, aggrecan, collagen VI and COMP in buffer I and significantly weaker signals for collagen II, collagen IX and COMP were detected in fraction III isolated from the cartilage of quadruple knockout mice compared with controls (**C**). At 4 weeks, the amount of aggrecan is increased in all fractions, the amount of collagen IX is slightly increased in fraction II and the amount of COMP is moderately decreased in fraction III in M *Matn1-4*^{–/–} mice compared with the control (**D**). Abbreviation: MW-molecular weight marker.

To assess the consequence of the lack of matrilins on the ultrastructural and biomechanical properties of the cartilaginous ECM, we applied atomic force microscopy (AFM) (Figure 6). We investigated the proliferative zone of the growth plate at two weeks of age on non-fixed, native sections and recorded high resolution images of the interterritorial matrix (ITM) representing the intercolumnar areas. Topographical images revealed an elaborated network of collagen fibrils in both control and *Matn1-4*^{–/–} mice (Figure 6A). Quantification of the diameter of heterotypic collagen fibrils revealed a significantly increased thickness of the fibers (Figure 6B), similar to the results reported earlier in *Matn1*^{–/–}/*Matn3*^{–/–} mice [36]. The mean fibril diameter was 45.64 ± 7.29 nm in control and 61.50 ± 12.38 nm in *Matn1-4*^{–/–} mice ($p < 0.001$). Interestingly, nanoindentation measurements indicated comparable compressive stiffness of the ITM. The frequency of the elastic moduli showed a bimodal distribution with a first peak (representing the proteoglycan moiety) at 45.17 ± 0.93 kPa in controls and at 47.91 ± 0.34 kPa in quadruple mutants, and with a second peak (representing the collagen fibrils) at 61.46 ± 7.79 kPa in controls and 59.48 ± 2.14 kPa in *Matn1-4*^{–/–} mice (Figure 6C).
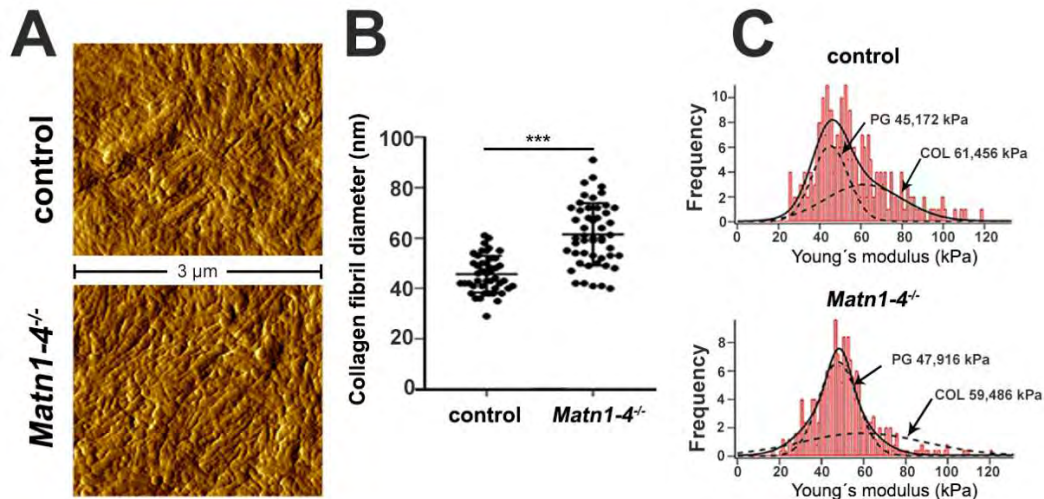
Figure 6. Normal growth plate cartilage stiffness but altered fibril diameter in *Matn1-4⁻/⁻* mice. (**A**) At 2 weeks of age, high-resolution AFM images on tibial sections show comparable organization of the collagenous networks in the interterritorial matrix in control and the mutant animals. (**B**) Quantification of the fibrillar diameter demonstrates significant thickening of the collagen fibrils in the *Matn1-4⁻/⁻* mice (*** $p < 0.001$). (**C**) Histograms depicting a comparable, bimodal stiffness distribution between the genotypes determined by nano-scale AFM indentation. On each histogram, the solid line represents the sum of two Gaussian functions, whereas the dashed lines indicate individual fits representing proteoglycans (first peak, PG) and the collagen fibrils (second peak, COL).

Taken together, although the expression and distribution of the analyzed matrilin binding partners were not obviously altered in the growth plate cartilage of *Matn1-4⁻/⁻* mice, the solubility of these proteins in the ECM is moderately affected by the loss of all matrilins. Despite this mild biochemical phenotype and the increased diameter of collagen fibrils, the biomechanical behavior of the cartilage ECM, characterized by the compressive stiffness, is apparently not affected in the growth plate of adolescent *Matn1-4⁻/⁻* mice.

2.5. Depletion of All Matrilins in the Articular Cartilage Leads to Severe Spontaneous Osteoarthritis in Mice

Next, we analyzed the consequence of the ablation of matrilin genes on age-associated changes of the articular cartilage. All matrilins are expressed in low amounts in peripheral articular cartilage areas of the knee joint in wild-type mice at one year of age (Figure 7A) [13]. We examined articular cartilage degeneration on HE-stained sections of control and *Matn1-4⁻/⁻* knee joints at six, 12, and 18 months of age. We found no difference in articular cartilage degradation between the genotypes at six months of age (data not shown), however, histological signs of articular cartilage damage were observed in *Matn1-4⁻/⁻* mice at 12 and 18 months of age (Figure 7B). Applying a scoring system for articular cartilage degradation, ranging from normal appearance (score 0) to exposure of the subchondral bone (score 5) [36], the mean histological score was 1.4 for control (*n* = 8) and 2.5 for *Matn1-4⁻/⁻* mice (*n* = 10) at 12 months of age. At 18 months of age, the mean histology score was 1.3 for control (*n* = 8) and 2.7 for mutant mice (*n* = 11) ($p < 0.05$) (Figure 7C). These results demonstrate that the lack of the complete matrilin family in cartilage leads to an osteoarthritic-like phenotype in aging mice from one year on, and strongly suggest that matrilins are protective for spontaneous osteoarthritis.

Analyzing the expression of matrilins in healthy and osteoarthritic human knee cartilage by immunohistochemical staining further supported the participation of matrilins in OA progression (Figure 7D). In normal human articular cartilage, matrilins are weakly expressed in the middle and deep zones: MATN1 is localized to the nucleus; MATN2 and MATN4 are associated with the cytoplasm and diffusely with the ECM; while MATN3 displays mainly pericellular/territorial matrix deposition. All matrilins are upregulated in human OA cartilage samples with severe articular

cartilage degeneration (Figure 7D), which may implicate an attempt of repair by enhancing the expression of matrilin family members in the diseased ECM.
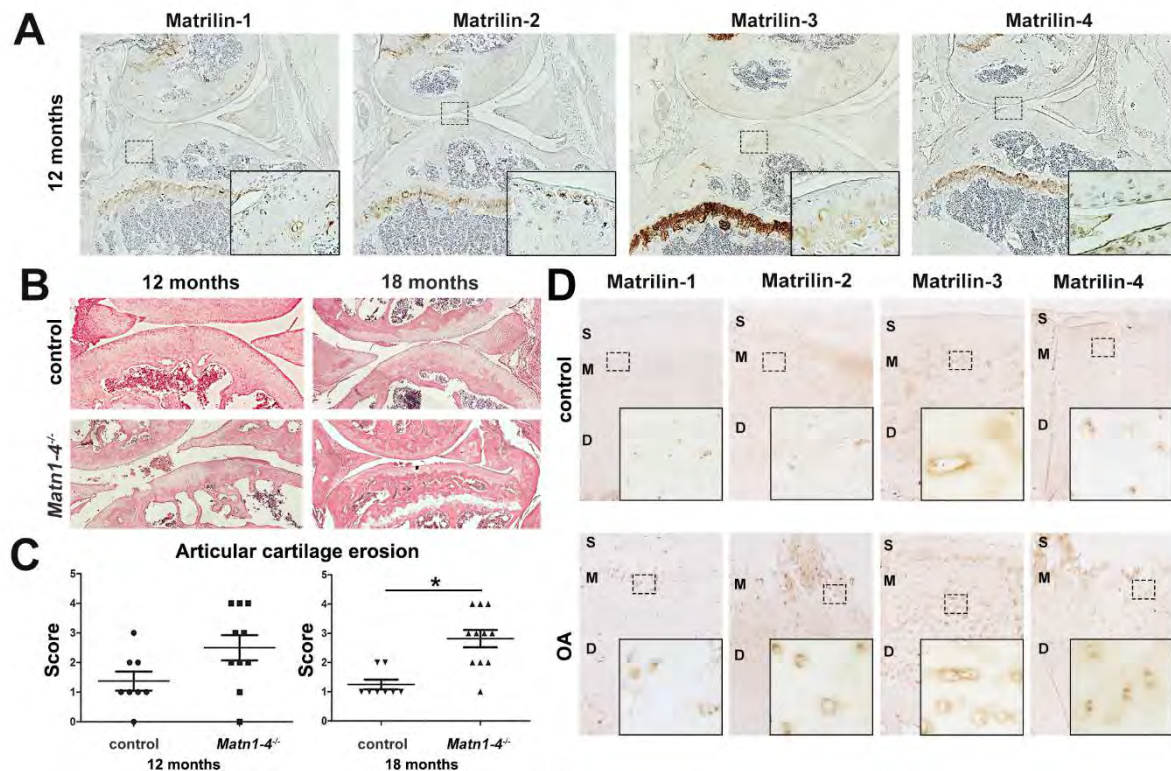

Figure 7. *Matn1-4−/−* mice develop age-associated osteoarthritis. (**A**) Immunohistochemistry of knee joints demonstrates the moderate expression of matrilins in the articular cartilage of wild-type mice at 12 months of age. All matrilins have strong expression in the growth plate cartilage. Original magnifications: × 5 for overview pictures and x 20 for inserts. (**B**) HE staining of the knee joint at 12 and 18 months old control and *Matn1-4−/−* mice. Original magnification × 10. (**C**) Histological grading for cartilage degradation indicates higher incidence and severity of osteoarthritic-like erosion in *Matn1-4−/−* mice compared to age-matched controls (* *p* < 0.05). (**D**) Analyzing the expression of matrilins in healthy (control) and osteoarthritic human knee articular cartilage derived from the tibia by immunohistochemistry demonstrates upregulation of all matrilins in the OA tissue. The depicted zones: S-superficial; M-middle and D-deep. Original magnifications: × 5 for overview pictures and x 20 for inserts.

The increased severity of spontaneous osteoarthritis in the *Matn1-4−/−* mice might be a consequence of the compromised biomechanical properties of the articular cartilage ECM. Therefore, we have investigated the topography and stiffness of the different articular cartilage zones by AFM on native tissue sections in quadruple mutant and control animals. High-resolution images at four months depicted the well-formed, striated collagen fibrillar network in both genotypes (Figure 8A). Quantification of the collagen fibril diameters revealed fibril thickening in the *Matn1-4−/−* mice (Figure 8B) supporting the findings observed in the growth plate collagen fibrils. In the middle zone, the mean fibrillar diameter was 81.07 ± 17.23 nm in control and 95.31 ± 16.76 nm in *Matn1-4−/−* mice (*p* < 0.01). In the deep zone, the mean fibrillar diameter was 75.52 ± 14.88 nm in control and 93.22 ± 14.71 nm in *Matn1-4−/−* mice (*p* < 0.001). AFM nanoindentation in the superficial, middle and deep zones of the articular cartilage showed bimodal stiffness distribution for proteoglycans and collagen fibrils. At four months of age, we observed a stiffer superficial zone in the mutant compared with wild type, while the elastic moduli in the middle and deep zone were not changed significantly (Figure 8C). At 12 months, in contrast, both peaks of the elastic moduli indicated softer superficial and middle zones

in the quadruple knockout mice compared to control (Figure 8D). Interestingly however, the deep zone was stiffer in the mutant articular cartilage than in the control (Figure 8D).
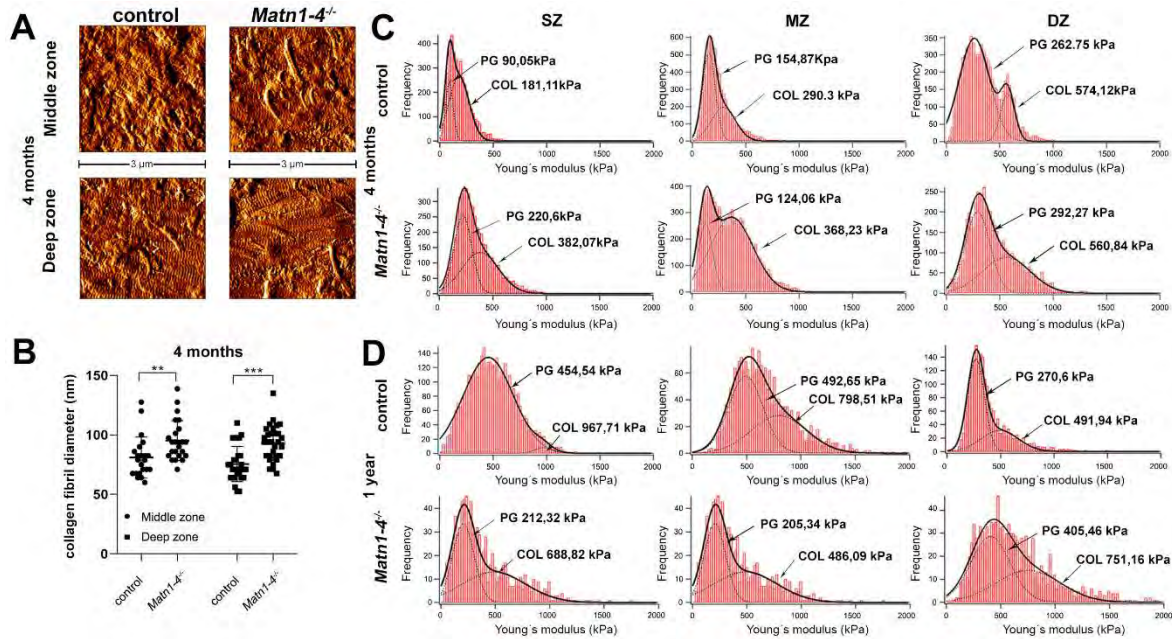

Figure 8. Altered biomechanical properties of articular cartilage in *Matn1-4⁻/⁻* mice. High resolution AFM images of articular cartilage at 4 months (**A**) showed comparable organization of the collagenous networks in control and mutant. (**B**) Significant thickening of the collagen fibrils was detected in the middle (** *p* < 0.01) and the deep zones (*** *p* < 0.001) of the articular cartilage of *Matn1-4⁻/⁻* mice. (**C**) Nanoindentation AFM demonstrated stiffer mutant matrix in the superficial zone (SZ) at four months. (**D**) At 1 year, softer ECM was detected in the superficial and middle (MZ) zones, whereas a stiffer matrix was observed in the deep zone (DZ) of the *Matn1-4⁻/⁻* mice. On each histogram, the solid line represents the sum of two Gaussian functions, whereas the dashed lines indicate individual fits representing proteoglycans (first peak, PG) and the collagen fibrils (second peak, COL).

To investigate whether matrilins may play a role in inflammation-mediated articular cartilage degradation, we performed an ex vivo explant culture experiment in which femoral heads were subjected or not to the influence of the pro-inflammatory cytokine interleukin-1 alpha (IL-1α). After four days in culture, the explants were investigated for proteoglycan loss by Safranin O staining on histological sections and for sulfated glycosaminoglycan (GAG) release into the medium (Figure 9A,B). Both the histochemical staining and the GAG-release assay indicated no difference in IL-1α—induced proteoglycan loss between the genotypes.
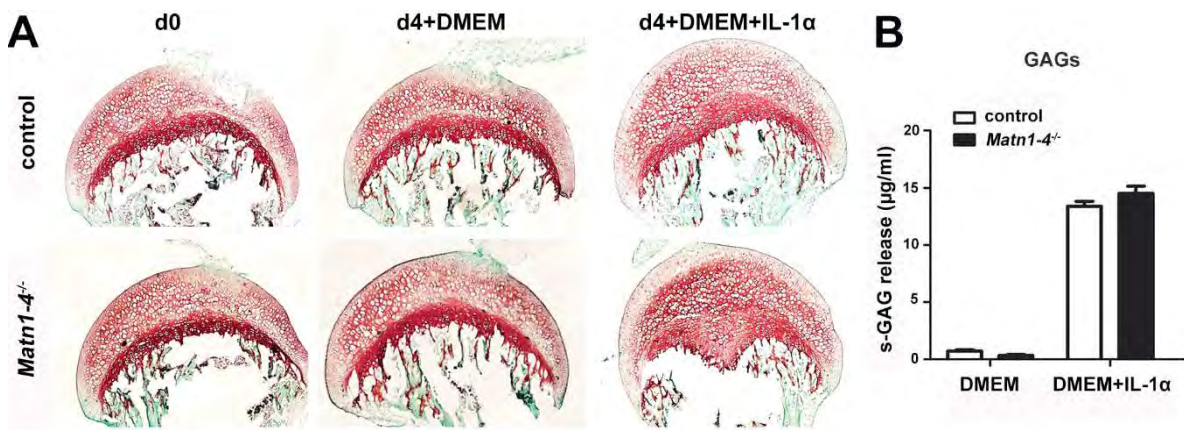

Figure 9. Matrilins are not involved in the interleukin-1-mediated proteoglycan loss of the articular cartilage. (**A**) Safranin-O and Fast Green staining of hip explants after culturing for 4 days (d4) with

or without 10 ng/mL IL-1α. Note the similar loss of proteoglycans at the articular cartilage surface after IL-1α stimulation in control and *Matn1-4$^{-/-}$* mice. (**B**) Quantification of the sulfated GAG release into the medium shows no difference after IL-1α stimulation between the genotypes.

2.6. MATN4-Deficiency Also Enhances Age-Associated Articular Cartilage Degradation

The development of spontaneous osteoarthritis in aged *Matn1-4$^{-/-}$* mice raised the question about the contribution of the individual matrilins to the phenotype. Previously, we had not observed age-associated osteoarthritis in single MATN1, MATN2, MATN3, or double MATN1/MATN3 deficient mice [12,31,32,36]. However, the MATN4 knockout mice (*Matn4$^{-/-}$*) have not been yet analyzed for articular cartilage degeneration. Thus, we investigated the pathology of the knee joint in 18–24 month old Matn4$^{-/-}$ mice on HE-stained histological sections (Figure 10). *Matn4$^{-/-}$* animals, similar to the *Matn1-4$^{-/-}$* mice, exhibited severe osteoarthritis-like phenotype at the age of 24 months often leading to complete erosion of the articular cartilage and exposure of the subchondral bone (Figure 10A). We found that the mean articular cartilage degeneration score was 1.70 in wild-type mice and was 3.67 in the *Matn4$^{-/-}$* mice ($p < 0.001$) (Figure 10B), implying that MATN4 may protect against osteoarthritis. Interestingly, immunohistochemistry demonstrated that the deposition of MATN2 and MATN3, but not the expression of MATN1, is upregulated in the articular cartilage of the knee joint of aged mice (Figure 10C).

Figure 10. The lack of matrilin-4 leads to age-associated, spontaneous osteoarthritis of the knee joint. (**A**) HE-stained *Matn4$^{-/-}$* knee joint (original magnification × 10) at 24 months of age exhibited severe osteoarthritis-like phenotype and (**B**) a significantly higher articular cartilage degeneration score compared to wild type (*** $p < 0.001$). (**C**) Immunohistochemistry demonstrates upregulated

expression of MATN2 and MATN3 in MATN4-deficient articular cartilage. Original magnifications: × 10 for overview pictures and x 20 for inserts.

3. Discussion

Cartilage extracellular matrix consists of macromolecular suprastructures containing the aggregates of aggrecan and hyaluronan, which are embedded into the network of collagen types II/IX/XI fibrils [42,43]. In order to fulfil biological and biomechanical functions, these macromolecular assemblies are interconnected and stabilized by various adaptor proteins including the FACIT (fibril associated collagen with interrupted triple helices) collagen type IX, family members of thrombospondins (e.g., COMP or thrombospondin-5), small leucine-rich repeat proteoglycans (e.g., decorin and biglycan) and matrilins [8,10,11]. Matrilins are von Willebrand factor A domain containing multi-subunit adaptors with prominent expression in the skeleton, especially in the cartilage [1,13]. All matrilins (MATN1, MATN2, MATN3 and MATN4) are expressed in the growth plate and the articular surface suggesting important roles for both developing, transient and permanent cartilages [1,13]. Despite the anticipated importance of matrilins in the cartilaginous skeleton, no or relatively mild cartilage abnormalities have been reported in knockout mice carrying single or double deletions for matrilin genes, suggesting functional redundancy among the family members [12,32,33,36]. In this study, we have generated and analyzed further single and compound matrilin-deficient mouse lines. We found evidence for biochemical compensation within the matrilin family, which showed that matrilins are important for patterning of the vertebral column and they, especially MATN-4, protect articular cartilage against spontaneous, age-associated osteoarthritis.

Sequential extraction of cartilage tissue is a well-established biochemical tool to assess the protein expression and ECM anchorage of matrilins, and to test their possible compensatory regulations [44]. MATN1 and MATN3 are largely insoluble and require strongly denaturing agent, like 4M GuHCl (buffer III), to be extracted from the tissue, while MATN2 and MATN4 can be partially extracted by milder buffers (e.g., high salt/EDTA, buffer II) [36,44]. We have previously shown by immunoblotting [36] and reproduced in this study (Figure 1C) that MATN4 is upregulated in buffers II and III in mouse strains lacking the matrilin-1 protein (*Matn1*$^{-/-}$ and *Matn1*$^{-/-}$/*Matn3*$^{-/-}$). We found even higher level of MATN4 upregulation when MATN2 was additionally missing in the cartilage of *Matn2*$^{-/-}$/*Matn3*$^{-/-}$ and *Matn1-3*$^{-/-}$ mice (Figure 1C). Numerous non-skeletal tissues co-express MATN2 and MATN4, including the brain, the eye, and the lung. Interestingly, in a previous study, we could not observe a similar upregulation of MATN4 protein in extracts of those tissues in *Matn2*$^{-/-}$ mice [12]. However, an increased level of *Matn4* mRNA was reported in damaged sciatic nerves of *Matn2*$^{-/-}$ mice compared with control [38]. As we did not find enhanced *Matn4* mRNA expression in cartilage of *Matn1*$^{-/-}$, *Matn3*$^{-/-}$, *Matn1*$^{-/-}$/*Matn3*$^{-/-}$ [36] and *Matn1-3*$^{-/-}$ mice (data not shown), our data implicate that MATN4 may exhibit compensatory upregulation for MATN2 only at protein levels, and specifically in cartilage. Importantly, we showed in this study that only MATN2 is upregulated in cartilage of *Matn4*$^{-/-}$ mice, while the protein levels of MATN1 and MATN3 were unchanged in matrilin-4-deficient mice compared with control (Figure 1E,F). Taken together, accumulated evidence from our previous [36] and current studies demonstrate that MATN2 and MATN4 compensate each other mutually at the protein level in mouse cartilage tissue.

The prominent expression of matrilins in the developing long bones and the chondrodysplasia phenotypes associated with dominant-negative mutations of the human *MATN3* gene suggest a role of matrilins for skeletal growth. We showed previously that mice lacking MATN1, MATN2, MATN3 and MATN1/MATN3 have normal skeleton, probably due to functional redundancy of the family members [12,31,32,36]. The lack of obvious cartilage abnormalities in *Matn4*$^{-/-}$ (Figure 1D) and *Matn1-3*$^{-/-}$ mice (Figure 1A,B) further support this hypothesis, which prompted us to analyze skeletal development and cartilage functions in details in mice lacking all matrilins. Surprisingly, *Matn1-4*$^{-/-}$ mice show normal growth indicated by the comparable body weights and the similar length of the skeletal elements of the appendicular skeleton in adolescent (four weeks) and adult (four months) *Matn1-4*$^{-/-}$ mice and control mice (Figure 2A,C,E,F). However, we observed slightly but significantly increased lengths of the femur, tibia, and humerus in *Matn1-4*$^{-/-}$ mice just shortly after birth (P2),

which could possibly be explained by the differences in the genetic background. All matrilin single and multiple mutants were on C57BL/6 × 129/Sv background and *Matn1-4⁻/⁻* mice were kept in homozygous breeding. As control, we used wild-type mice on the same, mixed genetic background. However, we could not ensure the same ratio of the C57BL/6 and the 129/Sv genetic material in control and *Matn1-4⁻/⁻* mice. Inbred 129/Sv mice have longer gestation length, smaller litter size, and increased body weight at birth compared to inbred C57BL/6 mice [45], which suggest that even a mild shift towards higher 129/Sv contribution in *Matn1-4⁻/⁻* mice compared to wild type could result in an enlarged skeleton perinatally. In accordance with our observation that the lengths of skeletal elements were normal from four weeks of age in *Matn1-4⁻/⁻* mice, the two inbred strains display a similar body weight at 16 weeks [46].

Importantly, careful histological assessment of the development of the tibia at various embryonic and postnatal stages did not reveal any abnormalities of chondrocyte differentiation, growth plate structure and function in *Matn1-4⁻/⁻* mice (Figures 3 and 4). A previous in vitro study by Yang et al. showed that MATN3 binds to and inhibits BMP-2, which in turn suppresses SMAD-1/5 promoter activity, reduces SMAD-1 phosphorylation and inhibits the expression of the hypertrophic chondrocyte marker gene collagen X (*Col10a1*) in cultured chondrocytes [41]. It has been also reported that *Matn3⁻/⁻* mice, established in the Chen laboratory, display premature hypertrophic differentiation in the embryonic tibial growth plate at E16.5 and E17.5 [35], but not at the newborn stage, which was associated with increased SMAD1 activation in the proliferative zone of the growth plate at E18.5 [41]. Interestingly, in another study, *MATN3* induced the chondrogenesis of murine ATDC5 chondroprogenitor cells by elevating the gene expression of aggrecan (*Acan*) and collagen II (*Col2a1*), but did not alter the expression of *Col10a1* [47]. In contrast, MED or SEMD mutant *MATN3* constructs abolished *Acan* and/or *Col2a1* mRNAs expression and upregulated *Col10a1* expression by interfering with TGF-β signaling [47]. Although these studies suggest a role of MATN3 for the modulation of hypertrophic differentiation of chondrocytes, *Matn1-4⁻/⁻* mice, however, do not show aberrant chondrogenic differentiation. Histomorphometry at different postnatal stages (Figure 3C,D,G,H) and in situ hybridization at P2 (Figure 4A) indicated normal lengths of growth plate zones and the normal expression of chondrocyte differentiation markers, respectively. At E15.5, the ratio of the total tibial length and the length of the hypertrophic core was comparable between wild-type and *Matn1-4⁻/⁻* animals indicating that the hypertrophic differentiation rate is not affected by the lack of matrilins during embryonic development of long bones (Figure 3A). Furthermore, the normal proliferation rate of growth plate chondrocytes, the proper and timely formation and mineralization of the chondro-osseous junctions, and the normal columnar structure in *Matn1-4⁻/⁻* mice clearly indicate that matrilins are dispensable for growth plate morphogenesis.

Matrilins interact through their VWA domains with other matrix constituents, including collagens (collagen types II, IX), proteoglycans (aggrecan, biglycan, decorin) [6], and COMP [9], and they can form both collagen-dependent and collagen-independent networks [3,48,49]. A growing body of evidence suggests that the disturbance of these interacting molecular assemblies could affect the integration of ECM molecules, collagen fibril formation and cartilage mechanical conditions. Ablation of collagen IX in mice results in abnormal perinatal organization of the growth plate architecture [50,51] associated with reduced integrations of COMP, MATN1, MATN3, and MATN4 into the ECM [8,52–54], softer cartilage matrix [54], and increased collagen fibril diameter [8,51]. COMP deficiency mildly impacts growth plate structure [55] and moderately influences the deposition and fibrillar integration of MATN3, but has no apparent effect on collagen fibrillogenesis [8,51]. While collagen fibrils with larger diameters were also reported in *Matn1⁻/⁻* and *Matn1⁻/⁻/Matn3⁻/⁻* knockout mice [33,36], the solubility of the matrilin interacting partners biglycan, decorin, COMP and collagen II were not altered in the cartilage of *Matn1⁻/⁻/Matn3⁻/⁻* double deficient mice [36]. In the epiphyseal cartilage of *Matn1-4⁻/⁻* knockout mice, we did not observe an obvious difference in the deposition of ECM molecules such as aggrecan, COMP and collagen types II, IX, and VI using immunohistochemistry (Figure 5A,B). However, alterations in their extractability were noticed by Western blotting. At the newborn stage, when the cartilage ECM is less mature, all investigated proteins showed increased solubility in neutral salt (buffer I), while collagens II, IX and

COMP were present in a clearly reduced extractable amount in chaotropic buffer containing GuHCl (buffer III) (Figure 5C). At four weeks, when the cartilage matrix is undergoing a maturation process, the amount of extractable aggrecan was increased in all fractions of the cartilage of $Matn1\text{-}4^{-/-}$ mice compared with that in the control, whereas the solubility of the other ECM proteins did not change significantly (Figure 5D). These results suggest that matrilins may have a matrix-stabilizing role by supporting the firm anchorage of their interaction partners into the ECM when the cartilage undergoes extensive perinatal growth. Using high-resolution AFM imaging, we found collagen fibrils with increased diameters in the growth plate cartilage of two-week old $Matn1\text{-}4^{-/-}$ mice (Figure 6B), confirming the established role of MATN1 and/or MATN3 in the control of lateral growth of collagen fibrils [33,36]. Nanoscale AFM indentation, however, demonstrated normal stiffness of the growth plate cartilage in $Matn1\text{-}4^{-/-}$ mice, which implies that matrilins are dispensable for cartilage biomechanics, at least at this stage of postnatal development.

In humans, chondrodysplasia-causing mutations in COMP, collagen IX, or MATN3 are frequently associated with premature osteoarthritis. Matrilin-3 is present at low levels in the joint articular surface and its deposition is upregulated in cartilage and in the synovial fluid of patients with OA as a consequence of cartilage degradation [56–60]. Studies with recombinant MATN3 and human primary chondrocytes have revealed that MATN3 exhibits a context-dependent anabolic or catabolic function by influencing the expression of pro-inflammatory cytokines, ECM degradation enzymes, and ECM synthesis [59,61–63] through the modulation of protein kinase B (AKT) [59], interleukin-6 [62], and interleukin-1 [63,64] signaling pathways. The neoexpression of MATN1 was also observed in the cartilage of OA or rheumatoid arthritis patients [65,66], and MATN2 was recently observed in total knee arthroplasty and suggested as a biomarker for OA [67]. In contrast to other matrilins, down-regulation of $MATN4$ gene expression was reported to be associated with knee OA progression [68]. In the present study, we have performed, for the first time, a comprehensive immunohistochemical study to assess the deposition of matrilins in normal and osteoarthritic human knee articular cartilage (Figure 7D). We observed that matrilins are present at various amounts in the healthy articular cartilage, preferentially in the middle and deep zones. MATN1 shows a very weak, cell-associated staining pattern; MATN3 displays predominantly pericellular expression; MATN2 and MATN4 exhibit moderate cellular staining. In severely damaged OA cartilage, all matrilins are upregulated, indicating that each member of the matrilin family participates in the cellular response for the advanced disease as an attempt to protect the tissue from further degradation.

Indeed, the most striking phenotype of the $Matn1\text{-}4^{-/-}$ mice was the development of severe osteoarthritis in aged mice (Figure 7B,C). In mice, matrilins are differentially expressed in the developing and mature articular cartilage. MATN2 and MATN4 are present, whereas MATN1 and MATN3 are absent at the superficial zone of the growing epiphysis [12,13,31,69,70]. In adult joints, immunohistochemistry demonstrated a very moderate deposition of matrilins in the articular cartilage [13] (Figure 7A). Interestingly, a lineage tracing experiment, in which the matrilin-1-Cre ($Matn1\text{-}Cre$) knock-in mice were crossed with the floxed ROSA26-LacZ reporter mouse line (R26R), demonstrated the lack of beta-galactosidase signal at the joint surface, suggesting that matrilin-1 is not expressed in the mature articular cartilage [70]. The OA phenotype in the $Matn1\text{-}4^{-/-}$ mice was accompanied by increased collagen fibril diameter (Figure 8A,B), confirming our similar results obtained on the growth plate cartilage, and changes in the nanomechanical properties of the knee joint cartilage. Nano-scale indentation-type AFM recorded the typical bimodal stiffness distribution of the articular cartilage (representing proteoglycans and collagens) [71,72] and showed higher stiffness of both macromolecular assemblies at the superficial zone of the articular cartilage in $Matn1\text{-}4^{-/-}$ mice compared to control already at 4 months of age before any histological sign of cartilage degeneration (Figure 8C). As the stiffness of the middle and deep zones were in the normal range at this age, it seems that matrilin-deficiency primarily affects ECM biomechanics in the outermost zone where the collagen fibrils are oriented parallel to the surface. Of note, a recent study found increased elastic moduli at the articular cartilage surface in $Matn1^{-/-}$ mice [34]. Furthermore, stiffening of the articular cartilage before the onset of OA has been also recently observed in hypomorphic aggrecan mutant mice [71]. When OA is histologically visible in one-year old $Matn1\text{-}4^{-/-}$ mice, the superficial

and middle zones exhibited a reduced Young's modulus for both proteoglycans and collagens (Figure 8D), probably reflecting the advanced deterioration of the ECM [73]. The increased stiffness in the deep zone may be the consequence of a mechanical adaptation mechanism to the weakened upper zones. Importantly, the lack of matrilins did not influence GAG release in IL-1α stimulated hip explant culture (Figure 9), therefore reasonable to speculate that matrilins protect against OA through biomechanical stabilization of the articular cartilage ECM.

Based on mouse models, the participation of the individual matrilins in OA is controversial. Spontaneous articular cartilage degradation was observed in 1 year old *Matn3*$^{-/-}$ mice generated by Chen and his colleagues [35], while *Matn3*$^{-/-}$ and *Matn1*$^{-/-}$/*Matn3*$^{-/-}$ mice established in our laboratory showed no obvious signs of accelerated articular cartilage degradation in aged animals [32,36]. Similarly, no OA-related phenotype was reported in mouse strains carrying a human *MATN3* MED mutation in wild-type [74] or in *Matn1* null background [75]. Interestingly, a recent study demonstrated that the microRNA miR-483-5p targeted *Matn3* and *Timp2* (tissue inhibitor of metalloproteinase 2), which in turn accelerated articular cartilage degradation in mice with experimental OA [76]. Age-related, spontaneous OA has not been reported in mice lacking MATN1 [31,33] or MATN2 [12]. However, more severe articular cartilage degeneration was observed after surgical destabilization of the medial meniscus in *Matn1*$^{-/-}$ mice compared to wild-type control [34]. Since the role of MATN4 in OA has not been investigated, we have also evaluated spontaneous articular cartilage degradation in aged *Matn4*$^{-/-}$ mice. MATN4 deficiency had a dramatic effect on the joint by exacerbating OA-like erosion of the articular cartilage at a similar level as we observed in the *Matn1-4*$^{-/-}$ mice (Figure 10). Consistent with the observation in the growth plate, we have also found a prominent upregulation of MATN2 expression in the MATN4 deficient articular cartilage (Figure 10C) which, however, was unable to compensate for the lack of MATN4. These findings indicate for the first time that MATN4 is essential to maintain the integrity of the articular cartilage and protect the joints against age-associated osteoarthritis.

The most surprising phenotype what we have observed in the *Matn1-4*$^{-/-}$ mice was the patterning defect of the axial skeleton manifested by the highly penetrant (nearly 90%) transition of the L6 vertebra into a sacral identity (Figure 2B–D and Table 1). Disturbance of the vertebral column specification at the lumbosacral junction was also present in *Matn1-4*$^{+/-}$ mice demonstrated by partial (asymmetric) or complete sacralization of L6 in two-thirds of the investigated animals (*n* = 6). Congenital skeletal anomalies including sacralization of 6th lumbar vertebra (or 26th pre-caudal vertebra) are common in some inbred strains including the strain 129 [77,78]. Depending on environmental factors, the three vertebral types (L6, L6 to S1, asymmetric L6 to S1) occur about the same frequency in this strain [40,77], and the proportion of the normal L6 identity is significantly increased when 129 animals were raised in 129 x C57BL hybrid females upon ovary transplantation [78]. As we have not observed patterning defects of the vertebral columns in previous single or double knockout matrilin mutant mice [12,31,32,36] maintained on the mixed C57BL/6 × 129/Sv genetic background, and the *Matn1-4*$^{-/-}$ mice do not display other skeletal abnormalities of the 129 strain (e.g., accessory sternebrae), we are convinced that the phenotype is the consequence of the lack of all matrilins in the axial skeleton. The molecular basis of how matrilins regulate vertebral specification is not clear and warrant further studies. Interestingly, it has been recently shown that mice lacking the nucleus accumbens-associated protein 1 (NAC1) also exhibit the L6 sacralization phenotype accompanied by the reduced mRNA expression of matrilins in *Nacc1*$^{-/-}$ chondrocytes, which is especially significant in case of *Matn3* and *Matn4* [79]. Furthermore, all matrilin family members are expressed in the developing vertebral bodies [12,13], and MATN1 and MATN3 have been implicated in chondrogenic differentiation in vitro [80].

4. Materials and Methods

4.1. Knockout Mice

Outbred mice (C57BL/6 × 129/Sv) knockout for matrilin-1 (*Matn1*$^{-/-}$), matrilin-2 (*Matn2*$^{-/-}$), matrilin-3 (*Matn3* $^{-/-}$), and matrilin-4 (*Matn 4*$^{-/-}$) were previously generated in our laboratory

[12,31,32,37]. Double knockout mice for matrilin-1 and -3 (*Matn1$^{-/-}$/Matn3$^{-/-}$*) [36], matrilin-2 and -3 (*Matn2$^{-/-}$/Matn3$^{-/-}$*), triple knockout mice lacking matrilin-1, -2, and -3 (*Matn1-3$^{-/-}$*), and quadruple knockout mice lacking all matrilins (*Matn1-4$^{-/-}$*) [37] were generated by intercrossing single and multiple matrilin deficient mice. Wild-type littermates were used as control for single and double knockout mice. Triple and quadruple knockout mice were maintained in homozygous mutant breeding. Age-matched wild-type non-littermates on the same C57BL/6 x 129/Sv background were used as control for the *Matn1-4$^{-/-}$* and *Matn1-3$^{-/-}$* mice. Mice were kept under 12 h light/dark cycle, constant temperature, in individually ventilated cages in the Central Animal Facility at the Medical Faculty of the Ludwig-Maximilians-University. Mice were housed in groups of 2–5 per cage and received food and water *ad libitium*. The handling and breeding of all mouse strains have been approved by the government of Upper Bavaria (Application number: 55.2-1-54-2532-15-2016).

4.2. Human Samples

Human tibial plateau were obtained from patients undergoing total knee arthroplasty after written consent according to the ethical approval no. 238-15. The whole tissue explant was collected in phosphate buffered saline (PBS) pH 7.4 in the operation room of the Schön Klinik (Munich, Germany) and immediately delivered to our laboratory. Afterwards, cylindrical osteochondral plugs from differently degenerated or non-degenerated areas of the plateau were harvested with the aid of a 7 mm diameter trephine drill, washed once in PBS and fixed in 4% paraformaldehyde (PFA)/PBS overnight at 4 °C. Osteochondral plugs were decalcified in 10% formic acid/dH$_2$O for 3 days at RT. After that, plugs were thoroughly washed in PBS, immersed in 20% sucrose/PBS for 24 h at 4 °C and embedded in Tissue-Tek cryomedia (Sakura Finetek, Alphen aan den Rijn, The Netherlands) and gradually frozen on a chilled copper plate placed on dry ice. Sagittal sections of 10 μm were cut using a cryotome (HM500 cryostat, Thermo Fischer Scientific, Waltham, MA, USA) and collected on Superfrost Plus glass slides (Thermo Fischer Scientific, Waltham, MA, USA).

4.3. Antibodies

For immunohistochemistry and Western blots, the following primary antibodies were used: Rabbit polyclonal antibodies against matrilin-1, matrilin-2, matrilin-3, matrilin-4, cartilage oligomeric protein (COMP) and collagen VI were described previously [36]. Antibodies against collagen IX were gifts of Susanne Grässel (University of Regensburg, Germany) and Frank Zaucke (Orthopaedic University Hospital Friedrichsheim, Germany). Rabbit polyclonal anti-aggrecan antibody (ab#1031) was obtained from Merck Millipore (Billerica, MA, USA); mouse monoclonal anti-collagen II antibody (CIIC1) was purchased from the Developmental Studies Hybridoma Bank (Iowa, IL, USA); and the rabbit monoclonal antibodies specific for SMAD-1 (D59D7, #6944) and for phospho-SMAD-1/5/8 (D5B10, #13820) were obtained from Cell Signaling Technology (Beverly, MA, USA). Primary antibodies were diluted 1:400 for immunohistochemistry and 1:1000 for immunoblotting.

4.4. Whole-Mount Skeletal Staining and X-ray Analysis

For skeletal staining, 2-day and 4-week old mice were euthanized with carbon dioxide. De-skinned and eviscerated specimens were fixed in 95% ethanol for 3 days and transferred into acetone for additional 2 days. The skeleton was stained with 0.6% Alcian Blue (for cartilage) and 0.02% Alizarin Red (for bone) (both Sigma-Aldrich, St. Louis, MO, USA) in 90% ethanol and 5% acetic acid for 3 days in a 37 °C incubator with continuous shaking. Samples were cleared by incubation in descending potassium hydroxide and ascending glycerol solutions, and were finally preserved in 100% glycerol. To determine the length of the long bones, the humerus, the femur, and the tibia were dissected from five control and five *Matn1-4$^{-/-}$* mice, photographed with a Stemi 1000 stereo microscope (Carl Zeiss, Jena, Germany) and measured with the ZEN software (Carl Zeiss, Jena, Germany).

For X-ray analysis, 4-week, 4-month, and 1-year old mice were euthanized, and radiographs were taken using a sealed X-ray cabinet (FAXITRON 43855 A) at 35 kV, 2 mA, and 2 s exposure time.

Total body length (from the snout to the end of the tail) and the length of the skeletal elements (tibia, femur, and humerus) were analyzed with the distance measurement plug-in of the syngo Imaging XS-VA60B software (Siemens, Erlangen, Germany).

4.5. Histology, Immunohistochemistry and In Situ Hybridization

Mouse limbs were dissected from 15.5 and 18 day-old embryos (E15.5 and E18), and from newborn, 2-day (P2), 2-week, 4-week, 2-month, 4-month, 8-month, and 15–24 month old animals. The specimens were routinely fixed in 4% PFA/PBS at 4 °C for 12–24 h. Additionally, forelimbs were fixed in 95% ethanol and 1% acetic acid for immunohistochemical analysis. Samples from 2 weeks of age were decalcified in 15% ethylenediaminetetraacetic acid (EDTA) (Sigma-Aldrich, St. Louis, MO, USA) dissolved in PBS (pH 8.0) for 1–3 weeks. Specimens were processed either for standard paraffin or for cryo embedding. All the embedded tissues were cut into 8-μm thick sections using a microtome or cryotome. For routine histology, the sections were stained with hematoxylin and eosin (HE), Safranin orange and fast green (SO/FG), and Safranin orange-von Kossa (SO/vK) according to the standard protocols. Morphometric analyses of the growth plate zones were performed as described previously [81]. TRAP (tartrate resistant acid phosphatase) staining to visualize chondroclasts/osteoclasts at the chondro-osseous junction was performed with the leukocyte acid phosphatase kit (Sigma-Aldrich, St. Louis, MO, USA) according to manufacturer instructions. To assess articular cartilage degeneration on HE stained sections, a histological grading score for structural alteration was applied as follow: 0-normal articular cartilage; 1-surface irregularities; 2-cleft to transition zone; 3-cleft to radial zone; 4-cleft extending to calcified zone; 5-exposure of subchondral bone [36].

For immunohistochemistry, paraffin sections were rehydrated in descending ethanol series, rinsed in PBS and treated with bovine testicular hyaluronidase (Sigma-Aldrich, St. Louis, MO, USA) (2 mg/mL in PBS, pH 5.0) for 30 min at 37 °C to facilitate antibody penetration. Primary antibodies were incubated overnight at 4 °C and the subsequent immunohistochemical detection was performed using the corresponding Vectastain ABC Elite kit (Vector Laboratories, Burlingame, CA, USA) and 3,3-diaminobenzidine (DAB, Sigma-Aldrich, St. Louis, MO, USA) as chromogenic substrate.

For non-radioactive in situ hybridization, deparaffinized sections were rinsed in Tris-buffered saline (TBS) pH 7.5, acetylated with 0.25% acetic anhydride (pH 8.0) for 10 min, rinsed in TBS and dehydrated in ethanol. Sections were hybridized at 70 °C overnight with digoxigenin (DIG)-UTP-labelled antisense riboprobes specific for mouse collagen II (*Col2a1*), collagen X (*Col10a1*), indian hedgehog (*Ihh*), parathyroid hormone/parathyroid hormone-related peptide receptor (*Ppr*) and matrix metalloproteinase-13 (*Mmp-13*) as previously described [32]. After hybridization and subsequent washing in 2 X sodium citrate-chloride buffer (SSC) at 70 °C for 30 min, the sections were blocked with 2% goat serum for 1 h and incubated with a 1:500 diluted alkaline phosphatase-coupled anti-DIG antibody (Roche, Penzberg, Germany) for 2 h. Hybridization signals were detected using the p-nitroblue tetrazolium chloride/5-bromo-4-chloro-3-indolyl phosphate (NBT/BCIP) solution (Roche, Penzberg, Germany) according to the recommendation of the manufacturer. Brightfield microscopy images were acquired with an AxioObserver microscope (Carl Zeiss, Jena, Germany).

4.6. Cell Proliferation and Cell Death Assays

In vivo chondrocyte proliferation was analysed using the 5-bromo-2′-deoxyuridine (BrdU) incorporation assay as described previously [32]. Briefly, mice were injected intraperitoneally (50 μg/g of body weight) with BrdU solution (10 mg/mL in PBS, pH 7.4). After 2 h, the animals were sacrificed, knee samples were dissected and embedded into paraffin. Deparaffinized sections were treated with 2 M HCl for 30 min, washed in PBS, and incubated with a peroxidase-conjugated antibody against BrdU (Roche, Penzberg, Germany). Detection of proliferative cells in the S phase of the cell cycle was performed with DAB as chromogen substrate. Analysis of apoptotic chondrocytes was carried out using the TUNEL assay according to the manufacturer's instructions (In Situ Cell Death Detection Kit, Roche, Penzberg, Germany).

4.7. Protein Extraction and Western Blotting

Knee joint cartilage was dissected from newborn and 4-week old *Matn1-4$^{-/-}$* and control mice (*n* = 10). Specimens were weighed, cut into small pieces, and incubated in ten volumes of chilled extraction buffer I (0.15 M NaCl, 50 mM Tris, pH 7.4) overnight at 4 °C with continuous stirring. Next day, the mixture was centrifuged at 14,000 rpm for 1 h and the supernatant was stored at −20 °C, and the obtained pellet was incubated as above in buffer II (1 M NaCl, 10 mM EDTA, 50 mM Tris, pH 7.4) and subsequently in buffer III (4 M guanidine hydrochloride, 10 mM EDTA, 50 mM Tris, pH 7.4). All extraction buffers contained EDTA-free proteinase inhibitor cocktail (Roche, Penzberg, Germany). Aliquots (100 μL) of all extracts were precipitated with 96% ethanol and the pellets were processed and re-suspended in non-reducing SDS-PAGE (sodium dodecyl sulfate–polyacrylamide gel electrophoresis) sample buffer as described previously [32]. Samples were applied to 4–15% pre-casted SDS-PAGE gels (Bio-Rad, Berkeley, CA, USA) and electrophoresis was performed using a Bio-Rad apparatus. For Western blotting, proteins were transferred to a PVDF membrane (GE Healthcare, Chicago, USA) and incubated with primary antibodies diluted either in 5% skim milk (Sigma-Aldrich, St. Louis, MO, USA) or 5% bovine serum albumin (BSA) (Sigma-Aldrich, St. Louis, MO, USA) in 1X TBST (0.5% Tween 20 in TBS). Bound antibodies were detected by HRP-conjugated secondary antibodies, and the signal was developed using Luminata ECL Forte (Merck Millipore) and acquired on the GE Healthcare imaging system ImageQuant LAS 4000.

Primary chondrocytes were isolated from newborn ribcage as described [71]. Single cell suspensions were lysed in RIPA buffer with phosphatase (PhosSTOP, Roche, Penzberg, Germany) and protease inhibitors. Total protein was normalized using the BCA assay (Themo Scientific, Waltham, MA, USA) and equal amounts of protein were subjected to 10% SDS-PAGE, transferred to PVDF membrane and imaged as above.

4.8. Explant Culture

Femoral heads were dissected from 4-week-old control and *Matn1-4$^{-/-}$* mice and cultured in serum-free Dulbecco's modified Eagle's medium (DMEM) supplemented with streptomycin-penicillin for 4 days at 37 °C and 5% CO_2 in the absence or presence of the catabolic cytokine IL-1α (10 ng/mL) (R&D Systems, Minneapolis, MN, USA). After the culture period, femoral heads were fixed in 4% PFA, cryo-embedded, cut, and stained with SO to examine the loss of proteoglycans. Conditioned culture medium was also collected and analyzed for released sulfated glycosaminoglycan (sGAG) using the Blyscan B1000 GAG assay (Biocolor Ltd., Carrickfergus, UK) according to the instructions of the manufacturers.

4.9. Atomic Force Microscopy (AFM)

Knee joints from 2-week, 4-month, and 1-year-old control and *Matn1-4$^{-/-}$* animals were dissected and immediately immersed into Tissue-Tek and snap frozen in a liquid nitrogen-cooled bath of isopentane. Sagittal sections (30 μm) of three animals per genotype were cut using two supportive tapes (one double adhesive and an adhesive) and a cryostat, and placed on Super Frost Plus glass slides as previously described [82]. Sections were stored at −20 °C until the analysis. AFM imaging and indentation measurements were carried out on sections equilibrated at room temperature using the NanoWizard 1 AFM (JPK Instruments, Berlin, Germany) in combination with an inverse optical microscope (Axiovert 200, Carl Zeiss, Göttingen, Germany) as previously described [82]. Briefly, for the growth plate measurements the Young's modulus was determined at each indentation position by fitting a modified Hertz model (pyramidal indenter) to the respective approach curve, using the JPK data processing software (versions 4.2.20 and 5.0.96; JPK Instruments). The contact point was determined manually for each force curve, and the fit range was limited to a maximum indentation depth of 500 nm. For the articular cartilage measurements, the contact point was determined by fitting the modified Hertz model to the entire force range first and then using this fix contact point to fit only the first 500 nm indentation depth. To generate histograms and fitting Gaussian distributions, the data analysis software Origin 8.0 (OriginLab Corporation, Northampton, MA, USA) and Igor Pro

6.37 (Wavemetrix, London, UK) were used for growth plate and articular cartilage data, respectively. AFM imaging of the middle and deep zone of the articular cartilage was performed on 20 μm thick, PFA-fixed sections.

4.10. Statistical Analysis

Data are presented as mean ± SD (standard deviation). Statistical significance was assessed using the Mann-Whitney *U* test, *p* values less than 0.05 were considered significant. Histology data are representative of a minimum of six animals for each group.

5. Conclusions

In summary, our data imply that the matrilin family of adaptor proteins is dispensable for the growth of the cartilaginous skeleton, but required for vertebral column specification and articular cartilage stability. Biochemical analyses of cartilages from various matrilin-deficient mouse lines showed compensation among the family members, and indicated that the lack of all four matrilins moderately changes the extractability of binding partners. Atomic force microscopy revealed that matrilins control collagen fibril diameters in the cartilage ECM and modulate the stiffness of the articular cartilage. *Matn1-4$^{-/-}$* and *Matn4$^{-/-}$* mice develop similar age-associated osteoarthritis suggesting a novel function of matrilin-4 for preventing articular cartilage degradation in the murine knee joint.

Conflicts of Interest: The authors declare no conflict of interest.

Abbreviations

ACAN	Aggrecan
AFM	Atomic force microscopy
BMP-2	Bone morphogenetic protein-2
BrdU	Bromodeoxyuridine
COL	Collagen
COMP	Cartilage oligomeric matrix protein
ECM	Extracellular matrix
EDTA	Ethylenediaminetetracetic acid
GAG	Glycosaminoglycan
HE	Hematoxylin and eosin
IL-1	Interleukin-1
ITM	Interterritorial matrix
MATN	Matrilin
MED	Multiple epiphyseal dysplasia
OA	Osteoarthritis
PBS	Phosphate buffered saline
PFA	Paraformaldehyde
P2	Postnatal day 2
SDS-PAGE	Sodium dodecyl sulfate-polyacrylamide gel electrophoresis
SEMD	Spondylo-meta-epiphyseal dysplasia
TRAP	Tartrate-resistant acid phosphatase

TUNEL   Terminal deoxynucleotidyl transferase dUTP nick end labeling

References

1.   Klatt, A.R.; Becker, A.K.; Neacsu, C.D.; Paulsson, M.; Wagener, R. The matrilins: Modulators of extracellular matrix assembly. *Int. J. Biochem. Cell. Biol.* **2011**, *43*, 320–330.

2.   Aszodi, A.; Hauser, N.; Studer, D.; Paulsson, M.; Hiripi, L.; Bosze, Z. Cloning, sequencing and expression analysis of mouse cartilage matrix protein cDNA. *Eur. J. Biochem.* **1996**, *236*, 970–977.

3.   Klatt, A.R.; Nitsche, D.P.; Kobbe, B.; Morgelin, M.; Paulsson, M.; Wagener, R. Molecular structure and tissue distribution of matrilin-3, a filament-forming extracellular matrix protein expressed during skeletal development. *J. Biol. Chem.* **2000**, *275*, 3999–4006.

4.   Piecha, D.; Muratoglu, S.; Morgelin, M.; Hauser, N.; Studer, D.; Kiss, I.; Paulsson, M.; Deak, F. Matrilin-2, a large, oligomeric matrix protein, is expressed by a great variety of cells and forms fibrillar networks. *J. Biol. Chem.* **1999**, *274*, 13353–13361.

5.   Klatt, A.R.; Nitsche, D.P.; Kobbe, B.; Macht, M.; Paulsson, M.; Wagener, R. Molecular structure, processing, and tissue distribution of matrilin-4. *J. Biol. Chem.* **2001**, *276*, 17267–17275.

6.   Hauser, N.; Paulsson, M.; Heinegård, D.; Mörgelin, M. Interaction of Cartilage Matrix Protein with Aggrecan. Increased covalent cross-linking with tissue maturation. *J. Biol. Chem.* **1996**, *271*, 32247–32252.

7.   Winterbottom, N.; Tondravi, M.M.; Harrington, T.L.; Klier, F.G.; Vertel, B.M.; Goetinck, P.F. Cartilage matrix protein is a component of the collagen fibril of cartilage. *Dev. Dyn.* **1992**, *193*, 266–276.

8.   Budde, B.; Blumbach, K.; Ylostalo, J.; Zaucke, F.; Ehlen, H.W.; Wagener, R.; Ala-Kokko, L.; Paulsson, M.; Bruckner, P.; Grassel, S. Altered integration of matrilin-3 into cartilage extracellular matrix in the absence of collagen IX. *Mol. Cell. Biol.* **2005**, *25*, 10465–10478.

9.   Mann, H.H.; Ozbek, S.; Engel, J.; Paulsson, M.; Wagener, R. Interactions between the cartilage oligomeric matrix protein and matrilins. Implications for matrix assembly and the pathogenesis of chondrodysplasias. *J. Biol. Chem.* **2004**, *279*, 25294–25298.

10. Wiberg, C.; Klatt, A.R.; Wagener, R.; Paulsson, M.; Bateman, J.F.; Heinegard, D.; Morgelin, M. Complexes of matrilin-1 and biglycan or decorin connect collagen VI microfibrils to both collagen II and aggrecan. *J. Biol. Chem.* **2003**, *278*, 37698–37704.

11. Wagener, R.; Ehlen, H.W.; Ko, Y.P.; Kobbe, B.; Mann, H.H.; Sengle, G.; Paulsson, M. The matrilins—Adaptor proteins in the extracellular matrix. *FEBS Lett.* **2005**, *579*, 3323–3329.

12. Mates, L.; Nicolae, C.; Morgelin, M.; Deak, F.; Kiss, I.; Aszodi, A. Mice lacking the extracellular matrix adaptor protein matrilin-2 develop without obvious abnormalities. *Matrix Biol.* **2004**, *23*, 195–204.

13. Klatt, A.R.; Paulsson, M.; Wagener, R. Expression of matrilins during maturation of mouse skeletal tissues. *Matrix Biol.* **2002**, *21*, 289–296.

14. Briggs, M.D.; Chapman, K.L. Pseudoachondroplasia and multiple epiphyseal dysplasia: Mutation review, molecular interactions, and genotype to phenotype correlations. *Hum. Mutat.* **2002**, *19*, 465–478.

15. Chapman, K.L.; Mortier, G.R.; Chapman, K.; Loughlin, J.; Grant, M.E.; Briggs, M.D. Mutations in the region encoding the von Willebrand factor A domain of matrilin-3 are associated with multiple epiphyseal dysplasia. *Nat. Genet.* **2001**, *28*, 393–396.

16. Mabuchi, A.; Haga, N.; Maeda, K.; Nakashima, E.; Manabe, N.; Hiraoka, H.; Kitoh, H.; Kosaki, R.; Nishimura, G.; Ohashi, H.; et al. Novel and recurrent mutations clustered in the von Willebrand factor A domain of MATN3 in multiple epiphyseal dysplasia. *Hum. Mutat.* **2004**, *24*, 439–440.

17. Jackson, G.C.; Barker, F.S.; Jakkula, E.; Czarny-Ratajczak, M.; Makitie, O.; Cole, W.G.; Wright, M.J.; Smithson, S.F.; Suri, M.; Rogala, P.; et al. Missense mutations in the beta strands of the single A-domain of matrilin-3 result in multiple epiphyseal dysplasia. *J. Med. Genet.* **2004**, *41*, 52–59.

18. Otten, C.; Wagener, R.; Paulsson, M.; Zaucke, F. Matrilin-3 mutations that cause chondrodysplasias interfere with protein trafficking while a mutation associated with hand osteoarthritis does not. *J. Med. Genet.* **2005**, *42*, 774–779.

19. Cotterill, S.L.; Jackson, G.C.; Leighton, M.P.; Wagener, R.; Makitie, O.; Cole, W.G.; Briggs, M.D. Multiple epiphyseal dysplasia mutations in MATN3 cause misfolding of the A-domain and prevent secretion of mutant matrilin-3. *Hum. Mutat.* **2005**, *26*, 557–565.

20. Nundlall, S.; Rajpar, M.H.; Bell, P.A.; Clowes, C.; Zeeff, L.A.; Gardner, B.; Thornton, D.J.; Boot-Handford, R.P.; Briggs, M.D. An unfolded protein response is the initial cellular response to the expression of mutant matrilin-3 in a mouse model of multiple epiphyseal dysplasia. *Cell Stress Chaperones* **2010**, *15*, 835–849.

21. Mostert, A.K.; Dijkstra, P.F.; Jansen, B.R.; van Horn, J.R.; de Graaf, B.; Heutink, P.; Lindhout, D. Familial multiple epiphyseal dysplasia due to a matrilin-3 mutation: Further delineation of the phenotype including 40 years follow-up. *Am. J. Med. Genet. A* **2003**, *120*, 490–497.

22. Borochowitz, Z.U.; Scheffer, D.; Adir, V.; Dagoneau, N.; Munnich, A.; Cormier-Daire, V. Spondylo-epi-metaphyseal dysplasia (SEMD) matrilin 3 type: Homozygote matrilin 3 mutation in a novel form of SEMD. *J. Med. Genet.* **2004**, *41*, 366–372.

23. Stefansson, S.E.; Jonsson, H.; Ingvarsson, T.; Manolescu, I.; Jonsson, H.H.; Olafsdottir, G.; Palsdottir, E.; Stefansdottir, G.; Sveinbjornsdottir, G.; Frigge, M.L.; et al. Genomewide scan for hand osteoarthritis: A novel mutation in matrilin-3. *Am. J. Hum. Genet.* **2003**, *72*, 1448–1459.

24. Min, J.L.; Meulenbelt, I.; Riyazi, N.; Kloppenburg, M.; Houwing-Duistermaat, J.J.; Seymour, A.B.; van Duijn, C.M.; Slagboom, P.E. Association of matrilin-3 polymorphisms with spinal disc degeneration and osteoarthritis of the first carpometacarpal joint of the hand. *Ann. Rheum. Dis.* **2006**, *65*, 1060–1066.

25. Pullig, O.; Tagariello, A.; Schweizer, A.; Swoboda, B.; Schaller, P.; Winterpacht, A. MATN3 (matrilin-3) sequence variation (pT303M) is a risk factor for osteoarthritis of the CMC1 joint of the hand, but not for knee osteoarthritis. *Ann. Rheum. Dis.* **2007**, *66*, 279–280.

26. Meulenbelt, I.; Bijkerk, C.; Breedveld, F.C.; Slagboom, P.E. Genetic linkage analysis of 14 candidate gene loci in a family with autosomal dominant osteoarthritis without dysplasia. *J. Med. Genet.* **1997**, *34*, 1024–1027.

27. Loughlin, J.; Dowling, B.; Mustafa, Z.; Smith, A.; Sykes, B.; Chapman, K. Analysis of the association of the matrillin-1 gene (CRTM) with osteoarthritis: Comment on the article by Meulenbelt et al. *Arthritis Rheum.* **2000**, *43*, 1423–1425.

28. Montanaro, L.; Parisini, P.; Greggi, T.; Di Silvestre, M.; Campoccia, D.; Rizzi, S.; Arciola, C.R. Evidence of a linkage between matrilin-1 gene (MATN1) and idiopathic scoliosis. *Scoliosis* **2006**, *1*, 21.

29. Jang, J.Y.; Park, E.K.; Ryoo, H.M.; Shin, H.I.; Kim, T.H.; Jang, J.S.; Park, H.S.; Choi, J.Y.; Kwon, T.G. Polymorphisms in the Matrilin-1 gene and risk of mandibular prognathism in Koreans. *J. Dent. Res.* **2010**, *89*, 1203–1207.

30. Chimusa, E.R.; Beighton, P.; Kumuthini, J.; Ramesar, R.S. Detecting genetic modifiers of spondyloepimetaphyseal dysplasia with joint laxity in the Caucasian Afrikaner community. *Hum. Mol. Genet.* **2019**, *28*, 1053–1063.

31. Aszodi, A.; Bateman, J.F.; Hirsch, E.; Baranyi, M.; Hunziker, E.B.; Hauser, N.; Bosze, Z.; Fassler, R. Normal skeletal development of mice lacking matrilin 1: Redundant function of matrilins in cartilage? *Mol. Cell. Biol.* **1999**, *19*, 7841–7845.

32. Ko, Y.; Kobbe, B.; Nicolae, C.; Miosge, N.; Paulsson, M.; Wagener, R.; Aszodi, A. Matrilin-3 is dispensable for mouse skeletal growth and development. *Mol. Cell. Biol.* **2004**, *24*, 1691–1699.

33. Huang, X.; Birk, D.E.; Goetinck, P.F. Mice lacking matrilin-1 (cartilage matrix protein) have alterations in type II collagen fibrillogenesis and fibril organization. *Dev. Dyn.* **1999**, *216*, 434–441.

34. Chen, Y.; Cossman, J.; Jayasuriya, C.T.; Li, X.; Guan, Y.; Fonseca, V.; Yang, K.; Charbonneau, C.; Yu, H.; Kanbe, K.; et al. Deficient mechanical activation of anabolic transcripts and post-traumatic cartilage degeneration in Matrilin-1 knockout mice. *PLoS ONE* **2016**, *11*, e0156676.

35. van der Weyden, L.; Wei, L.; Luo, J.; Yang, X.; Birk, D.E.; Adams, D.J.; Bradley, A.; Chen, Q. Functional knockout of the matrilin-3 gene causes premature chondrocyte maturation to hypertrophy and increases bone mineral density and osteoarthritis. *Am. J. Pathol.* **2006**, *169*, 515–527.

36. Nicolae, C.; Ko, Y.P.; Miosge, N.; Niehoff, A.; Studer, D.; Enggist, L.; Hunziker, E.B.; Paulsson, M.; Wagener, R.; Aszodi, A. Abnormal collagen fibrils in cartilage of matrilin-1/matrilin-3-deficient mice. *J. Biol. Chem.* **2007**, *282*, 22163–22175.

37. Uckelmann, H.; Blaszkiewicz, S.; Nicolae, C.; Haas, S.; Schnell, A.; Wurzer, S.; Wagener, R.; Aszodi, A.; Essers, M.A. Extracellular matrix protein Matrilin-4 regulates stress-induced HSC proliferation via CXCR4. *J. Exp. Med.* **2016**, *213*, 1961–1971.

38. Malin, D.; Sonnenberg-Riethmacher, E.; Guseva, D.; Wagener, R.; Aszodi, A.; Irintchev, A.; Riethmacher, D. The extracellular-matrix protein matrilin 2 participates in peripheral nerve regeneration. *J. Cell. Sci.* **2009**, *122*, 995–1004.

39. Green, E.L. Genetic and non-genetic factors which influence the type of the skeleton in an inbred strain of mice. *Genetics* **1941**, *26*, 192–222.

40. Mc, L.A.; Michie, D. Factors affecting vertebral variation in mice. 4. Experimental proof of the uterine basis of a maternal effect. *Development* **1958**, *6*, 645–659.

41. Yang, X.; Trehan, S.K.; Guan, Y.; Sun, C.; Moore, D.C.; Jayasuriya, C.T.; Chen, Q. Matrilin-3 inhibits chondrocyte hypertrophy as a bone morphogenetic protein-2 antagonist. *J. Biol. Chem.* **2014**, *289*, 34768–34779.

42. Gentili, C.; Cancedda, R. Cartilage and bone extracellular matrix. *Curr. Pharm. Des.* **2009**, *15*, 1334–1348.

43. Hedlund, H.; Hedbom, E.; Heineg rd, D.; Mengarelli-Widholm, S.; Reinholt, F.P.; Svensson, O. Association of the aggrecan keratan sulfate-rich region with collagen in bovine articular cartilage. *J. Biol. Chem.* **1999**, *274*, 5777–5781.

44. Paulsson, M.; Wagener, R. Matrilins. *Methods Cell. Biol.* **2018**, *143*, 429–446.

45. Murray, S.A.; Morgan, J.L.; Kane, C.; Sharma, Y.; Heffner, C.S.; Lake, J.; Donahue, L.R. Mouse gestation length is genetically determined. *PLoS ONE* **2010**, *5*, e12418.

46. Reed, D.R.; Bachmanov, A.A.; Tordoff, M.G. Forty mouse strain survey of body composition. *Physiol. Behav.* **2007**, *91*, 593–600.

47. Jayasuriya, C.T.; Zhou, F.H.; Pei, M.; Wang, Z.; Lemme, N.J.; Haines, P.; Chen, Q. Matrilin-3 chondrodysplasia mutations cause attenuated chondrogenesis, premature hypertrophy and aberrant response to TGF-beta in chondroprogenitor cells. *Int. J. Mol. Sci.* **2014**, *15*, 14555–14573.

48. Chen, Q.; Johnson, D.M.; Haudenschild, D.R.; Tondravi, M.; Goetinck, P. Cartilage matrix protein forms a type II collagen-independent filamentous network: Analysis in primary cell cultures with a retrovirus expression system. *Mol. Biol. Cell* **1995**, *6*, 1743–1753.

49. Chen, Q.; Zhang, Y.; Johnson, D.M.; Goetinck, P.F. Assembly of a novel cartilage matrix protein filamentous network: Molecular basis of differential requirement of von Willebrand factor A domains. *Mol. Biol. Cell* **1999**, *10*, 2149–2162.

50. Dreier, R.; Opolka, A.; Grifka, J.; Bruckner, P.; Grässel, S. Collagen IX-deficiency seriously compromises growth cartilage development in mice. *Matrix Biol.* **2008**, *27*, 319–329.

51. Blumbach, K.; Bastiaansen-Jenniskens, Y.; DeGroot, J.; Paulsson, M.; Van Osch, G.; Zaucke, F. Combined role of type IX collagen and cartilage oligomeric matrix protein in cartilage matrix assembly: Cartilage oligomeric matrix protein counteracts type IX collagen–induced limitation of cartilage collagen fibril growth in mouse chondrocyte cultures. *Arthritis Rheum.* **2009**, *60*, 3676–3685.

52. Blumbach, K.; Niehoff, A.; Paulsson, M.; Zaucke, F. Ablation of collagen IX and COMP disrupts epiphyseal cartilage architecture. *Matrix Biol.* **2008**, *27*, 306–318.

53. Brachvogel, B.; Zaucke, F.; Dave, K.; Norris, E.L.; Stermann, J.; Dayakli, M.; Koch, M.; Gorman, J.J.; Bateman, J.F.; Wilson, R. Comparative proteomic analysis of normal and collagen IX null mouse cartilage reveals altered extracellular matrix composition and novel components of the collagen IX interactome. *J. Biol. Chem.* **2013**, *288*, 13481–13492.

54. Kamper, M.; Hamann, N.; Prein, C.; Clausen-Schaumann, H.; Farkas, Z.; Aszodi, A.; Niehoff, A.; Paulsson, M.; Zaucke, F. Early changes in morphology, bone mineral density and matrix composition of vertebrae lead to disc degeneration in aged collagen IX−/− mice. *Matrix Biol.* **2016**, *49*, 132–143.

55. Posey, K.; Hecht, J. The role of cartilage oligomeric matrix protein (COMP) in skeletal disease. *Curr. Drug Targets* **2008**, *9*, 869–877.

56. Pullig, O.; Weseloh, G.; Klatt, A.; Wagener, R.; Swoboda, B. Matrilin-3 in human articular cartilage: Increased expression in osteoarthritis. *Osteoarthr. Cartil.* **2002**, *10*, 253–263.

57. Firner, S.; Zaucke, F.; Michael, J.; Dargel, J.; Schiwy-Bochat, K.-H.; Heilig, J.; Rothschild, M.A.; Eysel, P.; Brüggemann, G.-P.; Niehoff, A. Extracellular Distribution of Collagen II and Perifibrillar Adapter Proteins in Healthy and Osteoarthritic Human Knee Joint Cartilage. *J. Histochem. Cytochem.* **2017**, *65*, 593–606.

58. Hosseininia, S.; Önnerfjord, P.; Dahlberg, L.E. Targeted proteomics of hip articular cartilage in OA and fracture patients. *J. Orthop. Res.* **2019**, *37*, 131–135.

59. Vincourt, J.B.; Etienne, S.; Grossin, L.; Cottet, J.; Bantsimba-Malanda, C.; Netter, P.; Mainard, D.; Libante, V.; Gillet, P.; Magdalou, J. Matrilin-3 switches from anti- to pro-anabolic upon integration to the extracellular matrix. *Matrix Biol.* **2012**, *31*, 290–298, doi:10.1016/j.matbio.2012.03.004.

60. Vincourt, J.B.; Vignaud, J.M.; Lionneton, F.; Sirveaux, F.; Kawaki, H.; Marchal, S.; Lomazzi, S.; Plenat, F.; Guillemin, F.; Netter, P. Increased expression of matrilin-3 not only in osteoarthritic articular cartilage but also in cartilage-forming tumors, and down-regulation of SOX9 via epidermal growth factor domain 1-dependent signaling. *Arthritis Rheum.* **2008**, *58*, 2798–2808.

61. Klatt, A.R.; Klinger, G.; Paul-Klausch, B.; Kuhn, G.; Renno, J.H.; Wagener, R.; Paulsson, M.; Schmidt, J.; Malchau, G.; Wielckens, K. Matrilin-3 activates the expression of osteoarthritis-associated genes in primary human chondrocytes. *FEBS Lett.* **2009**, *583*, 3611–3617.

62. Klatt, A.; Paul-Klausch, B.; Klinger, G.; Hillebrand, U.; Kühn, G.; Kobbe, B.; Renno, J.; Johannis, W.; Paulsson, M.; Wagener, R. The matrilin-3 VWA1 domain modulates interleukin-6 release from primary human chondrocytes. *Osteoarthr. Cartil.* **2013**, *21*, 869–873.

63. Jayasuriya, C.T.; Goldring, M.B.; Terek, R.; Chen, Q. Matrilin-3 induction of IL-1 receptor antagonist is required for up-regulating collagen II and aggrecan and down-regulating ADAMTS-5 gene expression. *Arthritis Res. Ther.* **2012**, *14*, R197.

64. Yang, H.; Wu, D.; Li, H.; Chen, N.; Shang, Y. Downregulation of microRNA-448 inhibits IL-1β-induced cartilage degradation in human chondrocytes via upregulation of matrilin-3. *Cell. Mol. Biol. Lett.* **2018**, *23*, 7.

65. Okimura, A.; Okada, Y.; Makihira, S.; Pan, H.; Yu, L.; Tanne, K.; Imai, K.; Yamada, H.; Kawamoto, T.; Noshiro, M. Enhancement of cartilage matrix protein synthesis in arthritic cartilage. *Arthritis Rheum.* **1997**, *40*, 1029–1036.

66. Ohno, S.; Murakami, K.; Tanimoto, K.; Sugiyama, H.; Makihira, S.; Shibata, T.; Yoneno, K.; Kato, Y.; Tanne, K. Immunohistochemical study of matrilin-1 in arthritic articular cartilage of the mandibular condyle. *J. Oral Pathol. Med.* **2003**, *32*, 237–242.

67. Zhang, S.; Peng, J.; Guo, Y.; Javidiparsijani, S.; Wang, G.; Wang, Y.; Liu, H.; Liu, J.; Luo, J. Matrilin-2 is a widely distributed extracellular matrix protein and a potential biomarker in the early stage of osteoarthritis in articular cartilage. *BioMed Res. Int.* **2014**, *2014*:986127.

68. Chou, C.-H.; Lee, M.T.M.; Song, I.-W.; Lu, L.-S.; Shen, H.-C.; Lee, C.-H.; Wu, J.-Y.; Chen, Y.-T.; Kraus, V.B.; Wu, C.-C. Insights into osteoarthritis progression revealed by analyses of both knee tibiofemoral compartments. *Osteoarthr. Cartil.* **2015**, *23*, 571–580.

69. Aszódi, A.; Módis, L.; Páldi, A.; Rencendorj, A.; Kiss, I.; Bösze, Z. The zonal expression of chicken cartilage matrix protein in the developing skeleton of transgenic mice. *Matrix Biol.* **1994**, *14*, 181–190.

70. Hyde, G.; Dover, S.; Aszodi, A.; Wallis, G.A.; Boot-Handford, R.P. Lineage tracing using matrilin-1 gene expression reveals that articular chondrocytes exist as the joint interzone forms. *Dev. Biol.* **2007**, *304*, 825–833.

71. Alberton, P.; Dugonitsch, H.C.; Hartmann, B.; Li, P.; Farkas, Z.; Saller, M.M.; Clausen-Schaumann, H.; Aszodi, A. Aggrecan hypomorphism compromises articular cartilage biomechanical properties and is associated with increased incidence of spontaneous osteoarthritis. *Int. J. Mol. Sci.* **2019**, *20*, 1008.

72. Gronau, T.; Krüger, K.; Prein, C.; Aszodi, A.; Gronau, I.; Iozzo, R.V.; Mooren, F.C.; Clausen-Schaumann, H.; Bertrand, J.; Pap, T. Forced exercise-induced osteoarthritis is attenuated in mice lacking the small leucine-rich proteoglycan decorin. *Ann. Rheum. Dis.* **2017**, *76*, 442–449.

73. Mieloch, A.A.; Richter, M.; Trzeciak, T.; Giersig, M.; Rybka, J.D. Osteoarthritis Severely Decreases the Elasticity and Hardness of Knee Joint Cartilage: A Nanoindentation Study. *J. Clin. Med.* **2019**, *8*, 1865.

74. Leighton, M.P.; Nundlall, S.; Starborg, T.; Meadows, R.S.; Suleman, F.; Knowles, L.; Wagener, R.; Thornton, D.J.; Kadler, K.E.; Boot-Handford, R.P. Decreased chondrocyte proliferation and dysregulated apoptosis in the cartilage growth plate are key features of a murine model of epiphyseal dysplasia caused by a matn3 mutation. *Hum. Mol. Genet.* **2007**, *16*, 1728–1741.

75. Bell, P.A.; Pirog, K.A.; Fresquet, M.; Thornton, D.J.; Boot-Handford, R.P.; Briggs, M.D. Loss of matrilin 1 does not exacerbate the skeletal phenotype in a mouse model of multiple epiphyseal dysplasia caused by a Matn3 V194D mutation. *Arthritis Rheum.* **2012**, *64*, 1529–1539.

76. Wang, H.; Zhang, H.; Sun, Q.; Wang, Y.; Yang, J.; Yang, J.; Zhang, T.; Luo, S.; Wang, L.; Jiang, Y. Intra-articular delivery of antago-miR-483-5p inhibits osteoarthritis by modulating matrilin 3 and tissue inhibitor of metalloproteinase 2. *Mol. Ther.* **2017**, *25*, 715–727.

77. Runner, M.N. Inheritance of susceptibility to congenital deformity—Embryonic instability. *J. Natl. Cancer Inst.* **1954**, *15*, 637–649.

78. Russell, W.L. Maternal influence on number of lumbar vertebrae in mice raised from transplanted ovaries. *Genetics* **1948**, *33*, 627.

79. Yap, K.L.; Sysa-Shah, P.; Bolon, B.; Wu, R.-C.; Gao, M.; Herlinger, A.L.; Wang, F.; Faiola, F.; Huso, D.; Gabrielson, K. Loss of NAC1 expression is associated with defective bony patterning in the murine vertebral axis. *PLoS ONE* **2013**, *8*, e69099.

80. Pei, M.; Luo, J.; Chen, Q. Enhancing and maintaining chondrogenesis of synovial fibroblasts by cartilage extracellular matrix protein matrilins. *Osteoarthr. Cartil.* **2008**, *16*, 1110–1117.

81. Aszodi, A.; Hunziker, E.B.; Brakebusch, C.; Fassler, R. Beta1 integrins regulate chondrocyte rotation, G1 progression, and cytokinesis. *Genes Dev.* **2003**, *17*, 2465–2479.

82. Prein, C.; Warmbold, N.; Farkas, Z.; Schieker, M.; Aszodi, A.; Clausen-Schaumann, H. Structural and mechanical properties of the proliferative zone of the developing murine growth plate cartilage assessed by atomic force microscopy. *Matrix Biol.* **2016**, *50*, 1–15.

Paper II

Article

Aggrecan Hypomorphism Compromises Articular Cartilage Biomechanical Properties and Is Associated with Increased Incidence of Spontaneous Osteoarthritis

Paolo Alberton [1,2,*]**, Hans Christian Dugonitsch** [1]**, Bastian Hartmann** [1,2,3] **, Ping Li** [1]**, Zsuzsanna Farkas** [1]**, Maximilian Michael Saller** [1] **, Hauke Clausen-Schaumann** [2,3] **and Attila Aszodi** [1,2]

[1]   Laboratory of Experimental Surgery and Regenerative Medicine, Clinic for General, Trauma and Reconstructive Surgery, Ludwig-Maximilians University, 80336 Munich, Germany; Hans.Dugonitsch@med.uni-muenchen.de (H.C.D.); bastian.hartmann@hm.edu (B.H.); Ping.Li@med.uni-muenchen.de (P.L.); Zsuzsanna.Farkas@med.uni-muenchen.de (Z.F.); Maximilian.Saller@med.uni-muenchen.de (M.M.S.); Attila.Aszodi@med.uni-muenchen.de (A.A.)

[2]   Center for Applied Tissue Engineering and Regenerative Medicine, Munich University of Applied Sciences, 80533 Munich, Germany; hauke.clausen-schaumann@hm.edu;

[3]   Center for NanoScience, Ludwig-Maximilians University Munich, 80799 Munich, Germany

[*]   Correspondence: Paolo.Alberton@med.uni-muenchen.de; Tel.: +49-89-4400-55485

Received: 1 February 2019; Accepted: 21 February 2019; Published: 26 February 2019

check for
updates

Abstract: The gene encoding the proteoglycan aggrecan (*Agc1*) is abundantly expressed in cartilage during development and adulthood, and the loss or diminished deposition of the protein results in a wide range of skeletal malformations. Furthermore, aggrecan degradation is a hallmark of cartilage degeneration occurring in osteoarthritis. In the present study, we investigated the consequences of a partial loss of aggrecan in the postnatal skeleton and in the articular cartilage of adult mice. We took advantage of the previously described *Agc1^{tm(IRES-CreERT2)}* mouse line, which allows for conditional and timely-regulated deletion of floxed, cartilage-expressed genes. As previously reported, the introduction of the CreER^{T2} cassette in the 3'UTR causes a disruption of the normal expression of *Agc1* resulting in a hypomorphic deposition of the protein. In homozygous mice, we observed a dwarf phenotype, which persisted throughout adulthood supporting the evidence that reduced aggrecan amount impairs skeletal growth. Homozygous mice exhibited reduced proteoglycan staining of the articular cartilage at 6 and 12 months of age, increased stiffening of the extracellular matrix at six months, and developed severe cartilage erosion by 12 months. The osteoarthritis in the hypomorph mice was not accompanied by increased expression of catabolic enzymes and matrix degradation neoepitopes. These findings suggest that the degeneration found in homozygous mice is likely due to the compromised mechanical properties of the cartilage tissue upon aggrecan reduction.

Keywords: aggrecan; articular cartilage; osteoarthritis; atomic force microscopy

1. Introduction

Osteoarthritis (OA) is a degenerative disorder of the synovial joints causing significant disability and morbidity in the aging population. OA is the most common cause of disability in elderly with an estimated prevalence of 10–15% of adults aged over 60. According to the United Nations, 130 million people will suffer from OA by 2050, and among them one-third being severely disabled. Genetic and numerous environmental risk factors (e.g., obesity, trauma, joint overuse) are responsible for the

etiology of OA. Despite a widespread awareness of the disease, the pathogenesis of OA is not completely understood. It is generally accepted that uncontrolled homeostasis of the extracellular matrix (ECM) produced by chondrocytes is critical for the onset of the condition. Changes in the composition and structural organization of cartilage ECM proteins may activate catabolic processes degrading proteoglycans and the heterotypic collagen II/IX/XI fibrils, which in turn alter the biomechanical properties of the tissue compromising the correct function of articular cartilage (AC), therefore laying the foundations for the establishment of the disorder.

The large aggregating protein aggrecan is the most abundant proteoglycan of the typical cartilaginous structures such us the growth plate and the articular cartilage (reviewed in [1,2]). The 250 kDa aggrecan protein core is composed of three globular (G1, G2 and G3), and two interglobular domains. The large interglobular region between the G2 and G3 domains carries about 100 chondroitin sulphate (CS) and 30 keratan sulphate (KS) chains [3]. The high negative charge density of the CS chains attracts counter ions and draw water molecules into the tissue, thus creating a positive osmotic pressure which endows articular cartilage to resist compressive forces. Aggrecan molecules form huge tertiary complexes in the cartilage ECM through interaction of the N-terminal G1 domain with hyaluronan and link protein. The KS chains interact with fibrillar collagens [4], and the C-terminal G3 domain binds to multiple ECM proteins including tenascins and fibulins [1]. Apart from creating the basis for the viscoelastic properties of cartilage, aggrecan–hyaluronan aggregates with their numerous glycosaminoglycan chains are playing important roles in cell-ECM crosstalk, binding and release of growth factors and morphogens [5,6]. In normal cartilage, aggrecan gene expression is sustained and its protein turnover relatively rapid [7,8].

The critical importance of aggrecan for endochondral bone formation and the function of permanent cartilage structures is demonstrated by numerous mutations identified in the gene coding for aggrecan in both human and various animal species (reviewed in [9]). Mutations in the human aggrecan gene (*ACAN or AGC1*) lead to a broad range of non-lethal skeletal dysplasia including spondyloepimetaphyseal dysplasia (SEMD) [10], osteochondritis dissecans with early onset of OA [11], and various short stature syndromes with accelerated bone maturation [12]. It has been recently suggested that human aggrecanopathies are mechanistically caused by *AGC1* mutations resulting either in haploinsufficiency or disruption of the cartilage structure [9]. In animals including mice, chicken and cattle, naturally occurring homozygous null or functional null mutations result in embryonic lethality, while heterozygous animals display milder skeletal dysplasias [1,9]. In mice, the *cmd* (*cartilage matrix deficiency*) and the *cmd–bc* deletion mutations lead to truncated aggrecan molecules or the lack of aggrecan, respectively, and the lethal phenotype is characterized by disproportionate dwarfism, short snout, protruding tongue and enlarged abdomen [13,14]. Heterozygous *cmd/+* mice are hypomorphic showing a reduced aggrecan mRNA level in embryonic limb cartilage (81% of the wild type), and develop postnatal dwarfism, spinal misalignment and age-associated intervertebral disc degeneration [15].

In modern functional genetics, generation of mouse lines which allow inducible gene deletion is of great importance for studying gene function and generating animal models for human disorders. Recently, the $Agc1^{tm(IRES-CreERT2)}$ mouse line, further referred to here as $Agc1^{CreERT2}$, has been established for inducible, conditional inactivation of genes floxed with *loxP* elements in chondrocytes [16]. In this model, a transgene encoding the fusion polypeptide of the Cre recombinase and a mutant ligand binding domain of the estrogen receptor ($CreER^{T2}$) has been introduced (knocked in) into the 3' untranslated region (UTR) of the endogenous mouse *aggrecan* gene (*Agc1*). These mice represent a precious tool, allowing the inducible inactivation of genes involved in cartilage degenerative disorders in a spatially and temporally coordinated manner after tamoxifen administration [17–26]. However, we have noticed during breeding of the line in our animal facility that the homozygous knock-in mice develop a postnatal dwarf phenotype. Indeed, it has been recently published that $Agc1^{CreERT2/CreERT2}$ mice have reduced body weight and length, and shorter endochondral bones compared to wild type and heterozygous mice [27]. Histological analysis indicated reduced height

of the growth plate and the articular cartilage. Further molecular and biochemical investigation revealed that the homozygous animals express about 50% of both aggrecan mRNA and protein in cartilage compared to the normal levels in wild type [27]. It was suggested that the decreased *Agc1* expression may have been caused by the deletion of a 760 bp region of the 3'UTR, disrupting putative regulatory regions or by the negative effect of the targeting construct-derived *pgk* promoter on the activity of the endogenous *Agc1* promoter [27]. As a consequence of the disturbed skeletal growth in *Agc1^{CreERT2/CreERT2}* mice, only heterozygous *Agc1^{CreERT2/+}* mice were suggested to be used for conditional deletion of the floxed genes in chondrocytes [27].

In this study, we extended the analysis of the *Agc1^{CreERT2}* mice for the function of the articular cartilage. We found that *Agc1^{CreERT2/CreERT2}* mice develop severe cartilage erosion of the knee joint at 12 months of age. Importantly, heterozygous *Agc1^{CreERT2/+}* mice also exhibited a tendency for increased articular cartilage destruction compared with wild type animals. Applying nanoscale indentation-type atomic force microscopy (IT-AFM) to characterize cartilage biomechanics, we demonstrated that *Agc1^{CreERT2/CreERT2}* mice have stiffer cartilaginous ECM in the superficial, middle and deep zones of the AC compared to control and heterozygous mice. We believe that this alteration in biomechanical properties compromises the basic cushioning function of AC, eventually predisposing mice to develop spontaneous OA. Thus, the *Agc1^{CreERT2/CreERT2}* mouse is a valuable model to investigate articular cartilage degradation in dependence of aggrecan level.

2. Results

2.1. Agc1^{CreERT2/CreERT2} Dwarf Phenotype Persist through the Adulthood

In our breeding colony, we have observed that, after two weeks of age, both male and female *Agc1^{CreERT2/CreERT2}* mice were consistently smaller compared to wild type confirming the previously reported early postnatal dwarfism between one and three months [27]. We did not notice any other gross visual abnormalities up to one year of age: the *Agc1^{CreERT2/CreERT2}* mice had apparently normal gait and physical activity. X-ray analysis confirmed the dwarf phenotype of *Agc1^{CreERT2/CreERT2}* mice at 6 and 12 months of age without an apparent sign of spinal misalignment (Figure 1A).
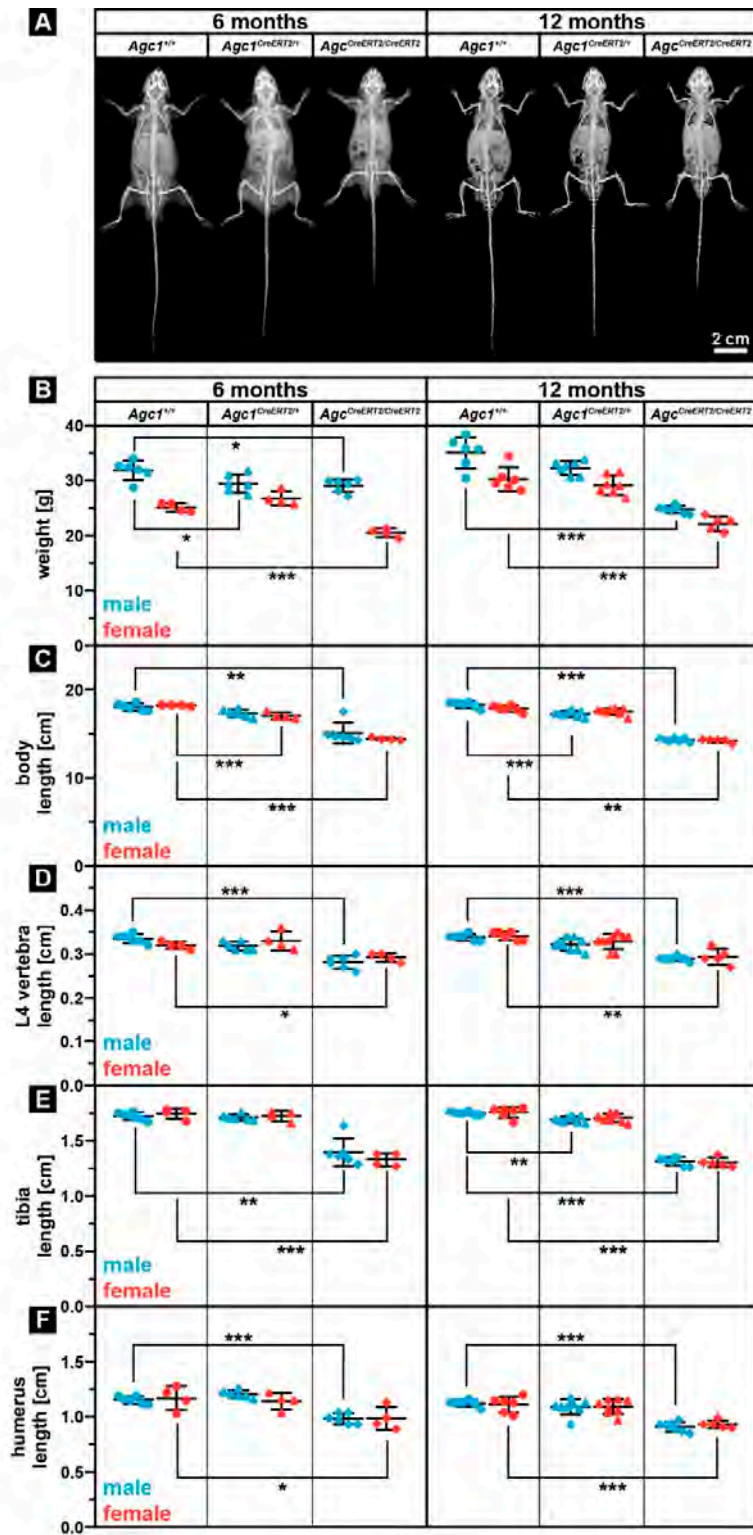
Figure 1. *Agc1^{CreERT2/CreERT2}* mice develop dwarfism which is maintained after skeletal maturation.
(A) representative X-ray images of *Agc1^{+/+}*, *Agc1^{CreERT2/+}* and *Agc1^{CreERT2/CreERT2}* mice at 6 and 12 months of age. (B–F) analysis of body weight (B), body length (C), L4 vertebra length (D), tibia length (E) and humerus length (F) at 6 and 12 months of age. Bars represent the mean ± standard deviation (SD). n > *Agc1^{+/+}*: 6(m)/4(f); *Agc1^{Cre/+}*: 6(m)/4(f); *Agc1^{Cre/Cre}*: 6(m)/4(f) at six months; and n > *Agc1^{+/+}*: 6(m)/6(f); *Agc1^{Cre/+}*: 7(m)/7(f); *Agc1^{Cre/Cre}*: 7(m)/5(f) at 12 months. Statistical significance calculated by one-way ANOVA where * $p < 0.5$; ** $p < 0.01$; *** $p < 0.001$.

In order to assess body parameters after the skeletal maturation, we have analyzed body weight, body length, the length of the fourth lumbar (L4) vertebra, and the length of long bones of the appendicular skeleton (tibia, femur and humerus) of homozygous $Agc1^{CreERT2/CreERT2}$, heterozygous $Agc1^{CreERT2/+}$ and wild type $Agc1^{+/+}$ animals at ages of 6 and 12 months. The body weight of both genders was significantly lower in $Agc1^{CreERT2/CreERT2}$ mice compared to $Agc1^{+/+}$ mice (males: 9% and 29% reduction at 6 and 12 months, respectively; females: 18% and 27% reduction at 6 and 12 months, respectively) (Figure 1B). Heterozygous $Agc1^{CreERT2/+}$ mice showed the tendency for reduced weight, which, however, only reached significance in 6-month-old males (7.6% reduction compared to wild type). X-ray micrographs were used to measure the length of the body (from snout to the end of the tail), the L4 vertebra, tibia, femur, and humerus, as characteristics for the size of the skeleton (Figure 1C,F and not shown). The body length of both gender was significantly reduced in $Agc1^{CreERT2/CreERT2}$ mice compared to $Agc1^{+/+}$ mice (males: 17% and 22% reduction at 6 and 12 months, respectively; females: 21% and 20% reduction at 6 and 12 months, respectively) (Figure 1C). Similarly, we found a statistical significant decrease in the length of the L4 vertebra when comparing $Agc1^{CreERT2/CreERT2}$ homozygous to control mice of both sex (males: 16% and 14% reduction at 6 and 12 months, respectively; females: 9% and 14% reduction at 6 and 12 months, respectively) (Figure 1D). Regarding long bones, the length of the total tibia was significantly decreased in both male and female $Agc1^{CreERT2/CreERT2}$ mice comparing to $Agc1^{+/+}$ mice (males: 17% and 22% reduction at 6 and 12 months, respectively; females: 21% and 20% reduction at 6 and 12 months, respectively) (Figure 1E). A similar trend was also observed in the length of the femur (data not shown). In the forelimbs, the length of the humerus was significantly reduced again in both male and female homozygous $Agc1^{CreERT2/CreERT2}$ mice compared to controls (males: 15% and 19% reduction at 6 and 12 months, respectively; females: 16% reduction at both 6 and 12 months) (Figure 1F). Interestingly, we found that heterozygous $Agc1^{CreERT2/+}$ mice occasionally exhibited significantly reduced skeletal parameters compared to $Agc1^{+/+}$ animals: 6% decreased body length in females at six months; 5.7% decreased body length in males at 12 months; 3.4% reduced tibia length in 12-month-old males (Figure 1C,E). Taken together, our results indicate that the dwarf phenotype of the $Agc1^{CreERT2/CreERT2}$ mice is maintained after the end of skeletal maturation (about four months of age) and there is no compensatory catch up during skeletal growth. It is important to note that heterozygous $Agc1^{CreERT2/+}$ mice displayed the tendency for reduced body weight, body length and tibia length at almost all investigated postnatal stages.

2.2. $Agc1^{CreERT2/CreERT2}$ Mice Are Characterized by Reduced Aggrecan Expression

As the expression level of aggrecan could crucially influence the phenotype, we have analyzed aggrecan mRNA and protein by quantitative RT-PCR and immunohistochemistry, respectively, in all genotypes. We have isolated total RNA from newborn rib cartilage (n = 3 for each genotype) and performed qPCR using $Agc1$-specific TaqMan probe. The mRNA expression was reduced to 74% and 64% of the control in $Agc1^{CreERT2/+}$ and $Agc1^{CreERT2/CreERT2}$ mice, respectively, indicating that insertion of the $CreER^{T2}$ transgene into the 3´UTR affect total $aggrecan$ gene expression in both homozygous and heterozygous knock-in animals (Figure 2A).

Next, we performed immunohistochemical staining in knee joints of 6- and 12-month-old animals using antibody against mouse aggrecan core protein (Figure 2B). The articular cartilage of the femur and tibia showed strong, predominantly pericellular/territorial matrix localization of the aggrecan protein in $Agc1^{+/+}$ mice at 6 and 12 months of age. In $Agc1^{CreERT2/CreERT2}$ mice, aggrecan was greatly reduced at 6 and 12 months of age, whereas, in $Agc1^{CreERT2/+}$ mice, aggrecan immunoreactivity was comparable to wild type at six months and decreased at 12 months. As the level of aggrecan core protein in the tissue correlates with the number of CS and KS chains, we also stained the knee joint sections with Toluidine blue at pH = 2.5 to detect sulphated glycosaminoglycans (sGAGs) (Figure 2B). The staining was intense in $Agc1^{+/+}$ and $Agc1^{CreERT2/+}$ cartilage, while the signal was reduced in $Agc1^{CreERT2/CreERT2}$ cartilage. Expression of cartilage fibril component type II collagen in the articular cartilage was comparable in each genotype.

Taken together, our expression analyses confirmed that *Agc1*^{CreERT2/CreERT2} mice are hypomorph, characterized by reduced *Agc1* RNA expression in primary chondrocytes isolated from newborn rib cartilage and greatly diminished aggrecan protein deposition in adult articular cartilage.
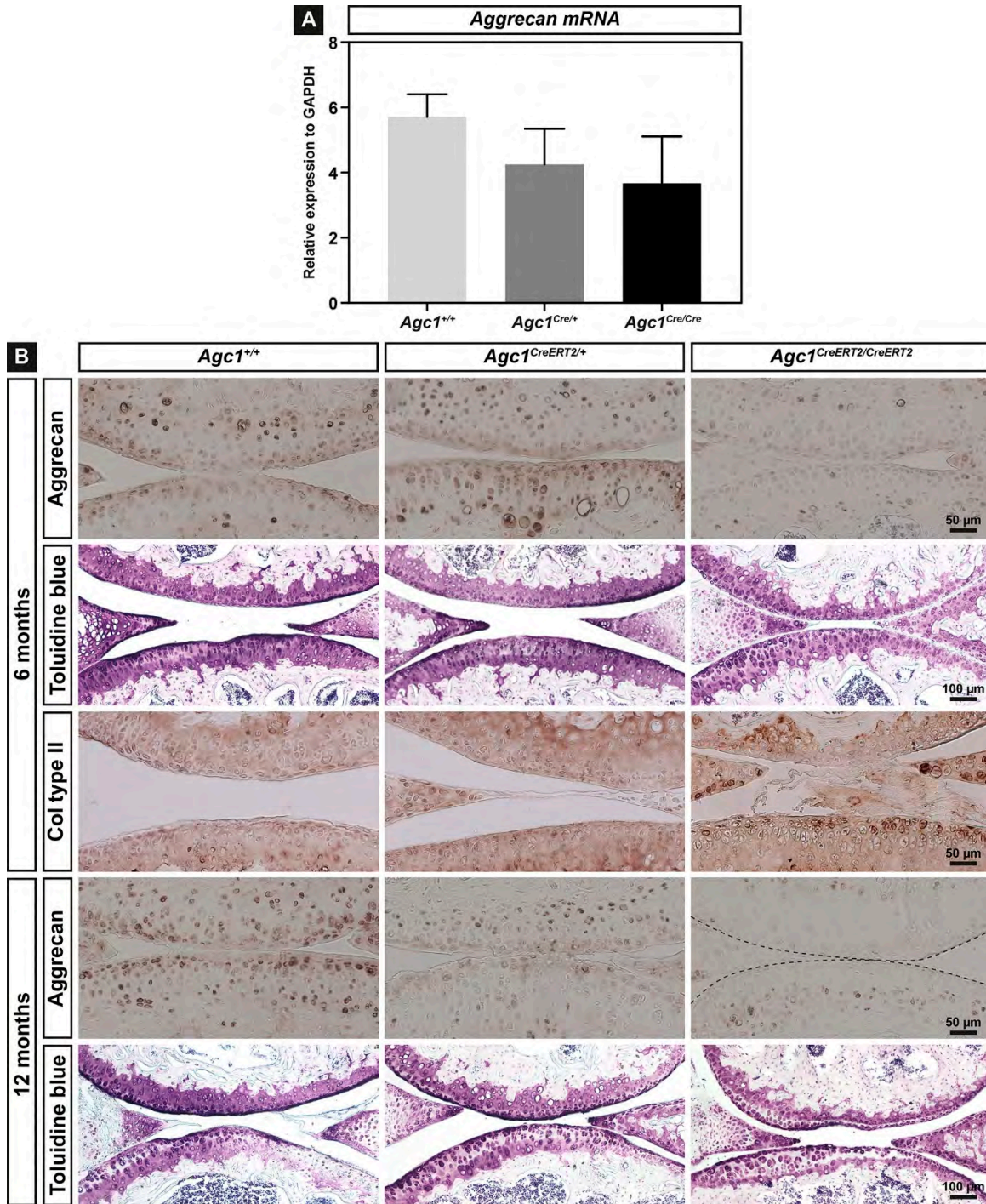

Figure 2. Expression of aggrecan in cartilage of mice carrying the *CreER*^{T2} transgene. (**A**) relative *Agc1*^{CreERT2/CreERT2}, mice. The mean values ± SD from three independent animals of each genotype are shown; (**B**) sagittal sections of the knee joint were stained with antibodies against aggrecan, collagen type II, and with Toluidine blue. n = 5 mice per genotype

2.3. Aggrecan Depletion Results in Stiffening of the Articular Cartilage

Reduced deposition of aggrecan and sulphated GAGs in the cartilage of Agc1$^{CreERT2/CreERT2}$ micev may result in alteration of the biomechanical properties of the tissue. In order to assess this possibility, we applied nano-scaled indentation-type atomic force microscopy (IT-AFM) on native knee sections and recorded the compressive stiffness in the various zones (superficial, middle and deep) of the AC at six months of age (Figure 3A,B). For all measurements, we observed a bimodal distribution of the Young's moduli, where the first peak (E1) on the histograms represents the softer proteoglycan moiety and the second peak (E2) is attributed to the stiffer collagen fibrils (Figure 3B) [28–30]. We found that, in the Agc1$^{CreERT2/CreERT2}$ mice, both peaks were shifted towards 60%–80% higher values in each AC zone compared to Agc1+/+ mice indicating a general stiffening of the cartilage extracellular matrix. The values in wild type and Agc1$^{CreERT2/CreERT2}$ superficial zone were E1 = 285.47/E2 = 484.61 kPa vs. E1 = 485.95 kPa/E2 = 800.04 kPa; in the middle zone were E1 = 374.30 kPa/E2 = 673.63 kPa vs. E1 = 699.07 kPa/E2 = 1.08 MPa; in the deep zone were E1 = 614.58 kPa/E2 = 1.01 MPa vs. E1 = 1.06 MPa/E2 = 1.84 MPa. In contrast, Agc1$^{CreERT2/+}$ mice showed comparable stiffness values with Agc1+/+ mice, in a range of 4% to 15% difference. All together, these data indicate that reduced amount of aggrecan in Agc1$^{CreERT2/CreERT2}$ mice severely compromises nanomechanical properties of the matrix, making the articular cartilage stiffer.
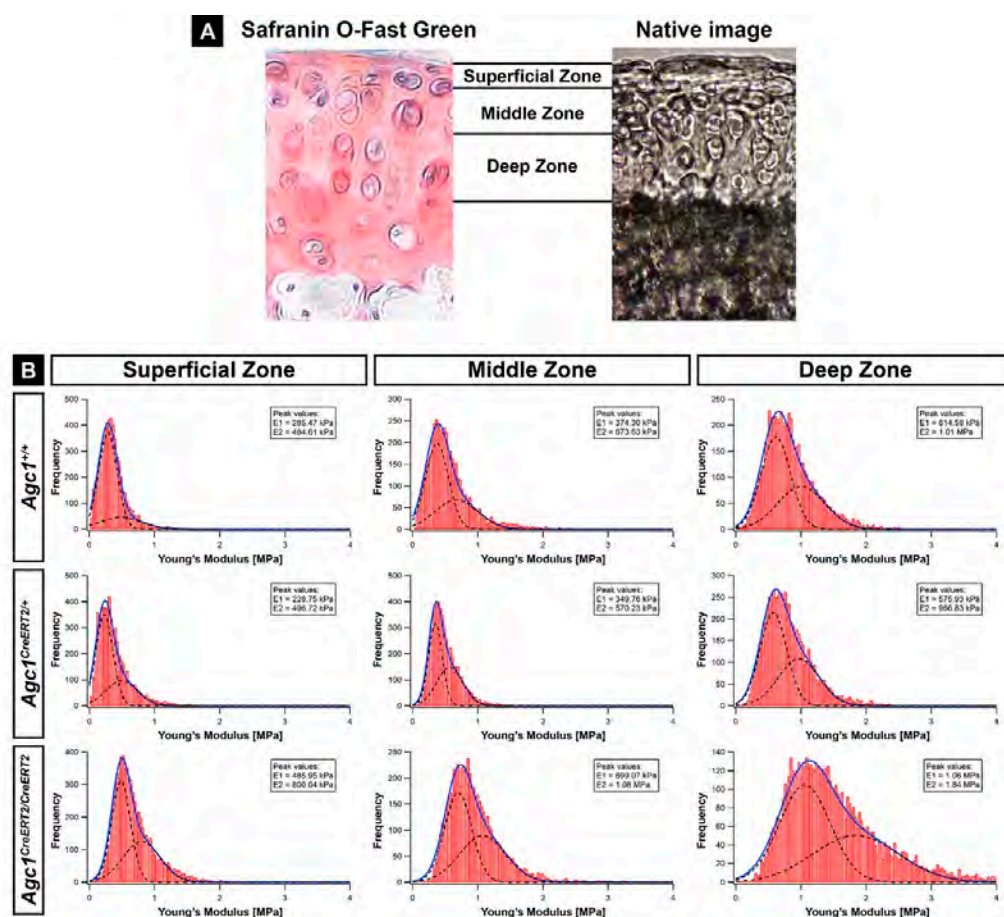

Figure 3. IT-AFM reveals stiffening of articular cartilage in *Agc1$^{CreERT2/CreERT2}$* mice at six months of age. (A) Safranin Orange /Fast Green staining and an overview image of a native articular cartilage section show the zones assessed by IT-AFM (40× magnification); (B) histograms showing the stiffness distribution in various zones of the tibial plateau cartilage determined by nano-indentation (n = 3 animals in each group). On each histogram, the solid line represents the sum of two Gaussian functions, whereas the dashed lines indicate individual fits. The first and the second stiffness peaks (E1 and E2) represent the proteoglycan gel and the collagen fibrils, respectively. n = 3 animals per genotype

2.4. Agc1CreERT2/CreERT2 Mice Develop Spontaneous Osteoarthritis during Aging

The development of articular cartilage deterioration was examined in control, heterozygous and homozygous knock-in animals at 6 and 12 months of age (Figure 4A). Safranin O-Fast Green staining on serial knee joint sections revealed normal or mildly affected articular cartilage at six months in each genotypes. At 12 months, all male $Agc1^{CreERT2/CreERT2}$ mice (n = 7) showed complete degeneration of the articular cartilage with exposure of the subchondral bone (arrow). At this age, wild type and heterozygous $Agc1^{CreERT2/+}$ mice frequently exhibited clefts extending into the calcified zone (arrow). Quantification of the cartilage damage according to the Osteoarthritis Research Society International (OARSI) histopathological recommendations (Figure 4B) revealed mildly decreased mean score in male $Agc1^{CreERT2/+}$ mice compared to control and homozygous knock-in mice at six months of age. At 12 months, male but not female $Agc1^{CreERT2/CreERT2}$ mice displayed significantly increased mean erosion score compared to wild type (males: 6.000 vs. 3.000, ** $p < 0.01$; females: 3.100 vs. 2.000). Control and heterozygous $Agc1^{CreERT2/+}$ mice showed similar mean cartilage erosion scores (male: 3.000 vs. 3.285; female: 2.000 vs. 2.333) in both genders. However, male heterozygous $Agc1^{CreERT2/+}$ mice had the tendency to develop more severe osteoarthritic damages exhibiting 25–50% erosion or complete eburnation of the AC surface. functions, whereas the dashed lines indicate individual fits. The first and the second stiffness peaks (E1 and E2) represent the proteoglycan gel and the collagen fibrils, respectively. n = 3 animals per genotype.
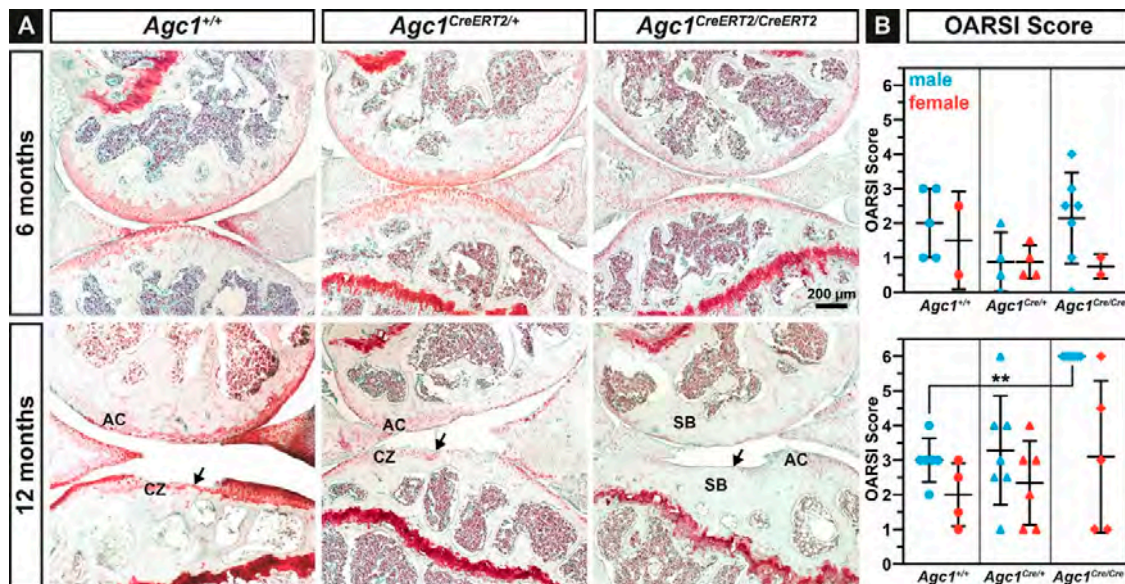
Figure 4. $Agc1^{CreERT2/CreERT2}$ mice exhibit severe cartilage erosion at 12 months of age. (A) representative images of Safranin O/Fast Green stained knee articular cartilage of 6 and 12 months old $Agc1^{+/+}$, Agc1$^{CreERT2/+}$ and $Agc1^{CreERT2/CreERT2}$ mice. Arrows indicate severe degeneration of the articular cartilage. Abbreviations: AC, articular cartilage; CZ, calcified zone; SB, subchondral bone. (B) quantification of spontaneous cartilage degeneration using the OARSI scoring system. Bars represent mean ± SD. n = $Agc1^{+/+}$: 5(m)/2(f); $Agc1^{Cre/+}$: 4(m)/4(f); $Agc1^{Cre/Cre}$: 7(m)/2(f) at six months; and n = $Agc1^{+/+}$: 6(m)/4(f); $Agc1^{Cre/+}$: 7(m)/6(f); $Agc1^{Cre/Cre}$: 7(m)/5(f) at 12 months. Statistical significance calculated by one-way ANOVA, where ** $p < 0.01$

In order to assess the possibility that the onset of cartilage degradation in the hypomorphic mice was partially induced by the different cartilage volume at the load-bearing regions of the knee joint, we measured total articular cartilage thickness in 6-month-old animals. We found that the thickness of both the medial and lateral tibial plateau was slightly reduced in the hypomorphic mice compared to control; however, the difference was statistically not significant. At the medial plateau, the AC thickness was 128.94 ± 11.33 μm for wild type (n = 5 animals), 114.46 ± 15.74 μm for $Agc1^{CreERT2/+}$ mice (n = 7) and 116.96 ± 12.92 μm for $Agc1^{CreERT2/CreERT2}$ mice (n = 6). At the lateral tibial plateau, the AC thickness was 107.18 ± 7.65 μm for wild type, 102.43 ± 5.48 μm for $Agc1^{CreERT2/+}$ mice and

105.54 $\pm$ 10.33 μm for $Agc1^{CreERT2/CreERT2}$ mice. These data indicate that articular cartilage thickness is apparently not affected by the decreased aggrecan levels, and the thickness of the cartilage does not contribute to cartilage degeneration in the hypomorphic mice *per se*.

2.5. Higher Incidence of OA in $Agc1^{CreERT2/CreERT2}$ Mice Is Not Correlated with Increased AC Catabolism

The reduced amount of aggrecan and the stiffer biomechanical environment in the articular cartilage might disturb metabolism inducing upregulation of catabolic enzymes which breakdown the ECM. Therefore, we have analyzed the expression of several proteases, which are able to degrade collagens or aggrecan by immunohistochemistry at 12 months of age. We found comparable expression of Matrix Metalloproteinase-13 (MMP-13), a typical collagenase upregulated during OA, and the aggrecanase A Disintegrin and Metalloproteinase with Thrombospondin Motifs-5 (ADAMTS-5) in each genotype (Figure 5A). Similarly, immunostaining for MMP-3, MMP-9 and ADAMTS-4 showed nodifference in the expression of these proteases in the articular cartilage of the $Agc1^{CreERT2/CreERT2}$, $Agc1^{CreERT2/+}$ and $Agc1^{+/+}$ mice (not shown). Immunostaining with the Collagen Type I and II Cleavage (C1,2C) antibody (Figure 5A) and the Collagen Type II Cleavage (C2C) Elisa assay (Figure 5B), which can detect collagen degradation products on tissue sections and in the urine, respectively, indicated no difference for collagen breakdown between the genotypes. Interestingly, when we stained the articular cartilage sections with an antibody recognizing the MMP-driven aggrecan degradation neo-epitope VIDIPEN, we found gradually decreasing immunoreactivity in $Agc1^{CreERT2/+}$ and $Agc1^{CreERT2/CreERT2}$ mice compared to wild type.
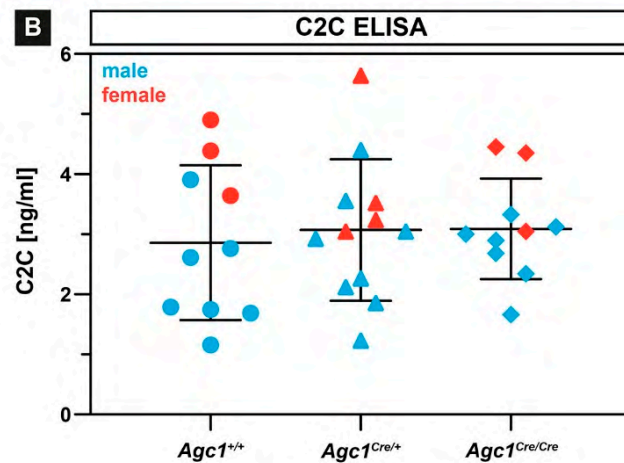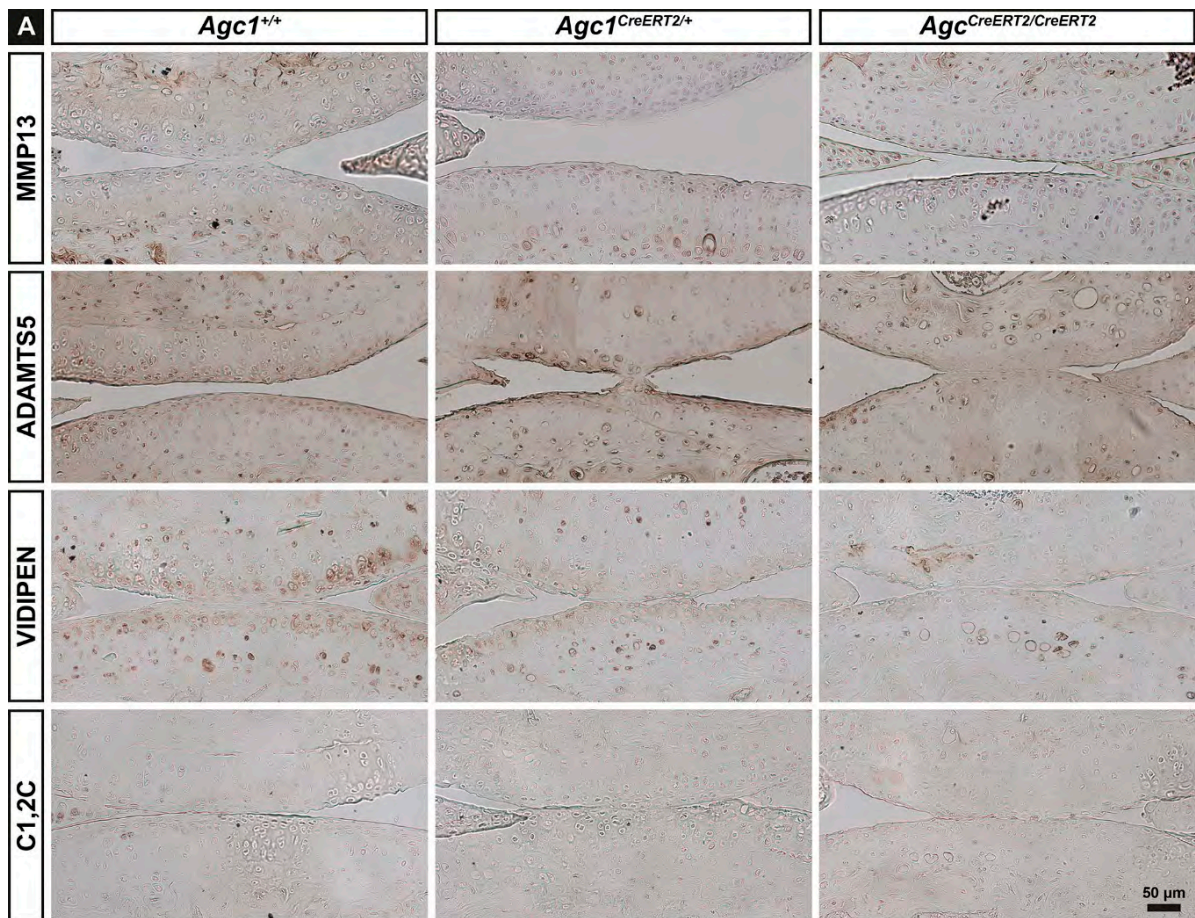
Figure 5. *Agc1^{CreERT2/CreERT2}* mice develop dwarfism which is maintained after skeletal maturation. (A) representative X-ray images of *Agc1^{+/+}*, *Agc1^{CreERT2/+}* and *Agc1^{CreERT2/CreERT2}* mice at 6 and 12 months of age. (B–F) analysis of body weight (B), body length (C), L4 vertebra length (D), tibia length (E) and humerus length (F) at 6 and 12 months of age. Bars represent the mean ± standard deviation (SD). n > *Agc1^{+/+}*: 6(m)/4(f); *Agc1^{Cre/+}*: 6(m)/4(f); *Agc1^{Cre/Cre}*: 6(m)/4(f) at six months; and n > *Agc1^{+/+}*: 6(m)/6(f); *Agc1^{Cre/+}*: 7(m)/7(f); *Agc1^{Cre/Cre}*: 7(m)/5(f) at 12 months. Statistical significance calculated by one-way ANOVA where * $p < 0.5$; ** $p < 0.01$; *** $p < 0.001$.

and permanent cartilaginous tissues. In this study, we have investigated the consequence of decreased aggrecan expression for articular cartilage function by analyzing the hypomorphic $Agc1^{CreERT2}$ mouse line. We found that reduced aggrecan leads to increased stiffness of the articular cartilage, which in turn results in severe age-associated osteoarthritis.

Mutations in the human aggrecan gene lead to aggrecanopathies, an increasing group of skeletal dysplasias ranging from mild idiopathic short stature to severe chondrodysplasias [9]. Missense mutations typically found in the C-terminal G3 domain of the aggrecan core protein are likely to disrupt interactions with other cartilage ECM proteins. The phenotypic spectrum of these neomorphic mutations includes mild short stature with accelerated bone maturation [12]; osteochondritis dissecans with short stature and early-onset osteoarthritis [11]; and extreme short stature with craniofacial and spinal abnormalities [10]. Heterozygous nonsense mutations accumulated at the G1–G2 and CS1–CS2 domains introduce premature termination codon resulting in the formation of truncated proteins or haploinsufficiency due to nonsense-mediated mRNA degradation [9,31]. These dominant mutations lead to spondyloepiphyseal dysplasia (SED) Kimberly type characterized by proportionate short stature and severe premature osteoarthritis [32] or idiopathic short stature associated with early-onset OA [12,33]. Null or functional null loss of function mutations in mice (cmd, cmd–bc) [13,14], chicken (nanomelia) [34,35] or cattle (Dexter bulldog dwarfism) [36] are perinatal lethal due to severely abnormal skeletal growth caused by the lack of aggrecan in the cartilage ECM.

Although the findings in human and other species indicate that the absence or reduction of the aggrecan in the cartilage ECM leads to chondrodysplasias and osteoarthritis, the correlation between the level of aggrecan expression and the clinical manifestation of the diseases is not clear. To date, only two mouse models have been investigated in order to link aggrecan gene expression to skeletal phenotype. The naturally occurring cartilage matrix deficiency (cmd) is caused by a 7 bp deletion in exon 5 of $Agc1$ which leads to a premature stop codon in exon 6 and formation of a short, truncated protein [13]. Homozygous (cmd/cmd) mice die at birth due to severe chondrodysplasia characterized by a cleft palate, abnormal tracheal cartilage formation and dwarfism [13] caused by the loss of the normal columnar structure of the growth plate [37]. Heterozygous cmd/+ mice, however, survive and develop moderate proportional dwarfism at around one month of age. Furthermore, cmd/+ mice exhibit misalignment of the spine at one year of age, which eventually results in premature death at 19 months due to eating difficulties [15]. In the $Agc1^{CreERT2}$ mouse model, the 3´ UTR of the aggrecan gene was disrupted by knocking in a Cre-ER^{T2} construct to generate an inducible, cartilage-specific deleter mouse line [16]. Although the original publication did not describe a phenotype, it has later been reported that $Agc1^{CreERT2/CreERT2}$ mice develop dwarfism by one month of age associated with shortening of the growth plate [27]. Now, here we show that the dwarf phenotype exists after the end of skeletal maturation having about 10–20% smaller skeletal elements of the $Agc1^{CreERT2/CreERT2}$ mice compared to wild type at 6 and 12 months of age (Figure 1). The size reduction affected both the axial and the appendicular skeleton. Interestingly, we observed a mild, but sometimes statistically significant, 3% to 6% reduction of the skeleton and body weight of $Agc1^{CreERT2/+}$ mice indicating that the skeletally mature heterozygous animals also exhibit a very slight dwarfism.

Insertion of an exogenous targeting construct with selection cassette into intronic or untranslated regions of an endogenous gene could disrupt important regulatory domains, affect splicing or directly influence promoter activity of the endogenous or neighboring genes [38–42]. The interference with the endogenous gene activity leads to hypomorphic alleles with reduced mRNA and protein expression, which is proved to be useful to study the effect of gene doses in various disorders [38,39,43]. It has been previously reported that insertion of the $CreER^{T2}$ targeting construct into the $Agc1$ gene causes the lack of 760 bp of the 3´-UTR. This could affect RNA stability resulting in 20% and 50% reduction of aggrecan mRNA in adult, three-month-old knee epiphyseal cartilage of heterozygous and homozygous knock-in mice, respectively [27]. We found that $Agc1$ mRNA levels were reduced in newborn rib cartilage to ~74% in $Agc1^{CreERT2/+}$ mice and to 64% in $Agc1^{CreERT2/CreERT2}$ mice compared to the wild type levels (Figure 2A). These observations indicate that disruption of the 3´UTR by the transgene

insertion causes a similar reduction of the *Agc1* mRNA levels in chondrocytes regardless of the age or location of the cartilage tissue. In the *cmd* model, the *Agc1* mRNA in embryonic limb cartilage is reduced to 41% in *cmd/cmd* mice and to 81% in *cmd/+* mice [15]. Although the direct comparison between the haploinsufficiency *cmd/+* model and the hypomorph *Agc1*^{CreERT2} model is difficult due to the different nature of the causative mutations, it is reasonable to speculate that about 25–50% reduction in the normal *Agc1* mRNA level is sufficient to generate a mild dwarf phenotype in mice. The reduction of mRNA expression in this range affects the deposition of the aggrecan protein into the ECM as demonstrated by 13% decreased the CS level in spinal cartilage from *cmd/+* mice [15], ~50% less aggrecan in knee joint extracts from *Agc1*$^{CreERT2/CreERT2}$ mice [27] and the greatly reduced aggrecan immunoreactivity in the articular cartilage of *Agc1*$^{CreERT2/CreERT2}$ knee joints (Figure 2B).

The most dramatic phenotype we found in the adult *Agc1*$^{CreERT2/CreERT2}$ mice is the severe degeneration of the knee articular cartilage typical for late stage osteoarthritis (Figure 4). Since OA was not described in aging *cdm/+* mice, we hypothesise that *Agc1*$^{CreERT2/CreERT2}$ mice have a greater loss of aggrecan in the articular cartilage which impairs its function and eventually leads to the complete erosion of the AC surface in males by 12 months of age. The aggrecan–hyaluronan aggregates have a crucial role for maintaining the biomechanical properties of the articular cartilage by immobilizing a vast amount of negative charges and generating an osmotic swelling pressure, which provides the tissue with resistance against compressive forces [3]. *Agc1*$^{CreERT2/CreERT2}$ mice displayed reduced aggrecan and GAG content in the knee joint suggesting alterations in the biomechanics of the articular cartilage. Applying nanoscale IT-AFM, we observed prominent stiffening of the AC from *Agc1*$^{CreERT2/CreERT2}$ mice (Figure 3B) at six months of age, when histological differences of AC degeneration were not evident between the genotypes (Figure 4B). The increased stiffness was detected in the superficial, middle and deep zones implying a systemic hardening of the whole articular cartilage.

In normal cartilage, the swelling pressure is balanced by the tensile force of the collagen network and modifying the collagen fibril-hydrated proteoglycan ratio could affect the swelling and biomechanical properties of the tissue. Earlier studies have shown that porcine articular cartilage incubated in hypotonic salt solution or digested with proteoglycan-degrading enzymes has increased cartilage nanostiffness [28,44]. Accordingly, the reduced negative charge density of the sGAG chains due to the decreased aggrecan level in the homozygous hypomorphic mice could result in reduced tissue hydration, decreased swelling pressure and increased constraining matrix stress, which in turn elevates cartilage stiffness. It is important to note, however, that the imbalance between osmotic swelling pressure and the tensile forces apparently does not affect cartilage volume, as the thickness of the tibial articular cartilage was not significantly altered in the *Agc1*$^{CreERT2/CreERT2}$ mice.

We have previously shown that nanoscale indentation is a sensitive tool to assess cartilage biomechanical properties of the growth plate, the articular cartilage and the intervertebral disc [29,30,45–47]. We showed that IT-AFM depicts subtle biomechanical differences between wild type and genetically modified mice carrying mutations, which affect the collagen network [45–47] or the proteoglycans [30]. The method is capable of resolving the biomechanical properties of the collagen fibrils and the entrapped proteoglycan gel resulting in a bimodal stiffness distribution on the recorded histograms [28,29]. We observed a shift for the stiffness of both the collagens and the proteoglycans in the *Agc1*$^{CreERT2/CreERT2}$ mice compared to wild type and *Agc1*$^{CreERT2/+}$ mice. This general increase in stiffness of the major components of the cartilage matrix could lead to a rigid AC surface, which is more susceptible for mechanical load-induced degradation. We have previously found that mice lacking collagen IX, an essential component of the heterotypic cartilage collagen fibrils, also display increased nanostiffness of the hip articular cartilage before obvious signs of joint degeneration and the onset of osteoarthritis [45]. In human AC, nanostiffness is increasing by age due to GAG loss-induced dehydration of the proteoglycan moiety [45] or stiffening of the collagen fibrils [48] and could predispose for OA. However, disintegration of the cartilage extracellular matrix

(e.g., the collagen meshwork) during the onset and progression of OA is accompanied by decreased compressive stiffness in both animal models and human patients [45,49,50].

During the course of OA, usually degradation of aggrecan followed by breakdown of the collagen network are critical steps for progressive cartilage destruction. In $Agc1^{CreERT2/CreERT2}$ mice, the reduced level of aggrecan apparently does not affect cartilage metabolism as demonstrated by the normal expression of MMP-13, ADAMTS-5 and collagen and aggrecan degradation neoepitopes (Figure 5). These findings suggest a physical activity-induced "wear and tear" mechanism for destruction of the mechanically abnormal AC in the $Agc1^{CreERT2/CreERT2}$ mice.

Epidemiological studies have shown that the prevalence, incidence and severity of osteoarthritis are higher in postmenopausal women than men due to hormonal, anatomical and genetic factors [51,52]. In murine, however, sex hormones, body weight, behavior and activity differences between genders lead to higher incidence of joint degeneration in male mice in both age-associated and experimentally-induced osteoarthritis models [53–55]. In line with this evidence, the cartilage destruction was more severe in male $Agc1^{CreERT2/CreERT2}$ mice than in female mice implying that physical activities (e.g., fighting) and high body weight could worsen the condition.

In summary, we have demonstrated that the hypomorphic $Agc1^{CreERT2/CreERT2}$ mice develop age-associated OA characterized by severe erosion of the articular cartilage by 12 months of age. The phenotype was associated with stiffening of the AC, indicating that aggrecan level crucially affects biomechanical properties of the cartilage matrix. As heterozygous mice occasionally show a tendency for reduced length of skeletal elements and increased cartilage destruction, we advise the cartilage field for a careful interpretation of experiments with cartilage specific-deletion of floxed genes using the $Agc1^{CreERT2}$ line. On the other hand, these hypomorphic mice are ideal models to study aggrecan gene doses and skeletal phenotype correlation through the entire postnatal life with implications for human aggrecanopathies.

4. Materials and Methods

4.1. Mouse Model and Husbandry

$Agc1^{tm(IRES-CreERT2)}$ [16] were purchased from the Jackson Laboratory (JAX stock #019148). Upon arrival, mice were bred with 129/Sv outbred mice for at least two generations. Mice were housed in groups of 2–4 per cage and received food and water *ad libitum*. They were maintained in a temperature- and air- controlled environment, with 12 h light/dark cycle. Animals were handled and housed according to the federal and institutional guidelines for the care and use of laboratory animals, approved by the Central Animal Facility of the LMU Munich and the government of Upper Bavaria (Application number: 55.2-1-54-2532-15-2016). For the sake of simplicity, control, heterozygous and homozygous mice are denoted as $Agc1^{+/+}$, $Agc1^{CreERT2/+}$ and $Agc1^{CreERT2/CreERT2}$, respectively. Newborn, 6- and 12-month-old male and female mice were included in the study. Genotyping was performed according to the Jackson Laboratory protocol. Mice were sacrificed via cervical dislocation and tissue collection performed *post mortem*.

4.2. Radiography and Morphometry

X-ray images of euthanized mice were taken with a Faxitron X-ray cabinet (model 43855A) at 35 kV, 2 mA and 2 sec exposure time. Total body length (from the snout to the end of the tail) and the length of the skeletal elements (4th lumbar vertebra, tibia, femur and humerus) were analyzed with the distance measurement plug-in of the syngo Imaging XS-VA60B software (Siemens, Erlangen, Germany).

4.3. Sample Preparation

Hind limbs of euthanized mice were de-skinned and partially cleaned from the muscles around the knee joints. For histology and immunohistochemistry, knee joints from the left side were fixed in 4% paraformaldehyde (PFA) in phosphate buffered saline (PBS) pH 7.4 (Sigma-Aldrich, Taufkirchen,

Germany), overnight at 4 °C. The next day, samples were washed 3 times in PBS and afterwards decalcified for approximately 4 weeks in a 20% ethylenediaminetetraacetic acid (EDTA)/PBS pH 8.0 solution (Sigma-Aldrich). Decalcified specimens were washed 3 times in PBS, then dehydrated through an ascending row of ethanol, cleared in xylol and finally embedded in paraffin. Samples were cut on a Rotary Microtome HM360 in 8 μm sagittal sections and placed on Superfrost plus glass slides (Thermo Scientific, Madison, WI, USA). For AFM measurements, the correspondent right knee joints were directly enclosed in Tissue-Tek cryomedia (Sakura, Zoeterwoude, NL, USA) on the base of plastic disposable cassettes, and gradually frozen by transferring them on a chilled copper plate placed on dry ice. Sagittal sections of 30 μm were cut with the aid of adhesive tape (as described in [29]) using a Microm HM500 cyostat (Thermo Scientific) and kept at −20 °C until use.

4.4. Histology

For the histological examination of proteoglycan content, Toluidine blue and Safranin O/Fast Green staining were performed. For Toluidine blue staining, tissue sections were deparaffinized, rehydrated and incubated for 10 min in 0.1% Toluidine blue in toluidine buffer pH 2.5. Excess stain, was adsorbed with Whatman paper and then slides were immersed in a 2% $K_3Fe(CN_6)$/dH2O solution for 3 min. Finally, sections were directly mount with Roti-histokit (Roth, Karlsruhe, Germany). For Safranin O/Fast Green staining a 0.5% hematoxylin staining solution (Roth) was used for 2 min and then washed with tap water for 5 min. After dipping in 1% acetic alcohol (Merck, Darmstadt, Germany). slides were incubated in a 0.02% fast green solution (Sigma-Aldrich) for 1 min. Next, tissue sections were immersed in 1% acetic acid for 30 s and then a 1% Safranin O solution (Sigma-Aldrich) was applied for 30 min. After three changes of 95% ethanol, and two of 100% ethanol, sections were cleared in xylol and mounted with Roti-Histokit. The thickness of the tibial articular cartilage in 6-month-old animals was measured as previously described [56]. Briefly, representative micrographs of Safranin O/Fast Green sections from the lateral and medial tibial plateau were analyzed by using the linear measure tool of the ZEN 2.3 Lite image capturing and processing software (Carl Zeiss, Jena, Germany). In each section, three regions of the articular cartilage extending from the surface to the subchondral bone were measured. The mean of the three values was used to characterize the total thickness of the articular cartilage. At least five animals of each genotype were evaluated.

4.5. Scoring of Articular Cartilage Erosion

The pathological scoring of AC has been performed on Safranin O/Fast Green stained sagittal tissue sections. To have a full representation of the entire knee, about 10 slides, harvested at approximately 80 μm intervals, were chosen. Slides were evaluated by two independent observers in a blinded fashion. To assess cartilage degeneration, the OARSI scoring system was used [57]. Evaluation of articular cartilage structure comprehends eight grades as follows: 0—normal cartilage; 0.5—loss of proteoglycan stain without cartilage damage; 1—Surface fibrillations; 2—Cleft extending just below the superficial zone; 3—Cleft/erosion to the calcified cartilage extending to < 25% of the articular surface; 4—25–50% loss of articular surface; 5—50–75% loss of articular surface; 6—Eburnation with > 75% loss of cartilage. The means of the two independent observers of the maximal histopathological scores obtained across the entire knee joints were presented

4.6. Immunohistochemistry

For immunohistochemistry, paraffin embedded sections were deparaffinized, rehydrated and digested with 2 mg/mL bovine testicular hyaluronidase/PBS pH 5.0 at 37 °C for 30 min. Endogenous peroxidase activity was quenched with a 0.3% H_2O_2/methanol solution for 30 min. Sections were blocked with 1% bovine serum albumin/PBS for 60 min at room temperature. Afterwards, slides were incubated overnight at 4 °C with the following antibodies diluted in blocking solution: aggrecan (Millipore ab1031, 1:200, Beverly, MA, USA), collagen type II (DSHB CIICI, 5 μg/mL), MMP-13 (Sigma Aldrich MAB13424, 1:100), ADAMTS-5 (Abcam ab13976, 1:500, Cambridge, MA, USA),

VIDIPEN (a gift of Amanda Fosang, University of Melbourne, 1:1000), and C1,2C (IBEX 50-1035, 1:400). The next day, sections were incubated with the correspondent biotinylated secondary antibodies and immunostained by the avidin-biotin complex (Vectastain ABC Elite kit) method or the Vector M.O.M kit (both Vector Laboratories, Burlingame, CA, USA) and the 3,3'-diaminobenzidine (Sigma) as chromogenic substrate. Finally, sections were counterstained with hematoxylin and mounted with Roti-Histokit.

4.7. RNA Isolation and Quantitative RT-PCR

Total RNA was isolated from primary chondrocytes of newborn mice. Briefly, rib cages from euthanized mice were dissected, cleaned from the attached tissues with forceps and digested for 30 min in a solution of 2 mg/mL collagenase type 2 (Worthington, Malvern, PA, USA) in Dulbecco's Modified Eagle's (DMEM)/Ham's F12 1:1 (Thermo Fischer Scientific) supplemented with $1\times$ penicillin/streptomycin (Biochrom, Berlin, Germany). After the first enzymatic digestion, the perichondrium was removed and cleaned ribs were re-placed in a new collagenase solution for 3 h at 37 °C in a humidified incubator with 5% CO_2. The obtained cell suspension was centrifuged at 500 g for 5 min and washed with PBS. Total RNA isolation and cDNA synthesis were performed with the Qiagen RNeasy Mini kit (Qiagen, Hilden, Germany) and the Transcriptor First-Strand cDNA Synthesis kit (Roche, Basel, Switzerland), respectively, according to the manufacturer's instructions. Quantitative RT-PCR was performed using the gene specific TaqMan probes from Integrated DNA Technologies for *glyceraldehyde 3-phosphate dehydrogenase (GAPDH)* (Mm.PT.39a.1) and *aggrecan* (Mm.PT.58.10174685). PrimeTime Gene Expression Master Mix, dH2O and cDNA samples were pipetted in triplicates in a 96-well plate and a PCR reaction was carried out in a LightCycler 96 thermocycler provided with the LightCycler 96 Software (Roche). The relative gene expression is calculated against the housekeeping gene *GAPDH* by the comparative ΔCt method. Results in graph show the mean ± standard deviation of two PCR runs from three mice per genotypes.

4.8. Atomic Force Microscopy

Nano-scale indentation-type atomic force microscopy (IT-AFM) was carried out using a JPK NanoWizard®1 (JPK Instruments, Berlin, Germany) mounted on an inverse Axiovert 200 optical microscope (Carl Zeiss, Jena, Germany) to enable a precise positioning of the AFM tip on the region of interest. For measurements, silicon nitride cantilevers (MLCT, Cantilever E, Bruker) with a nominal spring constant of 0.1 N/m and pyramidal tips with a nominal radius of 20 nm were used. All IT-AFM measurements were carried out in PBS at pH 7.4. In order to determine the actual cantilever spring constant, each cantilever was individually calibrated using the thermal noise method [58]. Every spring constant determination was repeated three times and the mean value was used for data analysis. In each cartilage zone (superficial, middle and deep) an area of 3×3 μm, 25×25 force-indentation curves were recorded with a constant vertical tip velocity of 15 μm/s and a sampling rate of 5 kHz. For data analysis, the JPK Data Processing Software was used (Version 6.1.102, JPK Instruments). The Young's modulus was extracted from the approach section of the force-indentation curves from the contact point up to a maximum indentation depth of 500 nm, using a modified Hertz model for a pyramidal indenter as described in [29,59]. For comparison, stiffness distributions (histograms) were calculated for each developmental stage and genotype. Two sections per animal were scanned with a total of 3×625 force-indentation curves for each cartilage zone. To locate the maxima of these histograms, a linear combination of two Gaussian distributions was fitted to each histogram using the Igor Pro software (Version 6.3.7.2, WaveMetrics, Portland, OR, USA).

4.9. Enzyme-Linked Immunosorbent Assay

In order to detect the levels of collagen type 2 degradation products, the commercially available Mouse Collagen Type 2 Cleavage ELISA kit (MyBioSource, MBS725817, San Diego, CA, USA) was used according to the manufacturer instructions. Urine samples were collected from 12-month-old

mice on the day of sacrification and kept at −80 °C until use. C2C levels are expressed in ng/mL and were normalized to urinary creatinine concentration. Quantitative determination of creatinine in urine samples was assessed with the Mouse Creatinine kit from Crystal Chem (Cat. 80350) as per manufacturer protocol.

4.10. Statistical Analysis

Statistical significance was calculated after determination of the Gaussian distribution using a one-way ANOVA test (GraphPad Prism, San Diego, CA, USA) with appropriate post hoc tests. Statistical significance was assumed at a *p*-value of ≤ 0.05. All values represent the mean and the standard deviation (SD). In all experiments, at least three animals were used (a list of the precise number of animals used in each experiment is stated in figure legends).

5. Conclusions

In conclusion, our data demonstrate that $Agc1^{CreERT2/CreERT2}$ mice have smaller skeleton, stiffer articular cartilage and are prone to spontaneous, age-associated osteoarthritis owing to reduced deposition of aggrecan in cartilage. Therefore, the homozygous $Agc1^{CreERT2/CreERT2}$ mice should not be used for conditional gene ablation experiments assessing gene function in the articular cartilage. However, the $Agc1^{CreERT2/CreERT2}$ mice could serve as valuable model for studying aggrecanopathies caused by reduced aggrecan expression in the cartilaginous skeleton.

Author Contributions: Study conception, design and manuscript writing: P.A., H.C.-S. and A.A. Performed experiments: P.A., H.C.D, B.H., P.L. and Z.F. Data visualization and statistical analysis: M.M.S. and B.H.

**Conflicts of Interest:** The authors confirm that there are no conflicts of interest.

References

1. Aspberg, A. The Different Roles of Aggrecan Interaction Domains. *J. Histochem. Cytochem.* **2012**, *60*, 987–996. [CrossRef] [PubMed]
2. Aspberg, A. Cartilage Proteoglycans. In *Cartilage*; Springer International Publishing: Cham, Switzerland, 2016; pp. 1–22.
3. Kiani, C.; Chen, L.; Wu, Y.J.; Yee, A.J.; Yang, B.B. Structure and function of aggrecan. *Cell Res.* **2002**, *12*, 19–32. [CrossRef] [PubMed]
4. Hedlund, H.; Hedbom, E.; Heinegrd, D.; Mengarelli-Widholm, S.; Reinholt, F.P.; Svensson, O. Association of the aggrecan keratan sulfate-rich region with collagen in bovine articular cartilage. *J. Biol. Chem.* **1999**, *274*, 5777–5781. [CrossRef] [PubMed]
5. Cortes, M.; Baria, A.T.; Schwartz, N.B. Sulfation of chondroitin sulfate proteoglycans is necessary for proper Indian hedgehog signaling in the developing growth plate. *Development* **2009**, *136*, 1697–1706. [CrossRef] [PubMed]
6. Mouw, J.K.; Ou, G.; Weaver, V.M. Extracellular matrix assembly: A multiscale deconstruction. *Nat. Rev. Mol. Cell Biol.* **2014**, *15*, 771–785. [CrossRef] [PubMed]
7. Chambers, M.G.; Kuffner, T.; Cowan, S.K.; Cheah, K.S.E.; Mason, R.M. Expression of collagen and aggrecan genes in normal and osteoarthritic murine knee joints. *Osteoarthr. Cartil.* **2002**, *10*, 51–61. [CrossRef] [PubMed]
8. Maroudas, A.; Bayliss, M.T.; Uchitel-Kaushansky, N.; Schneiderman, R.; Gilav, E. Aggrecan turnover in human articular cartilage: Use of aspartic acid racemization as a marker of molecular age. *Arch. Biochem. Biophys.* **1998**, *350*, 61–71. [CrossRef] [PubMed]
9. Gibson, B.G.; Briggs, M.D. The aggrecanopathies; an evolving phenotypic spectrum of human genetic skeletal diseases. *Orphanet J. Rare Dis.* **2016**, *11*, 86. [CrossRef] [PubMed]

10. Tompson, S.W.; Merriman, B.; Funari, V.A.; Fresquet, M.; Lachman, R.S.; Rimoin, D.L.; Nelson, S.F.; Briggs, M.D.; Cohn, D.H.; Krakow, D. A Recessive Skeletal Dysplasia, SEMD Aggrecan Type, Results from a Missense Mutation Affecting the C-Type Lectin Domain of Aggrecan. *Am. J. Hum. Genet.* **2009**, *84*, 72–79. [CrossRef] [PubMed]

11. Stattin, E.-L.; Tegner, Y.; Domellöf, M.; Dahl, N. Familial osteochondritis dissecans associated with early osteoarthritis and disproportionate short stature. *Osteoarthr. Cartil.* **2008**, *16*, 890–896. [CrossRef] [PubMed]

12. Nilsson, O.; Guo, M.H.; Dunbar, N.; Popovic, J.; Flynn, D.; Jacobsen, C.; Lui, J.C.; Hirschhorn, J.N.; Baron, J.; Dauber, A. Short stature, accelerated bone maturation, and early growth cessation due to heterozygous aggrecan mutations. *J. Clin. Endocrinol. Metab.* **2014**, *99*, E1510–E1518. [CrossRef] [PubMed]

13. Watanabe, H.; Kimata, K.; Line, S.; Strong, D.; Gao, L.Y.; Kozak, C.A.; Yamada, Y. Mouse cartilage matrix deficiency (cmd) caused by a 7 bp deletion in the aggrecan gene. *Nat. Genet.* **1994**, *7*, 154–157. [CrossRef] [PubMed]

14. Bell, L.; Juriloff, M.; Harris, M.J. A new mutation at the cmd locus in the mouse. *J. Hered.* **1986**, *77*, 205–206. [CrossRef] [PubMed]

15. Watanabe, H.; Nakata, K.; Kimata, K.; Nakanishi, I.; Yamada, Y. Dwarfism and age-associated spinal degeneration of heterozygote cmd mice defective in aggrecan. *Proc. Natl. Acad. Sci. USA* **1997**, *94*, 6943–6947. [CrossRef] [PubMed]

16. Henry, S.P.; Jang, C.-W.; Deng, J.M.; Zhang, Z.; Behringer, R.R.; de Crombrugghe, B. Generation of aggrecan-CreERT2 knockin mice for inducible Cre activity in adult cartilage. *Genesis* **2009**, *47*, 805–814. [CrossRef] [PubMed]

17. Alvarez-Garcia, O.; Matsuzaki, T.; Olmer, M.; Miyata, K.; Mokuda, S.; Sakai, D.; Masuda, K.; Asahara, H.; Lotz, M.K. FOXO are required for intervertebral disk homeostasis during aging and their deficiency promotes disk degeneration. *Aging Cell* **2018**, *17*, e12800. [CrossRef] [PubMed]

18. Wang, C.; Abu-Amer, Y.; O'Keefe, R.J.; Shen, J. Loss of Dnmt3b in Chondrocytes Leads to Delayed Endochondral Ossification and Fracture Repair. *J. Bone Miner. Res.* **2018**, *33*, 283–297. [CrossRef] [PubMed]

19. Diekman, B.O.; Sessions, G.A.; Collins, J.A.; Knecht, A.K.; Strum, S.L.; Mitin, N.K.; Carlson, C.S.; Loeser, R.F.; Sharpless, N.E. Expression of p16INK4ais a biomarker of chondrocyte aging but does not cause osteoarthritis. *Aging Cell* **2018**, *17*, e12771. [CrossRef] [PubMed]

20. Alkhatib, B.; Liu, C.; Serra, R. Tgfbr2 is required in Acan-expressing cells for maintenance of the intervertebral and sternocostal joints. *JOR Spine* **2018**, *1*, e1025. [CrossRef] [PubMed]

21. Liao, L.; Zhang, S.; Gu, J.; Takarada, T.; Yoneda, Y.; Huang, J.; Zhao, L.; Oh, C.D.; Li, J.; Wang, B.; et al. Deletion of Runx2 in Articular Chondrocytes Decelerates the Progression of DMM-Induced Osteoarthritis in Adult Mice. *Sci. Rep.* **2017**, *7*, 2371. [CrossRef] [PubMed]

22. Henry, S.P.; Liang, S.; Akdemir, K.C.; De Crombrugghe, B. The postnatal role of Sox9 in cartilage. *J. Bone Miner. Res.* **2012**, *27*, 2511–2525. [CrossRef] [PubMed]

23. Couasnay, G.; Bon, N.; Devignes, C.S.; Sourice, S.; Bianchi, A.; Véziers, J.; Weiss, P.; Elefteriou, F.; Provot, S.; Guicheux, J.; et al. PiT1/Slc20a1 Is Required for Endoplasmic Reticulum Homeostasis, Chondrocyte Survival, and Skeletal Development. *J. Bone Miner. Res.* **2018**, *34*, 387–398. [CrossRef] [PubMed]

24. Liao, L.; Jiang, H.; Fan, Y.; Lu, R.S.; Wei, C.; Takarada, T.; He, S.; Chen, D. Runx2 is required for postnatal intervertebral disc tissue growth and development. *J. Cell. Physiol.* **2019**, *234*, 6679–6687. [CrossRef] [PubMed]

25. Zhang, Y.; Sheu, T.; Hoak, D.; Shen, J.; Hilton, M.J.; Zuscik, M.J.; Jonason, J.H.; O'Keefe, R.J. CCN1 Regulates Chondrocyte Maturation and Cartilage Development. *J. Bone Miner. Res.* **2016**, *31*, 549–559. [CrossRef] [PubMed]

26. Zhou, X.; von der Mark, K.; Henry, S.; Norton, W.; Adams, H.; de Crombrugghe, B. Chondrocytes Transdifferentiate into Osteoblasts in Endochondral Bone during Development, Postnatal Growth and Fracture Healing in Mice. *PLoS Genet.* **2014**, *10*, e1004820. [CrossRef] [PubMed]

27. Rashid, H.; Chen, H.; Hassan, Q.; Javed, A. Dwarfism in homozygous Agc1CreERT mice is associated with decreased expression of aggrecan. *Genesis* **2017**, *55*, e23070. [CrossRef] [PubMed]

28. Loparic, M.; Wirz, D.; Daniels, A.U.; Raiteri, R.; Vanlandingham, M.R.; Guex, G.; Martin, I.; Aebi, U.; Stolz, M. Micro- and nanomechanical analysis of articular cartilage by indentation-type atomic force microscopy: Validation with a gel-microfiber composite. *Biophys. J.* **2010**, *98*, 2731–2740. [CrossRef] [PubMed]

29. Prein, C.; Warmbold, N.; Farkas, Z.; Schieker, M.; Aszodi, A.; Clausen-Schaumann, H. Structural and mechanical properties of the proliferative zone of the developing murine growth plate cartilage assessed by atomic force microscopy. *Matrix Biol.* **2016**, *50*, 1–15. [CrossRef] [PubMed]

30. Gronau, T.; Krüger, K.; Prein, C.; Aszodi, A.; Gronau, I.; Iozzo, R.V.; Mooren, F.C.; Clausen-Schaumann, H.; Bertrand, J.; Pap, T.; et al. Forced exercise-induced osteoarthritis is attenuated in mice lacking the small leucine-rich proteoglycan decorin. *Ann. Rheum. Dis.* **2017**, *76*, 442–449. [CrossRef] [PubMed]

31. Hauer, N.N.; Sticht, H.; Boppudi, S.; Büttner, C.; Kraus, C.; Trautmann, U.; Zenker, M.; Zweier, C.; Wiesener, A.; Jamra, R.A.; et al. Genetic screening confirms heterozygous mutations in ACAN as a major cause of idiopathic short stature. *Sci. Rep.* **2017**, *7*, 12225. [CrossRef] [PubMed]

32. Gleghorn, L.; Ramesar, R.; Beighton, P.; Wallis, G. A mutation in the variable repeat region of the aggrecan gene (AGC1) causes a form of spondyloepiphyseal dysplasia associated with severe, premature osteoarthritis. *Am. J. Hum. Genet.* **2005**, *77*, 484–490. [CrossRef] [PubMed]

33. Gkourogianni, A.; Andrew, M.; Tyzinski, L.; Crocker, M.; Douglas, J.; Dunbar, N.; Fairchild, J.; Funari, M.F.A.; Heath, K.E.; Jorge, A.A.L.; et al. Clinical Characterization of Patients With Autosomal Dominant Short Stature due to Aggrecan Mutations. *J. Clin. Endocrinol. Metab.* **2017**, *102*, 460–469. [CrossRef] [PubMed]

34. Primorac, D.; Stover, M.L.; Clark, S.H.; Rowe, D.W. Molecular basis of nanomelia, a heritable chondrodystrophy of chicken. *Matrix Biol.* **1994**, *14*, 297–305. [CrossRef]

35. Vertel, B.M.; Grier, B.L.; Li, H.; Schwartz, N.B. The chondrodystrophy, nanomelia: Biosynthesis and processing of the defective aggrecan precursor. *Biochem. J.* **1994**, *301*, 211–216. [CrossRef] [PubMed]

36. Cavanagh, J.A.L.; Tammen, I.; Windsor, P.A.; Bateman, J.F.; Savarirayan, R.; Nicholas, F.W.; Raadsma, H.W. Bulldog dwarfism in Dexter cattle is caused by mutations in ACAN. *Mamm. Genome* **2007**, *18*, 808–814. [CrossRef] [PubMed]

37. Lauing, K.L.; Cortes, M.; Domowicz, M.S.; Henry, J.G.; Baria, A.T.; Schwartz, N.B. Aggrecan is required for growth plate cytoarchitecture and differentiation. *Dev. Biol.* **2014**, *396*, 224–236. [CrossRef] [PubMed]

38. Fritsch, A.; Loeckermann, S.; Kern, J.S.; Braun, A.; Bösl, M.R.; Bley, T.A.; Schumann, H.; von Elverfeldt, D.; Paul, D.; Erlacher, M.; et al. A hypomorphic mouse model of dystrophic epidermolysis bullosa reveals mechanisms of disease and response to fibroblast therapy. *J. Clin. Investig.* **2008**, *118*, 1669–1679. [CrossRef] [PubMed]

39. Mohn, A.R.; Gainetdinov, R.R.; Caron, M.G.; Koller, B.H. Mice with reduced NMDA receptor expression display behaviors related to schizophrenia. *Cell* **1999**, *98*, 427–436. [CrossRef]

40. Nagy, A.; Moens, C.; Ivanyi, E.; Pawling, J.; Gertsenstein, M.; Hadjantonakis, A.K.; Pirity, M.; Rossant, J. Dissecting the role of N-myc in development using a single targeting vector to generate a series of alleles. *Curr. Biol.* **1998**, *8*, 661–664. [CrossRef]

41. Pan, Y.; Zhang, L.; Liu, Q.; Li, Y.; Guo, H.; Peng, Y.; Peng, H.; Tang, B.; Hu, Z.; Zhao, J.; et al. Insertion of a knockout-first cassette in Ampd1 gene leads to neonatal death by disruption of neighboring genes expression. *Sci. Rep.* **2016**, *6*, 35970. [CrossRef] [PubMed]

42. Pham, C.T.; MacIvor, D.M.; Hug, B.A.; Heusel, J.W.; Ley, T.J. Long-range disruption of gene expression by a selectable marker cassette. *Proc. Natl. Acad. Sci. USA* **1996**, *93*, 13090–13095. [CrossRef] [PubMed]

43. Raffai, R.L.; Weisgraber, K.H. Hypomorphic apolipoprotein E mice: A new model of conditional gene repair to examine apolipoprotein E-mediated metabolism. *J. Biol. Chem.* **2002**, *277*, 11064–11068. [CrossRef] [PubMed]

44. Stolz, M.; Raiteri, R.; Daniels, A.U.; VanLandingham, M.R.; Baschong, W.; Aebi, U. Dynamic elastic modulus of porcine articular cartilage determined at two different levels of tissue organization by indentation-type atomic force microscopy. *Biophys. J.* **2004**, *86*, 3269–3283. [CrossRef]

45. Stolz, M.; Gottardi, R.; Raiteri, R.; Miot, S.; Martin, I.; Imer, R.; Staufer, U.; Raducanu, A.; Düggelin, M.; Baschong, W.; et al. Early detection of aging cartilage and osteoarthritis in mice and patient samples using atomic force microscopy. *Nat. Nanotechnol.* **2009**, *4*, 186–192. [CrossRef] [PubMed]

46. Aro, E.; Salo, A.M.; Khatri, R.; Finnilä, M.; Miinalainen, I.; Sormunen, R.; Pakkanen, O.; Holster, T.; Soininen, R.; Prein, C.; et al. Severe Extracellular Matrix Abnormalities and Chondrodysplasia in Mice Lacking Collagen Prolyl 4-Hydroxylase Isoenzyme II in Combination with a Reduced Amount of Isoenzyme I. *J. Biol. Chem.* **2015**, *290*, 16964–16978. [CrossRef] [PubMed]

47. Kamper, M.; Hamann, N.; Prein, C.; Clausen-Schaumann, H.; Farkas, Z.; Aszodi, A.; Niehoff, A.; Paulsson, M.; Zaucke, F. Early changes in morphology, bone mineral density and matrix composition of vertebrae lead to disc degeneration in aged collagen IX -/- mice. *Matrix Biol.* **2016**, *49*, 132–143. [CrossRef] [PubMed]

48. Wen, C.-Y.; Wu, C.-B.; Tang, B.; Wang, T.; Yan, C.-H.; Lu, W.W.; Pan, H.; Hu, Y.; Chiu, K.-Y. Collagen fibril stiffening in osteoarthritic cartilage of human beings revealed by atomic force microscopy. *Osteoarthr. Cartil.* **2012**, *20*, 916–922. [CrossRef] [PubMed]

49. Kleemann, R.U.; Krocker, D.; Cedraro, A.; Tuischer, J.; Duda, G.N. Altered cartilage mechanics and histology in knee osteoarthritis: Relation to clinical assessment (ICRS Grade). *Osteoarthr. Cartil.* **2005**, *13*, 958–963. [CrossRef] [PubMed]

50. Wilusz, R.E.; Zauscher, S.; Guilak, F. Micromechanical mapping of early osteoarthritic changes in the pericellular matrix of human articular cartilage. *Osteoarthr. Cartil.* **2013**, *21*, 1895–1903. [CrossRef] [PubMed]

51. O'Connor, M.I. Sex differences in osteoarthritis of the hip and knee. *J. Am. Acad. Orthop. Surg.* **2007**, *15*, S22–S25. [CrossRef] [PubMed]

52. Palazzo, C.; Nguyen, C.; Lefevre-Colau, M.-M.; Rannou, F.; Poiraudeau, S. Risk factors and burden of osteoarthritis. *Ann. Phys. Rehabil. Med.* **2016**, *59*, 134–138. [CrossRef] [PubMed]

53. Sokoloff, L. Natural history of degenerative joint disease in small laboratory animals. I. Pathological anatomy of degenerative joint disease in mice. *AMA Arch. Pathol.* **1956**, *62*, 118–128. [PubMed]

54. van Osch, G.J.; van der Kraan, P.M.; Vitters, E.L.; Blankevoort, L.; van den Berg, W.B. Induction of osteoarthritis by intra-articular injection of collagenase in mice. Strain and sex related differences. *Osteoarthr. Cartil.* **1993**, *1*, 171–177. [CrossRef]

55. Ma, H.-L.; Blanchet, T.J.; Peluso, D.; Hopkins, B.; Morris, E.A.; Glasson, S.S. Osteoarthritis severity is sex dependent in a surgical mouse model. *Osteoarthr. Cartil.* **2007**, *15*, 695–700. [CrossRef] [PubMed]

56. Raducanu, A.; Hunziker, E.B.; Drosse, I.; Aszodi, A. B1 Integrin Deficiency Results in Multiple Abnormalities of the Knee Joint. *J. Biol. Chem.* **2009**, *284*, 23780–23792. [CrossRef] [PubMed]

57. Glasson, S.S.; Chambers, M.G.; Van Den Berg, W.B.; Little, C.B. The OARSI histopathology initiative—Recommendations for histological assessments of osteoarthritis in the mouse. *Osteoarthr. Cartil.* **2010**, *18*, S17–S23. [CrossRef] [PubMed]

58. Butt, H.-J.; Jaschke, M. Calculation of thermal noise in atomic force microscopy. *Nanotechnology* **1995**, *6*. [CrossRef]

59. Sneddon, I.N. The relation between load and penetration in the axisymmetric boussinesq problem for a punch of arbitrary profile. *Int. J. Eng. Sci.* **1965**, *3*, 47–57. [CrossRef]
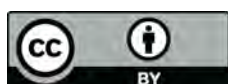
REFERENCES

1. Buck DW, 2nd, Dumanian GA: **Bone biology and physiology: Part I. The fundamentals**. *Plastic and reconstructive surgery* 2012, **129**(6):1314-1320.

2. Kothari ML, Mehta LA, Natrajan M: **The nature of bones and joints: a new perspective**. *Journal of postgraduate medicine* 1990, **36**(3):143-146.

3. Caplan AI: **Bone development**. *Ciba Foundation symposium* 1988, **136**:3-21.

4. Mackie EJ, Ahmed YA, Tatarczuch L, Chen KS, Mirams M: **Endochondral ossification: how cartilage is converted into bone in the developing skeleton**. *The international journal of biochemistry & cell biology* 2008, **40**(1):46-62.

5. Hunter WL, Arsenault AL: **Vascular invasion of the epiphyseal growth plate: analysis of metaphyseal capillary ultrastructure and growth dynamics**. *The Anatomical record* 1990, **227**(2):223-231.

6. Reddi AH: **Bone and cartilage differentiation**. *Curr Opin Genet Dev* 1994, **4**(5):737-744.

7. Zaleske DJ: **Cartilage and bone development**. *Instr Course Lect* 1998, **47**:461-468.

8. Hayes AJ, MacPherson S, Morrison H, Dowthwaite G, Archer CW: **The development of articular cartilage: evidence for an appositional growth mechanism**. *Anatomy and embryology* 2001, **203**(6):469-479.

9. Kuettner KE, Schleyerbach R, Hascall VC: **Articular cartilage biochemistry**. In.: Raven Press, New York, NY; 1986.

10. Kuettner KEJCb: **Biochemistry of articular cartilage in health and disease**. 1992, **25**(3):155-163.

11. Cohen NP, Foster RJ, Mow VCJJoO, Therapy SP: **Composition and dynamics of articular cartilage: structure, function, and maintaining healthy state**. 1998, **28**(4):203-215.

12. Buckwalter J, Mankin HJJoB, surgery j: **Articular cartilage: part I**. 1997, **79**(4):600.

13. Theocharis AD, Skandalis SS, Gialeli C, Karamanos NK: **Extracellular matrix structure**. *Advanced drug delivery reviews* 2016, **97**:4-27.

14. Velleman SG: **The role of the extracellular matrix in skeletal development**. *Poultry science* 2000, **79**(7):985-989.

15. Suzuki F: **Roles of cartilage matrix proteins, chondromodulin-I and -II, in endochondral bone formation: a review**. *Connect Tissue Res* 1996, **35**(1-4):303-307.

16. Thompson JR, Oegema JTJTJob, volume jsA: **Metabolic activity of articular cartilage in osteoarthritis. An in vitro study**. 1979, **61**(3):407-416.

17. Kuivaniemi H, Tromp G, Prockop DJJHm: **Mutations in fibrillar collagens (types I, II, III, and XI), fibril-associated collagen (type IX), and network-forming collagen (type X) cause a spectrum of diseases of bone, cartilage, and blood vessels**. 1997, **9**(4):300-315.

18. Mundlos S, Olsen BJTFj: **Heritable diseases of the skeleton. Part II: Molecular insights into skeletal development-matrix components and their homeostasis**. 1997, **11**(4):227-233.

19. Patterson SE, Dealy CN: **Mechanisms and models of endoplasmic reticulum stress in chondrodysplasia**. *Developmental dynamics : an official publication of the American Association of Anatomists* 2014, **243**(7):875-893.

20. Berendsen AD, Olsen BR: **Bone development**. *Bone* 2015, **80**:14-18.

21. Carter DR, Orr TE: **Skeletal development and bone functional adaptation**. *Journal of bone and mineral research : the official journal of the American Society for Bone and Mineral Research* 1992, **7 Suppl 2**:S389-395.

22. Hoenderop JG, van Leeuwen JP, van der Eerden BC, Kersten FF, van der Kemp AW, Merillat AM,

Waarsing JH, Rossier BC, Vallon V, Hummler E *et al*: **Renal Ca²⁺ wasting, hyperabsorption, and reduced bone thickness in mice lacking TRPV5**. *The Journal of clinical investigation* 2003, **112**(12):1906-1914.

23. Sugiki T, Uyama T, Toyoda M, Morioka H, Kume S, Miyado K, Matsumoto K, Saito H, Tsumaki N, Takahashi Y *et al*: **Hyaline cartilage formation and enchondral ossification modeled with KUM5 and OP9 chondroblasts**. *J Cell Biochem* 2007, **100**(5):1240-1254.

24. Yang Y: **Skeletal morphogenesis during embryonic development**. *Critical reviews in eukaryotic gene expression* 2009, **19**(3):197-218.

25. Long F, Ornitz DM: **Development of the endochondral skeleton**. *Cold Spring Harbor perspectives in biology* 2013, **5**(1):a008334.

26. Horton WA, Degnin CR: **FGFs in endochondral skeletal development**. *Trends in endocrinology and metabolism: TEM* 2009, **20**(7):341-348.

27. Gerstenfeld L, Shapiro FJJocb: **Expression of bone-specific genes by hypertrophic chondrocytes: Implications of the complex functions of the hypertrophic chondrocyte during endochondral bone development**. 1996, **62**(1):1-9.

28. Shen G: **The role of type X collagen in facilitating and regulating endochondral ossification of articular cartilage**. *Orthodontics & craniofacial research* 2005, **8**(1):11-17.

29. Gabner S, Hausler G, Bock P: **Vascular Canals in Permanent Hyaline Cartilage: Development, Corrosion of Nonmineralized Cartilage Matrix, and Removal of Matrix Degradation Products**. *Anatomical record (Hoboken, NJ : 2007)* 2017, **300**(6):1067-1082.

30. Blumer MJ, Longato S, Fritsch H: **Structure, formation and role of cartilage canals in the developing bone**. *Annals of anatomy = Anatomischer Anzeiger : official organ of the Anatomische Gesellschaft* 2008, **190**(4):305-315.

31. Blumer MJ, Longato S, Richter E, Perez MT, Konakci KZ, Fritsch H: **The role of cartilage canals in endochondral and perichondral bone formation: are there similarities between these two processes?***Journal of anatomy* 2005, **206**(4):359-372.

32. Xie Y, Zhou S, Chen H, Du X, Chen LJJome: **Recent research on the growth plate: Advances in fibroblast growth factor signaling in growth plate development and disorders**. 2014, **53**(1):T11-T34.

33. Bell DM, Leung KK, Wheatley SC, Ng LJ, Zhou S, Ling KW, Sham MH, Koopman P, Tam PP, Cheah KS: **SOX9 directly regulates the type-II collagen gene**. *Nature genetics* 1997, **16**(2):174-178.

34. Dy P, Wang W, Bhattaram P, Wang Q, Wang L, Ballock RT, Lefebvre V: **Sox9 directs hypertrophic maturation and blocks osteoblast differentiation of growth plate chondrocytes**. *Developmental cell* 2012, **22**(3):597-609.

35. Akiyama H, Chaboissier MC, Martin JF, Schedl A, de Crombrugghe B: **The transcription factor Sox9 has essential roles in successive steps of the chondrocyte differentiation pathway and is required for expression of Sox5 and Sox6**. *Genes & development* 2002, **16**(21):2813-2828.

36. Smits P, Li P, Mandel J, Zhang Z, Deng JM, Behringer RR, de Crombrugghe B, Lefebvre V: **The transcription factors L-Sox5 and Sox6 are essential for cartilage formation**. *Developmental cell* 2001, **1**(2):277-290.

37. Suda N: **Parathyroid hormone-related protein (PTHrP) as a regulating factor of endochondral bone formation**. *Oral diseases* 1997, **3**(4):229-231.

38. Adams SL, Cohen AJ, Lassova L: **Integration of signaling pathways regulating chondrocyte differentiation during endochondral bone formation**. *Journal of cellular physiology* 2007, **213**(3):635-641.

39. Lu C, Wan Y, Cao J, Zhu X, Yu J, Zhou R, Yao Y, Zhang L, Zhao H, Li H *et al*: **Wnt-mediated reciprocal regulation between cartilage and bone development during endochondral ossification**. *Bone* 2013, **53**(2):566-574.

40. Yamashiro T, Wang XP, Li Z, Oya S, Aberg T, Fukunaga T, Kamioka H, Speck NA, Takano-Yamamoto T, Thesleff I: **Possible roles of Runx1 and Sox9 in incipient intramembranous ossification**. *Journal of bone and mineral research : the official journal of the American Society for Bone and Mineral Research* 2004, **19**(10):1671-1677.

41. Yoshida CA, Yamamoto H, Fujita T, Furuichi T, Ito K, Inoue K, Yamana K, Zanma A, Takada K, Ito Y *et al*: **Runx2 and Runx3 are essential for chondrocyte maturation, and Runx2 regulates limb growth through induction of Indian hedgehog**. *Genes & development* 2004, **18**(8):952-963.

42. Ding M, Lu Y, Abbassi S, Li F, Li X, Song Y, Geoffroy V, Im HJ, Zheng Q: **Targeting Runx2 expression in hypertrophic chondrocytes impairs endochondral ossification during early skeletal development**. *Journal of cellular physiology* 2012, **227**(10):3446-3456.

43. Huber M, Trattnig S, Lintner FJIr: **Anatomy, biochemistry, and physiology of articular cartilage**. 2000, **35**(10):573-580.

44. Buckwalter J, Mankin HJIcl: **Articular cartilage: tissue design and chondrocyte-matrix interactions**. 1998, **47**:477-486.

45. Vanderploeg EJ, Wilson CG, Levenston MEJO, cartilage: **Articular chondrocytes derived from distinct tissue zones differentially respond to in vitro oscillatory tensile loading**. 2008, **16**(10):1228-1236.

46. Francis SL, Di Bella C, Wallace GG, Choong PFM: **Cartilage Tissue Engineering Using Stem Cells and Bioprinting Technology—Barriers to Clinical Translation**. 2018, **5**(70).

47. Carballo CB, Nakagawa Y, Sekiya I, Rodeo SA: **Basic Science of Articular Cartilage**. *Clinics in sports medicine* 2017, **36**(3):413-425.

48. Sakata R, Iwakura T, Reddi AH: **Regeneration of Articular Cartilage Surface: Morphogens, Cells, and Extracellular Matrix Scaffolds**. *Tissue engineering Part B, Reviews* 2015, **21**(5):461-473.

49. Armiento AR, Stoddart MJ, Alini M, Eglin D: **Biomaterials for articular cartilage tissue engineering: Learning from biology**. *Acta biomaterialia* 2018, **65**:1-20.

50. Watanabe H, Yamada Y, Kimata K: **Roles of aggrecan, a large chondroitin sulfate proteoglycan, in cartilage structure and function**. *Journal of biochemistry* 1998, **124**(4):687-693.

51. Hay ED: **Cell biology of extracellular matrix**: Springer Science & Business Media; 2013.

52. Hedlund H, Hedbom E, Heinegård D, Mengarelli-Widholm S, Reinholt FP, Svensson OJJoBC: **Association of the aggrecan keratan sulfate-rich region with collagen in bovine articular cartilage**. 1999, **274**(9):5777-5781.

53. Cortes M, Baria AT, Schwartz NBJD: **Sulfation of chondroitin sulfate proteoglycans is necessary for proper Indian hedgehog signaling in the developing growth plate**. 2009, **136**(10):1697-1706.

54. Nia HT, Ortiz C, Grodzinsky A: **Aggrecan: approaches to study biophysical and biomechanical properties**. In: *Glycosaminoglycans.* Springer; 2015: 221-237.

55. Bonnans C, Chou J, Werb ZJNrMcb: **Remodelling the extracellular matrix in development and disease**. 2014, **15**(12):786-801.

56. Alexopoulos LG, Setton LA, Guilak FJAb: **The biomechanical role of the chondrocyte pericellular matrix in articular cartilage**. 2005, **1**(3):317-325.

57. Waldman SD, Spiteri CG, Grynpas MD, Pilliar RM, Kandel RAJJoor: **Long-term intermittent shear deformation improves the quality of cartilaginous tissue formed in vitro**. 2003, **21**(4):590-596.

58. Allen DM, Mao JJJJosb: **Heterogeneous nanostructural and nanoelastic properties of pericellular and**

interterritorial matrices of chondrocytes by atomic force microscopy. 2004, **145**(3):196-204.

59.   Rojas FP, Batista MA, Lindburg CA, Dean D, Grodzinsky AJ, Ortiz C, Han L: **Molecular adhesion between cartilage extracellular matrix macromolecules**. *Biomacromolecules* 2014, **15**(3):772-780.

60.   Wilusz RE, Sanchez-Adams J, Guilak FJMb: **The structure and function of the pericellular matrix of articular cartilage**. 2014, **39**:25-32.

61.   Responte DJ, Natoli RM, Athanasiou KA: **Collagens of articular cartilage: structure, function, and importance in tissue engineering**. *Critical reviews in biomedical engineering* 2007, **35**(5):363-411.

62.   Eyre D: **Collagen of articular cartilage**. *Arthritis research* 2002, **4**(1):30-35.

63.   Eyre DR: **Collagens and cartilage matrix homeostasis**. *Clinical orthopaedics and related research* 2004(427 Suppl):S118-122.

64.   Budde B, Blumbach K, Ylostalo J, Zaucke F, Ehlen HW, Wagener R, Ala-Kokko L, Paulsson M, Bruckner P, Grassel S: **Altered integration of matrilin-3 into cartilage extracellular matrix in the absence of collagen IX**. *Molecular and cellular biology* 2005, **25**(23):10465-10478.

65.   Jansen ID, Hollander AP, Buttle DJ, Everts V: **Type II and VI collagen in nasal and articular cartilage and the effect of IL-1alpha on the distribution of these collagens**. *Journal of molecular histology* 2010, **41**(1):9-17.

66.   Linsenmayer TF, Long F, Nurminskaya M, Chen Q, Schmid TM: **Type X collagen and other up-regulated components of the avian hypertrophic cartilage program**. *Progress in nucleic acid research and molecular biology* 1998, **60**:79-109.

67.   Hjorten R, Hansen U, Underwood RA, Telfer HE, Fernandes RJ, Krakow D, Sebald E, Wachsmann-Hogiu S, Bruckner P, Jacquet R *et al*: **Type XXVII collagen at the transition of cartilage to bone during skeletogenesis**. *Bone* 2007, **41**(4):535-542.

68.   Athens AA, Makris EA, Hu JC: **Induced collagen cross-links enhance cartilage integration**. *PloS one* 2013, **8**(4):e60719.

69.   Dreier R, Opolka A, Grifka J, Bruckner P, Grassel S: **Collagen IX-deficiency seriously compromises growth cartilage development in mice**. *Matrix biology : journal of the International Society for Matrix Biology* 2008, **27**(4):319-329.

70.   Lindahl AJPTotRSBBS: **From gristle to chondrocyte transplantation: treatment of cartilage injuries**. 2015, **370**(1680):20140369.

71.   Watanabe H: **[Cartilage proteoglycan aggregate: structure and function]**. *Clinical calcium* 2004, **14**(7):9-14.

72.   Knudson CB, Knudson W: **Cartilage proteoglycans**. *Seminars in cell & developmental biology* 2001, **12**(2):69-78.

73.   Roughley PJ, Lee ER: **Cartilage proteoglycans: structure and potential functions**. *Microscopy research and technique* 1994, **28**(5):385-397.

74.   Miwa HE, Gerken TA, Huynh TD, Flory DM, Hering TM: **Mammalian expression of full-length bovine aggrecan and link protein: formation of recombinant proteoglycan aggregates and analysis of proteolytic cleavage by ADAMTS-4 and MMP-13**. *Biochimica et biophysica acta* 2006, **1760**(3):472-486.

75.   Nia HT, Ortiz C, Grodzinsky A: **Aggrecan: approaches to study biophysical and biomechanical properties**. *Methods in molecular biology (Clifton, NJ)* 2015, **1229**:221-237.

76.   Dudhia J: **Aggrecan, aging and assembly in articular cartilage**. *Cellular and molecular life sciences : CMLS* 2005, **62**(19-20):2241-2256.

77.   Alberton P, Dugonitsch HC, Hartmann B, Li P, Farkas Z, Saller MM, Clausen-Schaumann H, Aszodi A:

Aggrecan Hypomorphism Compromises Articular Cartilage Biomechanical Properties and Is Associated with Increased Incidence of Spontaneous Osteoarthritis. *International journal of molecular sciences* 2019, **20**(5).

78. Hedlund H, Hedbom E, Heineg rd D, Mengarelli-Widholm S, Reinholt FP, Svensson O: **Association of the aggrecan keratan sulfate-rich region with collagen in bovine articular cartilage**. *The Journal of biological chemistry* 1999, **274**(9):5777-5781.

79. Cortes M, Baria AT, Schwartz NB: **Sulfation of chondroitin sulfate proteoglycans is necessary for proper Indian hedgehog signaling in the developing growth plate**. *Development (Cambridge, England)* 2009, **136**(10):1697-1706.

80. Flannery CRJAr, therapy: **Usurped SLRPs: novel arthritis biomarkers exposed by catabolism of small leucine-rich proteoglycans?** 2006, **8**(2):106.

81. Roughley PJ, Lee ERJMr, technique: **Cartilage proteoglycans: structure and potential functions**. 1994, **28**(5):385-397.

82. Bianco P, Fisher LW, Young MF, Termine JD, Robey PGJJoH, Cytochemistry: **Expression and localization of the two small proteoglycans biglycan and decorin in developing human skeletal and non-skeletal tissues**. 1990, **38**(11):1549-1563.

83. Eyre DR, Pietka T, Weis MA, Wu JJ: **Covalent cross-linking of the NC1 domain of collagen type IX to collagen type II in cartilage**. *The Journal of biological chemistry* 2004, **279**(4):2568-2574.

84. Brachvogel B, Zaucke F, Dave K, Norris EL, Stermann J, Dayakli M, Koch M, Gorman JJ, Bateman JF, Wilson R: **Comparative proteomic analysis of normal and collagen IX null mouse cartilage reveals altered extracellular matrix composition and novel components of the collagen IX interactome**. *The Journal of biological chemistry* 2013, **288**(19):13481-13492.

85. Olsen BR: **Collagen IX**. *The international journal of biochemistry & cell biology* 1997, **29**(4):555-558.

86. Hedbom E, Antonsson P, Hjerpe A, Aeschlimann D, Paulsson M, Rosa-Pimentel E, Sommarin Y, Wendel M, Oldberg A, Heinegård DJJobc: **Cartilage matrix proteins. An acidic oligomeric protein (COMP) detected only in cartilage**. 1992, **267**(9):6132-6136.

87. ZAUCKE F, DINSER R, MAURER P, PAULSSON MJBJ: **Cartilage oligomeric matrix protein (COMP) and collagen IX are sensitive markers for the differentiation state of articular primary chondrocytes**. 2001, **358**(1):17-24.

88. Blumbach K, Niehoff A, Paulsson M, Zaucke FJMb: **Ablation of collagen IX and COMP disrupts epiphyseal cartilage architecture**. 2008, **27**(4):306-318.

89. Wu W, Mwale F, Tchetina E, Kojima T, Yasuda T, Poole AR: **Cartilage matrix resorption in skeletogenesis**. *Novartis Foundation symposium* 2001, **232**:158-166; discussion 166-170.

90. Tan K, Duquette M, Joachimiak A, Lawler J: **The crystal structure of the signature domain of cartilage oligomeric matrix protein: implications for collagen, glycosaminoglycan and integrin binding**. *Faseb j* 2009, **23**(8):2490-2501.

91. DiCesare PE, Morgelin M, Carlson CS, Pasumarti S, Paulsson M: **Cartilage oligomeric matrix protein: isolation and characterization from human articular cartilage**. *Journal of orthopaedic research : official publication of the Orthopaedic Research Society* 1995, **13**(3):422-428.

92. Rock MJ, Holden P, Horton WA, Cohn DH: **Cartilage oligomeric matrix protein promotes cell attachment via two independent mechanisms involving CD47 and alphaVbeta3 integrin**. *Molecular and cellular biochemistry* 2010, **338**(1-2):215-224.

93. Firner S, Zaucke F, Michael J, Dargel J, Schiwy-Bochat KH, Heilig J, Rothschild MA, Eysel P, Bruggemann GP, Niehoff A: **Extracellular Distribution of Collagen II and Perifibrillar Adapter Proteins in Healthy**

and Osteoarthritic Human Knee Joint Cartilage. *The journal of histochemistry and cytochemistry : official journal of the Histochemistry Society* 2017, **65**(10):593-606.

94.   Klatt AR, Becker AK, Neacsu CD, Paulsson M, Wagener R: **The matrilins: modulators of extracellular matrix assembly**. *The international journal of biochemistry & cell biology* 2011, **43**(3):320-330.

95.   Klatt AR, Paulsson M, Wagener R: **Expression of matrilins during maturation of mouse skeletal tissues**. *Matrix biology : journal of the International Society for Matrix Biology* 2002, **21**(3):289-296.

96.   Deak F, Wagener R, Kiss I, Paulsson M: **The matrilins: a novel family of oligomeric extracellular matrix proteins**. *Matrix biology : journal of the International Society for Matrix Biology* 1999, **18**(1):55-64.

97.   Schubert A, Schminke B, Miosge N: **Fibulins and matrilins are novel structural components of the periodontium in the mouse**. *Archives of oral biology* 2017, **82**:216-222.

98.   Huang X, Birk DE, Goetinck PF: **Mice lacking matrilin-1 (cartilage matrix protein) have alterations in type II collagen fibrillogenesis and fibril organization**. *Developmental dynamics : an official publication of the American Association of Anatomists* 1999, **216**(4-5):434-441.

99.   Hauser N, Paulsson M, Heinegård D, Mörgelin MJJoBC: **Interaction of Cartilage Matrix Protein with Aggrecan INCREASED COVALENT CROSS-LINKING WITH TISSUE MATURATION**.   1996, **271**(50):32247-32252.

100.   Winterbottom N, Tondravi MM, Harrington TL, Klier FG, Vertel BM, Goetinck PFJDd: **Cartilage matrix protein is a component of the collagen fibril of cartilage**. 1992, **193**(3):266-276.

101.   Budde B, Blumbach K, Ylöstalo J, Zaucke F, Ehlen HW, Wagener R, Ala-Kokko L, Paulsson M, Bruckner P, Grässel SJM *et al*: **Altered integration of matrilin-3 into cartilage extracellular matrix in the absence of collagen IX**. 2005, **25**(23):10465-10478.

102.   Mann HH, Özbek S, Engel J, Paulsson M, Wagener RJJoBC: **Interactions between the Cartilage Oligomeric Matrix Protein and Matrilins IMPLICATIONS FOR MATRIX ASSEMBLY AND THE PATHOGENESIS OF CHONDRODYSPLASIAS**. 2004, **279**(24):25294-25298.

103.   Wiberg C, Klatt AR, Wagener R, Paulsson M, Bateman JF, Heinegård D, Mörgelin MJJoBC: **Complexes of matrilin-1 and biglycan or decorin connect collagen VI microfibrils to both collagen II and aggrecan**. 2003, **278**(39):37698-37704.

104.   Wagener R, Ehlen HW, Ko Y-P, Kobbe B, Mann HH, Sengle G, Paulsson MJFl: **The matrilins– adaptor proteins in the extracellular matrix**. 2005, **579**(15):3323-3329.

105.   Wagener R, Kobbe B, Paulsson MJFl: **Matrilin-4, a new member of the matrilin family of extracellular matrix proteins 1**. 1998, **436**(1):123-127.

106.   Segat D, Frie C, Nitsche PD, Klatt AR, Piecha D, Korpos E, Deak F, Wagener R, Paulsson M, Smyth N: **Expression of matrilin-1, -2 and -3 in developing mouse limbs and heart**. *Matrix biology : journal of the International Society for Matrix Biology* 2000, **19**(7):649-655.

107.   Aszodi A, Bateman JF, Hirsch E, Baranyi M, Hunziker EB, Hauser N, Bosze Z, Fassler R: **Normal skeletal development of mice lacking matrilin 1: redundant function of matrilins in cartilage?** *Molecular and cellular biology* 1999, **19**(11):7841-7845.

108.   Deák F, Wagener R, Kiss I, Paulsson MJMB: **The matrilins: a novel family of oligomeric extracellular matrix proteins**. 1999, **18**(1):55-64.

109.   Paulsson M, Wagener R: **Matrilins**. *Methods in cell biology* 2018, **143**:429-446.

110.   Malin D, Sonnenberg-Riethmacher E, Guseva D, Wagener R, Aszódi A, Irintchev A, Riethmacher DJJocs: **The extracellular-matrix protein matrilin 2 participates in peripheral nerve regeneration**. 2009, **122**(7):995-1004.

111.   Deák F, Mátés L, Korpos É, Zvara Á, Szénási T, Kiricsi M, Mendler L, Keller-Pintér A, Ózsvári B, Juhász

HJJCS: **Extracellular matrilin-2 deposition controls the myogenic program timing during muscle regeneration**. 2014:jcs. 141556.

112. Fullar A, Baghy K, Deak F, Peterfia B, Zsak Y, Tatrai P, Schaff Z, Dudas J, Kiss I, Kovalszky IJPo: **Lack of Matrilin-2 favors liver tumor development via Erk1/2 and GSK-3β pathways in vivo**. 2014, **9**(4).

113. Jonas A, Thiem S, Kuhlmann T, Wagener R, Aszodi A, Nowell C, Hagemeier K, Laverick L, Perreau V, Jokubaitis VJTJoci: **Axonally derived matrilin-2 induces proinflammatory responses that exacerbate autoimmune neuroinflammation**. 2014, **124**(11):5042-5056.

114. Otten C, Hansen U, Talke A, Wagener R, Paulsson M, Zaucke F: **A matrilin-3 mutation associated with osteoarthritis does not affect collagen affinity but promotes the formation of wider cartilage collagen fibrils**. *Human mutation* 2010, **31**(3):254-263.

115. Nicolae C, Ko Y-P, Miosge N, Niehoff A, Studer D, Enggist L, Hunziker EB, Paulsson M, Wagener R, Aszodi AJJobc: **Abnormal collagen fibrils in cartilage of matrilin-1/matrilin-3-deficient mice**. 2007, **282**(30):22163-22175.

116. van der Weyden L, Wei L, Luo J, Yang X, Birk DE, Adams DJ, Bradley A, Chen QJTAjop: **Functional knockout of the matrilin-3 gene causes premature chondrocyte maturation to hypertrophy and increases bone mineral density and osteoarthritis**. 2006, **169**(2):515-527.

117. Wang H, Zhang H, Sun Q, Wang Y, Yang J, Yang J, Zhang T, Luo S, Wang L, Jiang Y *et al*: **Intra-articular Delivery of Antago-miR-483-5p Inhibits Osteoarthritis by Modulating Matrilin 3 and Tissue Inhibitor of Metalloproteinase 2**. *Molecular therapy : the journal of the American Society of Gene Therapy* 2017, **25**(3):715-727.

118. Uckelmann H, Blaszkiewicz S, Nicolae C, Haas S, Schnell A, Wurzer S, Wagener R, Aszodi A, Essers MAGJJoEM: **Extracellular matrix protein Matrilin-4 regulates stress-induced HSC proliferation via CXCR4**. 2016, **213**(10):1961-1971.

119. Spranger JW: **Metaphyseal chondrodysplasia**. *Postgraduate medical journal* 1977, **53**(622):480-487.

120. Rimoin DL, Cohn D, Krakow D, Wilcox W, Lachman RS, Alanay Y: **The skeletal dysplasias: clinical-molecular correlations**. *Annals of the New York Academy of Sciences* 2007, **1117**:302-309.

121. Olsen BR: **Mutations in collagen genes resulting in metaphyseal and epiphyseal dysplasias**. *Bone* 1995, **17**(2 Suppl):45s-49s.

122. Otten C, Wagener R, Paulsson M, Zaucke F: **Matrilin-3 mutations that cause chondrodysplasias interfere with protein trafficking while a mutation associated with hand osteoarthritis does not**. *Journal of medical genetics* 2005, **42**(10):774-779.

123. Jayasuriya CT, Zhou FH, Pei M, Wang Z, Lemme NJ, Haines P, Chen Q: **Matrilin-3 chondrodysplasia mutations cause attenuated chondrogenesis, premature hypertrophy and aberrant response to TGF-beta in chondroprogenitor cells**. *International journal of molecular sciences* 2014, **15**(8):14555-14573.

124. Zaucke F, Grassel S: **Genetic mouse models for the functional analysis of the perifibrillar components collagen IX, COMP and matrilin-3: Implications for growth cartilage differentiation and endochondral ossification**. *Histology and histopathology* 2009, **24**(8):1067-1079.

125. Cotterill SL, Jackson GC, Leighton MP, Wagener R, Makitie O, Cole WG, Briggs MD: **Multiple epiphyseal dysplasia mutations in MATN3 cause misfolding of the A-domain and prevent secretion of mutant matrilin-3**. *Hum Mutat* 2005, **26**(6):557-565.

126. Borochowitz Z, Scheffer D, Adir V, Dagoneau N, Munnich A, Cormier-Daire V: **Spondylo-epi-metaphyseal dysplasia (SEMD) matrilin 3 type: homozygote matrilin 3 mutation in a novel form of SEMD**. *Journal of medical genetics* 2004, **41**(5):366-372.

127. van der Weyden L, Wei L, Luo J, Yang X, Birk DE, Adams DJ, Bradley A, Chen Q: **Functional knockout of the matrilin-3 gene causes premature chondrocyte maturation to hypertrophy and increases bone mineral density and osteoarthritis**. *The American journal of pathology* 2006, **169**(2):515-527.

128. Hyde G, Dover S, Aszodi A, Wallis GA, Boot-Handford RP: **Lineage tracing using matrilin-1 gene expression reveals that articular chondrocytes exist as the joint interzone forms**. *Developmental biology* 2007, **304**(2):825-833.

129. Watanabe H, Yamada Y: **Chondrodysplasia of gene knockout mice for aggrecan and link protein**. *Glycoconjugate journal* 2002, **19**(4-5):269-273.

130. Watanabe H, Nakata K, Kimata K, Nakanishi I, Yamada Y: **Dwarfism and age-associated spinal degeneration of heterozygote cmd mice defective in aggrecan**. *Proceedings of the National Academy of Sciences of the United States of America* 1997, **94**(13):6943-6947.

131. Watanabe H, Kimata K, Line S, Strong D, Gao LY, Kozak CA, Yamada Y: **Mouse cartilage matrix deficiency (cmd) caused by a 7 bp deletion in the aggrecan gene**. *Nature genetics* 1994, **7**(2):154-157.

132. Gleghorn L, Ramesar R, Beighton P, Wallis G: **A mutation in the variable repeat region of the aggrecan gene (AGC1) causes a form of spondyloepiphyseal dysplasia associated with severe, premature osteoarthritis**. *American journal of human genetics* 2005, **77**(3):484-490.

133. Gibson BG, Briggs MDJOjord: **The aggrecanopathies; an evolving phenotypic spectrum of human genetic skeletal diseases**. 2016, **11**(1):86.

134. Gardner DL: **The nature and causes of osteoarthrosis**. *British medical journal (Clinical research ed)* 1983, **286**(6363):418-424.

135. Schafer M, Dreinhofer K: **[Sports and osteoarthrosis]**. *Zeitschrift fur Rheumatologie* 2009, **68**(10):804-810.

136. Cicuttini FM, Spector TD: **Genetics of osteoarthritis**. *Ann Rheum Dis* 1996, **55**(9):665-667.

137. Bierma-Zeinstra SM, Koes BW: **Risk factors and prognostic factors of hip and knee osteoarthritis**. *Nat Clin Pract Rheumatol* 2007, **3**(2):78-85.

138. Hawker GA, Mian S, Bednis K, Stanaitis I: **Osteoarthritis year 2010 in review: non-pharmacologic therapy**. *Osteoarthritis and cartilage* 2011, **19**(4):366-374.

139. Lane NE, Shidara K, Wise BL: **Osteoarthritis year in review 2016: clinical**. *Osteoarthritis and cartilage* 2017, **25**(2):209-215.

140. Taruc-Uy RL, Lynch SA: **Diagnosis and treatment of osteoarthritis**. *Primary care* 2013, **40**(4):821-836, vii.

141. Rahmati M, Nalesso G, Mobasheri A, Mozafari M: **Aging and osteoarthritis: Central role of the extracellular matrix**. *Ageing research reviews* 2017, **40**:20-30.

142. Miyaki S, Lotz MK: **Extracellular vesicles in cartilage homeostasis and osteoarthritis**. *Current opinion in rheumatology* 2018, **30**(1):129-135.

143. Burton-Wurster N, Vernier-Singer M, Farquhar T, Lust G: **Effect of compressive loading and unloading on the synthesis of total protein, proteoglycan, and fibronectin by canine cartilage explants**. *Journal of orthopaedic research : official publication of the Orthopaedic Research Society* 1993, **11**(5):717-729.

144. Bader DL, Salter DM, Chowdhury TT: **Biomechanical influence of cartilage homeostasis in health and disease**. *Arthritis* 2011, **2011**:979032.

145. Torzilli PA, Grigiene R, Borrelli J, Jr., Helfet DL: **Effect of impact load on articular cartilage: cell metabolism and viability, and matrix water content**. *Journal of biomechanical engineering* 1999, **121**(5):433-441.

146. Loening AM, James IE, Levenston ME, Badger AM, Frank EH, Kurz B, Nuttall ME, Hung HH, Blake SM,

Grodzinsky AJ *et al*: **Injurious mechanical compression of bovine articular cartilage induces chondrocyte apoptosis**. *Archives of biochemistry and biophysics* 2000, **381**(2):205-212.

147. Milentijevic D, Torzilli PA: **Influence of stress rate on water loss, matrix deformation and chondrocyte viability in impacted articular cartilage**. *Journal of biomechanics* 2005, **38**(3):493-502.

148. Stefánsson SE, Jónsson H, Ingvarsson T, Manolescu I, Jónsson HH, Ólafsdóttir G, Pálsdóttir E, Stefánsdóttir G, Sveinbjörnsdóttir G, Frigge MLJTAJoHG: **Genomewide scan for hand osteoarthritis: a novel mutation in matrilin-3**. 2003, **72**(6):1448-1459.

149. Min JL, Meulenbelt I, Riyazi N, Kloppenburg M, Houwing-Duistermaat JJ, Seymour AB, van Duijn CM, Slagboom PEJAotrd: **Association of matrilin-3 polymorphisms with spinal disc degeneration and osteoarthritis of the first carpometacarpal joint of the hand**. 2006, **65**(8):1060-1066.

150. Pullig O, Tagariello A, Schweizer A, Swoboda B, Schaller P, Winterpacht AJAotrd: **MATN3 (matrilin-3) sequence variation (pT303M) is a risk factor for osteoarthritis of the CMC1 joint of the hand, but not for knee osteoarthritis**. 2007, **66**(2):279-280.

151. Pullig O, Weseloh G, Klatt A, Wagener R, Swoboda BJO, cartilage: **Matrilin-3 in human articular cartilage: increased expression in osteoarthritis**. 2002, **10**(4):253-263.

152. Firner S, Zaucke F, Michael J, Dargel J, Schiwy-Bochat K-H, Heilig J, Rothschild MA, Eysel P, Brüggemann, Niehoff AJJoH *et al*: **Extracellular distribution of collagen II and perifibrillar adapter proteins in healthy and osteoarthritic human knee joint cartilage. 2017, 65(10):593-606.**

153. Vincourt JB, Vignaud JM, Lionneton F, Sirveaux F, Kawaki H, Marchal S, Lomazzi S, Plénat F, Guillemin F, Netter PJA *et al*: **Increased expression of matrilin-3 not only in osteoarthritic articular cartilage but also in cartilage-forming tumors, and down-regulation of SOX9 via epidermal growth factor domain 1–dependent signaling**. 2008, **58**(9):2798-2808.

154. Vincourt J-B, Gillet P, Rat A-C, Guillemin F, Netter P, Mainard D, Magdalou JJO, cartilage: **Measurement of matrilin-3 levels in human serum and synovial fluid using a competitive enzyme-linked immunosorbent assay**. 2012, **20**(7):783-786.

155. Vincourt J-B, Etienne S, Grossin L, Cottet J, Bantsimba-Malanda C, Netter P, Mainard D, Libante V, Gillet P, Magdalou JJMB: **Matrilin-3 switches from anti-to pro-anabolic upon integration to the extracellular matrix**. 2012, **31**(5):290-298.

156. Klatt AR, Klinger G, Paul-Klausch B, Kühn G, Renno JH, Wagener R, Paulsson M, Schmidt J, Malchau G, Wielckens KJFl: **Matrilin-3 activates the expression of osteoarthritis-associated genes in primary human chondrocytes**. 2009, **583**(22):3611-3617.

157. Jayasuriya CT, Goldring MB, Terek R, Chen QJAr, therapy: **Matrilin-3 induction of IL-1 receptor antagonist is required for up-regulating collagen II and aggrecan and down-regulating ADAMTS-5 gene expression**. 2012, **14**(5):R197.

158. Meulenbelt I, Bijkerk C, De Wildt S, Miedema H, Valkenburg H, Breedveld F, Pols H, Te Koppele J, Sloos V, Hofman AJA *et al*: **Investigation of the association of the CRTM and CRTL1 genes with radiographically evident osteoarthritis in subjects from the Rotterdam study**. 1997, **40**(10):1760-1765.

159. Okimura A, Okada Y, Makihira S, Pan H, Yu L, Tanne K, Imai K, Yamada H, Kawamoto T, Noshiro MJA *et al*: **Enhancement of cartilage matrix protein synthesis in arthritic cartilage**. 1997, **40**(6):1029-1036.

160. Zhang S, Peng J, Guo Y, Javidiparsijani S, Wang G, Wang Y, Liu H, Liu J, Luo JJBri: **Matrilin-2 is a widely distributed extracellular matrix protein and a potential biomarker in the early stage of osteoarthritis in articular cartilage**. 2014, **2014**.

161. Chou C-H, Lee MTM, Song I-W, Lu L-S, Shen H-C, Lee C-H, Wu J-Y, Chen Y-T, Kraus VB, Wu C-CJO *et al*:

Insights into osteoarthritis progression revealed by analyses of both knee tibiofemoral compartments. 2015, **23**(4):571-580.

162. Rizkalla G, Reiner A, Bogoch E, Poole AR: **Studies of the articular cartilage proteoglycan aggrecan in health and osteoarthritis. Evidence for molecular heterogeneity and extensive molecular changes in disease**. *The Journal of clinical investigation* 1992, **90**(6):2268-2277.

163. Fraser A, Fearon U, Billinghurst RC, Ionescu M, Reece R, Barwick T, Emery P, Poole AR, Veale DJ: **Turnover of type II collagen and aggrecan in cartilage matrix at the onset of inflammatory arthritis in humans: relationship to mediators of systemic and local inflammation**. *Arthritis and rheumatism* 2003, **48**(11):3085-3095.

164. Wen CY, Wu CB, Tang B, Wang T, Yan CH, Lu WW, Pan H, Hu Y, Chiu KY: **Collagen fibril stiffening in osteoarthritic cartilage of human beings revealed by atomic force microscopy**. *Osteoarthritis and cartilage* 2012, **20**(8):916-922.

165. Stolz M, Gottardi R, Raiteri R, Miot S, Martin I, Imer R, Staufer U, Raducanu A, Duggelin M, Baschong W *et al*: **Early detection of aging cartilage and osteoarthritis in mice and patient samples using atomic force microscopy**. *Nature nanotechnology* 2009, **4**(3):186-192.

166. Roughley PJ, Mort JS: **The role of aggrecan in normal and osteoarthritic cartilage**. *Journal of experimental orthopaedics* 2014, **1**(1):8.

167. Matyas JR, Huang D, Chung M, Adams MEJA, Rheumatology ROJotACo: **Regional quantification of cartilage type II collagen and aggrecan messenger RNA in joints with early experimental osteoarthritis**. 2002, **46**(6):1536-1543.

168. Nilsson O, Guo MH, Dunbar N, Popovic J, Flynn D, Jacobsen C, Lui JC, Hirschhorn JN, Baron J, Dauber AJTJoCE *et al*: **Short stature, accelerated bone maturation, and early growth cessation due to heterozygous aggrecan mutations**. 2014, **99**(8):E1510-E1518.

169. Tompson SW, Merriman B, Funari VA, Fresquet M, Lachman RS, Rimoin DL, Nelson SF, Briggs MD, Cohn DH, Krakow DJTAJoHG: **A recessive skeletal dysplasia, SEMD aggrecan type, results from a missense mutation affecting the C-type lectin domain of aggrecan**. 2009, **84**(1):72-79.

170. Stattin E-L, Wiklund F, Lindblom K, Önnerfjord P, Jonsson B-A, Tegner Y, Sasaki T, Struglics A, Lohmander S, Dahl NJTAJoHG: **A missense mutation in the aggrecan C-type lectin domain disrupts extracellular matrix interactions and causes dominant familial osteochondritis dissecans**. 2010, **86**(2):126-137.

ACKNOWLEDGEMENTS